Dissertation

submitted to the

Combined Faculty of Natural Sciences and Mathematics

of the Ruperto Carola University Heidelberg, Germany

for the degree of

Doctor of Natural Sciences

Presented by

M.Sc. Sebastian Kruse

born in Detmold, Germany

Oral examination: 14th of January 2019

Therapeutic vaccination against HPV-positive tumors in a MHC-humanized mouse model

Referees: Prof. Dr. Martin Müller

PD Dr. Dr. Angelika Riemer

This work was performed from June 2015 – August 2018 under scientific supervision of PD Dr. Dr. Angelika Riemer in the Junior Research Group Immunotherapy and Immunoprevention at the German Cancer Research Center, Heidelberg.

Peer-reviewed publication based on this study

Kruse S., Büchler M., Uhl P., Sauter M., Scherer P., Lan T.C.T., Zottnick S., Klevenz A., Yang R., Rösl F., Mier W., and Riemer AB. *Therapeutic vaccination using minimal HPV16 epitopes in a novel MHC-humanized murine HPV tumor model.* (10/2018) Oncoimmunology. doi: 10.1080/2162402X.2018.1524694

Conference and workshop presentations based on this study

Kruse S. *Anti-tumor vaccination with mass spectrometry-confirmed HPV16 epitopes in a HLA-humanized mouse model.* (06/2016): Oral presentation at the IIC (Infection, Inflammation and Cancer) retreat 2016, Schöntal, Germany

Kruse S., Büchler M., Yang R., Will R., Fehr J., Rösl F., Blatnik R., Riemer A. B. *Therapeutic vaccination against HPV-induced tumors in a MHC-humanized mouse model.* (11/16): Poster presentation at the DKFZ PhD Poster Presentation, Heidelberg, Germany

Kruse S., Büchler M., Yang R., Will R., Fehr J., Rösl F., Blatnik R., Riemer A. B. *Therapeutic vaccination against HPV-induced tumors in a MHC-humanized mouse model.* (11/16): Oral presentation and poster presentation at the 8th German-Israeli Cancer Research School "Cancer Immunotherapy", Neve Ilan, Israel

Kruse S. *Therapeutic vaccination against HPV16 E6/E7-positive tumors in a MHC-humanized mouse model.* (07/17): Oral presentation at the DKFZ PhD retreat, Weil der Stadt, Germany

Kruse S., Büchler M., Klevenz A., Scherer P., Lan T.C.T., Yang R., Rösl F., Blatnik R., Riemer A.B. *Induction of HPV16 E7-specific CD8^{+} T cells in MHC-humanized A2.DR1 mice via minimal epitope vaccination.* (09/17): Poster presentation at the 3rd CRI-CIMT-EATI-AACR International Cancer Immunotherapy Conference, Mainz, Germany

Kruse S., Büchler M., Klevenz A., Scherer P., Lan T.C.T., Yang R., Rösl F., Blatnik R., Riemer A.B. *Therapeutic vaccination using a minimal HPV16 E7 epitope in a MHC-humanized mouse model.* (09/17): Poster presentation at the 47th Annual Meeting of the German Society for Immunology, Erlangen, Germany

Abstract

Human papillomaviruses (HPV) are responsible for 5 % of all annual cancer cases worldwide and thus present a major health problem. HPVs can cause oropharyngeal and anogenital cancers. More than 60 % of the HPV-induced cancers are caused by HPV16. Therapeutic anti-tumor vaccination against the two HPV oncoproteins E6 and E7 represents an attractive treatment option because these proteins are expressed in all tumor stages and are indispensable for tumor initiation and survival. Therapeutic vaccination could combine long-term immunity with reduced treatment side effects compared to conventional therapies such as surgery and chemotherapy. Preclinical studies for the development of a therapeutic HPV vaccine have yielded promising results. However, most clinical studies could not reproduce these findings. One obstacle to achieving better translatability of preclinical findings is the absence of a mouse model that allows the exclusive study of human HPV epitopes. A2.DR1 mice express two of the most common major histocompatibility complex (MHC) molecules, HLA-A2 and HLA-DR1, without the expression of any interfering murine MHCs. The aim of this PhD project was to develop a HPV16 tumor model for these mice, and to test various formulations of epitope-specific therapeutic anti-HPV16 vaccines. This work shows that the newly established PAP-A2 tumor cells express HPV16 E6/E7 and present four epitopes on HLA-A2 that can also be found on HPV16-transformed human tumor cells. The immunogenicity of all four epitopes in A2.DR1 mice was shown by the induction of $CD8^+$ T cell responses after vaccination with these epitopes. Comparing emulsion-based, mRNA-based and different amphiphilic peptide-based vaccines, it was observed that amphiphilic peptides induced the highest frequencies of E7/11-19-specific $CD8^+$ T cells. Furthermore, it could be demonstrated that therapeutic vaccination with an amphiphilic version of the minimal epitope E7/11-19 induces complete PAP-A2 tumor rejection in 50 % of animals. Interestingly, upon vaccination with the other three epitopes or combination vaccination with the four different epitopes we observed decreased anti-tumor responses compared to single E7/11-19 vaccination. In summary, this study presents the first HPV16 E6/E7-positive tumor model that allows the exclusive analysis of HPV16 epitopes in fully MHC-humanized mice and shows pronounced anti-tumor effects by minimal epitope vaccination. These results emphasize the need for the careful selection and combination of minimal epitope vaccines and could improve the efficacy of future therapeutic HPV vaccines.

Zusammenfassung

Humane Papillomviren (HPV) verursachen 5 % aller Krebsfälle weltweit und stellen somit ein wichtiges Gesundheitsproblem dar. HPVs können sowohl oropharyngeale als auch anogenitale Tumoren auslösen. Mehr als 60 % aller HPV-induzierten Krebsfälle werden von HPV16 ausgelöst. Therapeutische anti-Tumor Impfungen gegen die zwei HPV Onkoproteine E6 und E7 stellen eine attraktive Behandlungsoption dar, da diese Proteine in allen Tumorstadien exprimiert werden und unentbehrlich für die Tumorentstehung und das Tumorwachstum sind. Therapeutische Impfungen könnten Langzeit-Immunität mit reduzierten Nebenwirkungen, verglichen zu konventionellen Therapien wie operative Eingriffe und Chemotherapien, verbinden. Präklinische Studien für die Entwicklung einer therapeutischen HPV Impfung konnten vielversprechende Ergebnisse generieren, die meisten klinischen Studien konnten diese Ergebnisse jedoch nicht reproduzieren. Ein Hindernis, das der besseren Übertragbarkeit von präklinischen Studien zu klinischen Ergebnissen im Wege steht, ist das Fehlen eines Maus Modells, welches die exklusive Erforschung von humanen HPV Epitopen erlaubt. A2.DR1 Mäuse exprimieren zwei der häufigsten Haupthistokompatibilitätskomplex (MHC) Moleküle, HLA-A2 und HLA-DR1, ohne die Expression von interferierenden murinen MHC Molekülen. Das Ziel dieser Doktorarbeit war die Entwicklung eines HPV16 Tumor Modells für diese Mäuse, und die Evaluierung verschiedener Formulierungen therapeutischer HPV16 Impfungen mit definierten Minimalepitopen. Diese Arbeit zeigt, dass die neu entwickelte PAP-A2 Tumorzelllinie HPV16 E6/E7 exprimiert und vier HLA-A2-restringierte Epitope präsentiert, die auch auf HPV16-transformierten humanen Tumorzelllinien gefunden werden. Die Immunogenität von allen vier Epitopen in A2.DR1 Mäusen konnte durch die Induktion von $CD8^+$ T Zell-Antworten nach Impfung mit den vier Epitopen gezeigt werden. Im Vergleich von Emulsionsformulierungen, mRNA Vakzinen und Vakzinen basierend auf amphiphilen Peptiden konnte beobachtet werden, dass amphiphile Vakzine die höchsten Frequenzen von E7/11-19-spezifischen $CD8^+$ T Zellen induzierten. Weiterhin konnte gezeigt werden, dass eine therapeutische Impfung mit einer amphiphilen Version des Minimalepitops E7/11-19 eine vollständige Tumorabstoßung in 50 % der Tiere induziert. Interessanterweise wurden geringere anti-Tumor Effekte als die durch Einfach-Impfung mit E7/11-19 nach Impfung mit den drei anderen Epitopen oder Kombinationsimpfungen beobachtet. Zusammengefasst präsentiert

diese Arbeit das erste HPV16 E6/E7-positive Tumormodell, dass die exklusive Analyse von HPV16 Epitopen in vollständig MHC-humanisierten Mäusen erlaubt und zeigt starke anti-Tumor Effekte durch Impfung mit Minimalepitopen. Diese Ergebnisse betonen die Notwendigkeit der sorgfältigen Auswahl und Kombination von Vakzinen basierend auf Minimalepitopen und könnten die Wirksamkeit von zukünftigen therapeutischen HPV Impfungen verbessern.

Danksagung

An dieser Stelle möchte ich mich bei allen Personen bedanken, die mich beim Erstellen meiner Doktorarbeit unterstützt haben.

Zuerst möchte ich PD Dr. Dr. **Angelika Riemer** für die Möglichkeit danken, diese Doktorarbeit in ihrer Arbeitsgruppe anzufertigen. Dein Vertrauen in meine Fähigkeiten und deine Ratschläge, nicht nur wissenschaftlicher Art, waren immer ein großer Rückhalt für mich.

Des Weiteren möchte ich Prof. **Martin Müller** dafür danken, dass er die Erstbetreuung dieser Arbeit übernommen hat. Auch für die guten Anregungen in meinen TAC Meetings, das Gegenlesen der Thesis sowie für den unverzichtbaren NM2 Antikörper möchte ich ihm danken. Prof. **Suat Özbek** und Prof. **Viktor Umansky** danke ich für ihre Teilnahme als Prüfer an meiner Disputation. Ebenso bedanken möchte ich mich bei meinem dritten TAC Mitglied Prof. **Alexander Dalpke** für die anregenden Diskussionen in meinen TAC Meetings.

Ich danke Dr. **Philipp Uhl**, Dr. **Max Sauter** und der **Peptid Core Facility** (insbesondere **Mario Koch**) für ihren wertvollen Beitrag durch die Synthese von Peptid-Konstrukten. **Ruwen Yang** danke ich für ihren Vektor, der maßgeblich zum Gelingen des PAP-A2 Modells beigetragen hat. Ich danke dem Team von **BioNTech** und insbesondere Dr. **Christian Grunwitz** für das Zurverfügungstellen von mRNA Konstrukten und die gute Zusammenarbeit. Ebenso danke ich dem Team von **Silvacx** und hier besonders Dr. **Armin Kübelbeck** für die Nanopartikel und die gute Kooperation. Dr. **Theresa Bunse** danke ich für die 2277NS Zellen. Dr. **Matthias Bozza** danke ich für das Teilen seiner Vektoren und seiner Cloning-Expertise. Dr. **Frank Momburg** danke ich für seine single-chain trimer Konstrukte. Auch **Marten Meyer** danke ich für diese Konstrukte und für seine immunologische Expertise und die guten Diskussionen.

Alexandra Klevenz, **Lena Postawa** und **Florian Müller** möchte ich für ihre technische Assistenz danken.

Ein besonderer Dank gebührt den Studenten, die ich im Rahmen dieses Projekts betreut habe - **Jana Fehr**, **Marleen Büchler**, **Philipp Scherer** und **Tammy Lan** - für die Arbeit, die sie in dieses Projekt gesteckt haben und für die gute Zeit, die wir zusammen hatten.

Samantha Zottnick gebührt ganz besonderer Dank für lange wissenschaftliche Diskussionen auf dem Weg zum Unishop, ihren Humor, der so manchen Tag gerettet hat, und ihren unermüdlichen Einsatz für den Passierschein A38.

Monika Bock möchte ich für ihre administrative Unterstützung und ganz besonders für ihr offenes Ohr danken.

Ebenso danke ich allen Praktikanten, PhD-Studenten und Postdocs vom **Team F130** von Herzen für die wissenschaftliche und moralische Unterstützung und für die Gespräche, die den Alltag interessant gemacht haben. Ganz besonders zu nennen sind hier **Stephanie Hoppe**, **Alina Steinbach**, **Maria Bonsack**, **Nitya Mohan, Mogjib Salek, Mine Özcan** und **Jonas Förster**.

Die Core Facilities des DKFZ haben mich nach Kräften unterstützt, besonders hervorzuheben sind hier das Team des **Zentralen Tierlabors** und die **DKFZ Flow cytometry Core Facility**.

Der **Helmholtz International Graduate School for Cancer Research** möchte ich für die Beratung und Unterstützung danken.

Einen weiteren Dank möchte ich den **Mitgliedern des PhD Student Council 2015/2016** aussprechen für die intensive und interessante Zeit, in der ich vieles lernen durfte.

Ein gigantisches Dankeschön gilt meinen **Freunden** aus Heidelberg, Konstanz, Detmold und der ganzen Welt. Ohne eure Unterstützung hätte etwas ganz Essentielles gefehlt.

Meiner Freundin **Taga Lerner** danke ich für ihre Geduld auch in den schwierigen Situationen, exzellentes Essen, erholsame Urlaube und ihre Unterstützung. Du bist die Beste. Mindestens!

Meiner Familie, **Kristina**, **Ute** und **Friedrich Kruse,** danke ich für ihre Unterstützung in allen Lebenslagen. Auch meiner weiteren Familie möchte ich für ihr Interesse und ihre Unterstützung dieser Doktorarbeit herzlich danken.

List of figures

Several figures shown in this thesis were also published in the publication Kruse *et al.*, 2018. In particular, these are the following figures: Figure 16, Figure 23, Figure 24, Figure 29, Figure 33, Figure 34, Figure 36, Figure 37, Figure 38, Figure 39, Figure 40, Figure 41, Figure 42, Figure 43, Figure 44.

List of tables

Abbreviations

AB	antibody
AHSS	aluminum hydroxyphosphate sulfate
APC	antigen-presenting cell
APC	allophycocyanin
β2m	β2 microglobulin
BCR	B cell receptor
BSA	bovine serum albumin
CD	cluster of differentiation
CFSE	carboxyfluorescein succinimidyl ester
CIN	cervical intraepithelial neoplasia
CTL	cytotoxic T cell
DC	dendritic cell
DC	detergent compatible
DKFZ	Deutsches Krebsforschungszentrum
DMEM	Dulbecco's Modified Eagle Medium
DMSO	dimethyl sulfoxide
DNA	deoxyribonucleic acid
DTT	dithiothreitol
ECL	enhanced chemiluminescence
EDTA	ethylenediaminetetraacetic acid
EGFR	epidermal growth factor receptor
ELISpot	enzyme-linked immuno spot assay
ERAP I	endoplasmic reticulum aminopeptidase I
FACS	fluorescence-activated cell sorting
FCS	fetal calf serum
FITC	fluorescein isothiocyanate
Foxp3	forkhead box P3
FR	far red dye
HLA	human leukocyte antigen

HPLC	high performance liquid chromatography
HPV	human papillomavirus
HRP	horseradish peroxidase
ICS	intracellular staining
IFA	incomplete Freund's adjuvant
IFN	interferon
IL	interleukin
IVT	*in vitro* transcription
KO	knockout
LPP	lipo-PEG-peptide
LPX	lipoplex
MACS	magnetic-activated cell sorting
MCA	methylcholanthrene
MEM	minimal essential medium
MHC	major histocompatibility complex
MPLA	monophosphoryl lipid A
mRNA	messenger ribonucleic acid
MS	mass spectrometry
NGS	next generation sequencing
NK	natural killer
PADRE	pan HLA-DR binding epitope
PAGE	polyacrylamide gel electrophoresis
PAMP	pathogen-associated molecular pattern
Pap-test	Papanicolaou-test
PBS	phosphate-buffered saline
PCR	polymerase chain reaction
PD-L1	programmed death ligand 1
PE	phycoerythrin
PEG	polyethylene glycol
PMA	phorbol myristate acetate

pMHC	peptide loaded MHC
poly I:C, pIC	polyinosinic:polycytidylic acid
pRB	retinoblastoma protein
PRR	pattern recognition receptor
RNA	ribonucleic acid
RPMI	Roswell Park Memorial Institute medium
RT	room temperature
SCT	single-chain trimer
SDS	sodium dodecyl sulfate
SLP	synthetic long peptide
SSP	synthetic short peptide
TAP	transporter associated with antigen processing
Taq	Thermus aquaticus
TCR	T cell receptor
T_H	T-helper cell
TLR	Toll-like receptor
TNF	tumor necrosis factor
T_{reg}	regulatory T cell
TRIS	Tris(hydroxymethyl)aminomethane
URR	upstream regulatory region
VIN	vulvar intraepithelial neoplasia
VLP	virus-like particle
WB	Western blot
WT	wildtype

Table of Contents

1 Introduction

1.1 The immune system

The human body is under constant attack by pathogens like bacteria, viruses, fungi and parasites. The immune system evolved to counter these attacks and consists of two major parts: The innate and the adaptive immune system. The immune system is made up of organs, cellular components and soluble components. The organs that make up the immune system are the primary lymphoid organs with the bone marrow and thymus and the secondary lymphoid organs with the spleen, lymph nodes and the lymph system (Murphy *et al.*, 2016).

1.1.1 Innate immune system

The innate immune system is able to detect and attack pathogens quickly due to their expression of conserved features that are shared by many pathogens. This recognition is achieved by pattern recognition receptors (PRR) expressed on cells of the innate immune system. In general, the components of the innate immune system comprise cellular components such as natural killer (NK) cells, macrophages, dendritic cells (DC), neutrophils and the soluble components of the complement system. Macrophages and especially DCs are at the interface of the innate and the adaptive immune system due to their ability to present components of pathogens to cells of the adaptive immune system and thus trigger an adaptive immune response (Murphy *et al.*, 2016).

1.1.2 Adaptive immune system

The adaptive immune system cannot respond to the first encounter with a pathogen as quickly as the innate immune system but its highly specific and powerful effector mechanisms often eradicate a pathogen that is only kept in check by the innate immune system. Additionally, it can provide protection for the host, i.e. make it immune, to subsequent exposure to the same pathogen by its memory function. Like the innate immune system, the adaptive immune system is made up of cellular and soluble components. Lymphocytes make up the cellular part of the adaptive immune system and they are categorized into B lymphocytes (B cells) and T lymphocytes (T cells). The soluble components are called antibodies (ABs), which can bind to virtually all structures, and thus inactivate

them and mark them for phagocytosis by cells of the innate immune system. The names B and T cell stem from the site of their maturation, the bone marrow for B cells and the thymus for T cells (Murphy *et al.*, 2016). Both cell types carry a receptor, the B cell receptor (BCR) and T cell receptor (TCR), respectively. A high diversity of receptors is generated from a limited number of receptor genes by a process called V(D)J recombination and by the random addition of nucleotides to these genes during the development of these cells (Hozumi and Tonegawa, 1976; Schatz, 2004). Due to the partly random nature of the generation process, the receptor is unique to a clonal cell. The important distinguishing factor between the adaptive immune system and the innate immune system is that the adaptive immune system does not have to rely on conserved pathogen structures but that its cells can recognize virtually all structures of pathogens via the BCRs and TCRs. B and T cell antigen recognition results in activation and rapid clonal expansion after which they exercise their effector functions. The B cell receptor recognizes unprocessed structures that are present on pathogens (Murphy *et al.*, 2016). After activation and clonal expansion, B cells differentiate into plasma cells that secrete ABs into the blood stream. In contrast, the receptors of T cells recognize processed peptides that are presented on membrane-bound molecules called major histocompatibility complex (MHC). T cells are divided into $CD4^+$ and $CD8^+$ T cells, which differ in their function and the MHCs they recognize. $CD4^+$ T cells are also called helper T cells (T_H) and recognize epitopes presented on MHC class II, whereas $CD8^+$ T cells are also called cytotoxic T cells and recognize epitopes presented on MHC class I. The function of $CD4^+$ T cells is to provide B cells and macrophages with signals that allow them to fulfill their specific functions, hence their name. Due to their helper function they can also improve the activation of $CD8^+$ T cells. Cytotoxic $CD8^+$ T cells recognize tumor cells and cells infected with intracellular pathogens, such as viruses, and kill the cell to prevent a spread of the infection or the tumor (Murphy *et al.*, 2016).

Peptides that bind MHC and can be recognized by T cells are called epitopes and can be derived from self or non-self proteins. The name MHC is derived from the finding that tissue cannot be transplanted between two individuals who differ in their MHC molecules (Snell and Higgins, 1951). MHC molecules are divided into classical and non-classical MHCs, the focus here will be on classical MHCs. Non-classical MHCs have diverse functions such as iron uptake, tasks in the innate immune system and protection of the fetus from a maternal

immune response. The classical MHCs are categorized into MHC class I and MHC class II (Figure 1).

The MHC loci are highly polymorphic and each allele has different binding affinities for different epitopes (Murphy *et al.*, 2016). It is assumed that this variety evolved to enable MHCs to present epitopes from as many pathogens as possible. In humans, MHCs are called human leukocyte antigen (HLA). Despite this variety, certain MHC class I alleles are more common in the human population than others, e.g. HLA-A*0201, often abbreviated as HLA-A2, is the most frequent HLA class I allele in the Caucasian population. For example, in the USA, it has a frequency of 47.8 % among Caucasians (González-Galarza *et al.*, 2015).

MHC class I is expressed by virtually all nucleated cells and is formed by the association of a membrane-bound heavy chain consisting of five domains (α1, α2 and α3, a transmembrane domain and a cytoplasmic tail with the soluble β2 microglobulin (β2m) (Figure 1, left side). α1 and α2 make up the peptide-binding groove to which peptides of 8-11 amino acids can bind (Murphy *et al.*, 2016).

MHC class II molecules are expressed by professional antigen-presenting cells (APC) such as B lymphocytes, DCs and macrophages. This MHC class is formed by the association of two membrane-bound subunits, which are called α chain and β chain (Figure 1, right side). Since the peptide binding groove is open at both ends, MHC class II molecules bind longer epitopes (12-14 amino acids) than MHC class I molecules (Murphy *et al.*, 2016).

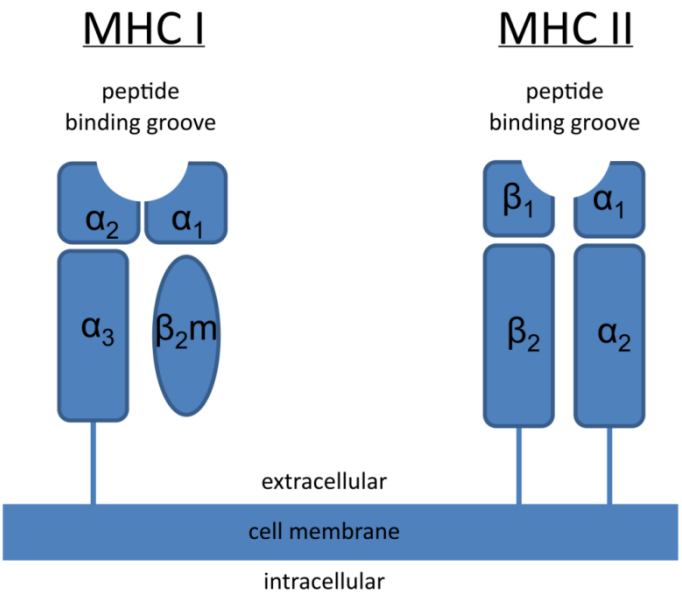

Figure 1. MHC class I und class II

The two classes of MHCs are characterized by different structures. MHC class I consists of one heavy chain (the alpha chain), consisting of three extracellular domains (α1-α3), a transmembrane domain and a cytoplasmic tail (not depicted) and the associated β2 microglobulin. MHC class II molecules are formed by the association of two proteins, the α chain and the β chain (Murphy *et al.*, 2016).

The peptides that are loaded onto MHC class I and class II differ not only in their length but also in the way they are produced and in their place of origin. Peptides that are presented on MHC class I are derived from intracellular proteins that get degraded by the proteasome, a cytosolic multi-subunit protease. The generated peptides are transported via the transporter associated with antigen processing (TAP) into the endoplasmic reticulum (ER) where they get further trimmed to the correct length by aminopeptidases such as the endoplasmic reticulum amino-peptidase I (ERAP I). After this, the peptides are loaded onto a MHC class I molecule that assembles with β2m. Subsequently, the newly assembled MHC class I:peptide complexes are transported to the cell surface and present the peptides to $CD8^+$ T cells. MHC class I molecules are expressed on all nucleated cells, thus allowing $CD8^+$ T cells to recognize infected cells by their presentation of endogenously produced, pathogen-derived epitopes. Furthermore, the expression of MHC class I inhibits killing by NK cells (Kärre *et al.*, 1986).

MHC class II-presented epitopes are derived from extracellular proteins that professional APCs such as DCs, macrophages or B cells have taken up by phagocytosis. These peptides are generated in the endosome. The MHC class II molecules are transported from the ER to the endosomes. These MHC II molecules are loaded with a placeholder peptide called invariant chain to prevent premature binding of self-peptides. The vesicles containing MHC class II molecules fuse with the endosome and the invariant chain is exchanged with a peptide that was generated in the endosome. Subsequently, the fully assembled MHC class II:peptide complexes are transported to the cell surface where patrolling $CD4^+$ T cells can recognize their epitope. By a process called cross-presentation, epitopes derived from phagocytosed proteins can also be presented on MHC class I. For this, APCs load endosome-derived epitopes onto MHC class I by processes that have not been fully elucidated yet (Murphy *et al.*, 2016).

Peptide presentation on MHC class I and MHC class II by professional APCs activates naïve T cells that carry the T cell receptor for the respective epitope. Generally, macrophages, B cells and DCs are classified as professional APCs since they have the ability to activate $CD4^+$ and $CD8^+$ T cells. The cell type most professionalized for this process is the DC. To activate a T cell, three signals are necessary.

1.1.3 Initiation of an immune response

Once a pathogen has breached the anatomical barriers of the body, it comes into contact with the immune system. Cells of the innate immune system, for example DCs, phagocytose the pathogen and get activated when their PRRs recognize conserved pathogen patterns, for instance in the case of viruses, double stranded RNA, which is recognized by the DC's toll-like receptor 3 (TLR3). The DC responds to this activation with the expression of costimulatory molecules on its surface, such as CD80/CD86, and with the secretion of immune stimulatory molecules, such as interleukin 6 (IL-6) or interferon-γ (IFN-γ). Additionally, MHC expression is upregulated. The generation of epitopes by the DC and their presentation on MHC results in the presence of all three signals required to activate T cells (Figure 2). The first signal is the binding of the TCR to a peptide-loaded MHC molecule on the DC. The second signal is provided by the binding of the DC's costimulatory molecules (e.g. CD80/CD86) to their counterpart on T cell side (CD28). The third signal is provided by soluble molecules, such as interferons or interleukins. Taken together, these three factors fully

activate the T cell and clonal expansion is induced. The DC's expression of CD80/CD86 and thus the activation of T cells can further be increased by a CD40/CD40L-mediated feedback process when a $CD4^+$ T_H recognizes its epitope presented on MHC class II on the DC (Bennett *et al.*, 1998; Ridge, Di Rosa and Matzinger, 1998; Schoenberger *et al.*, 1998).

After expansion, these clonal $CD8^+$ T cells patrol the whole body and kill cells presenting this epitope. When the pathogen has been eliminated from the body, the majority of the pathogen-specific T cells dies and only a few differentiate into long-lived memory T cells that can expand rapidly after renewed exposure to the pathogen's epitope (Murphy *et al.*, 2016).

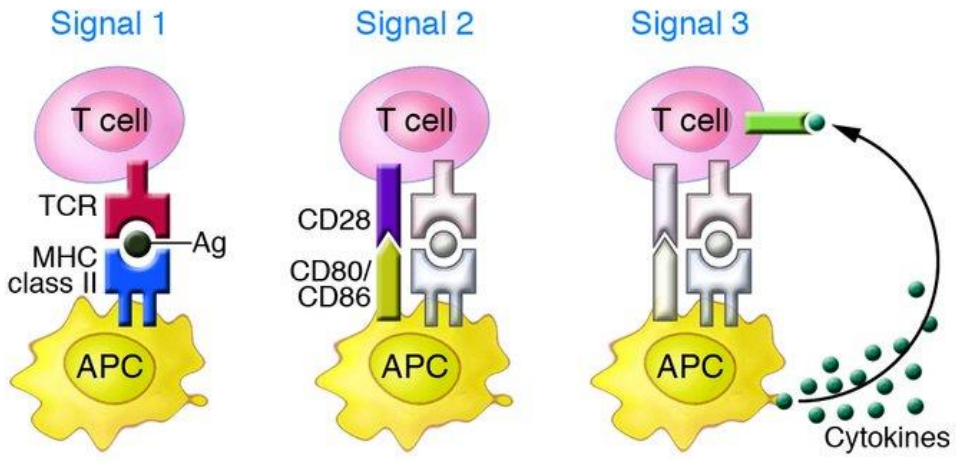

Figure 2. T cell activation requires three signals from professional antigen-presenting cells

The activation of T cells requires three signals: Signal 1 is the recognition of the peptide presented on MHC on the surface of the professional APC. Signal 2 is made up by the recognition of the APC's costimulatory molecules CD80/CD86 by the T cell's CD28. Last, cytokines secreted by the APC provide signal 3 and thus fully activate the T cell. Figure taken from (Gutcher and Becher, 2007).

To prevent an overshooting immune response, cells can express inhibitory molecules on their surface, such as programmed death-ligand 1 (PD-L1), which decrease the activity of T cells (Freeman *et al.*, 2000). These "brakes" of the immune system have become a very important field of research since their manipulation, e.g. with blocking ABs, allows to reinvigorate an anti-cancer immune response that was dampened by the cancer cells' expression of inhibitory molecules (Iwai *et al.*, 2002).

1.1.4 Basic principles of prophylactic and therapeutic vaccination

The term vaccination describes the process of exposing the immune system of an individual to a stimulus, e.g. dead or attenuated strains of a pathogen, which activates the adaptive immune system to generate immunity against this pathogen. In general, there are two kinds of vaccinations: Prophylactic and therapeutic vaccination. In the case of prophylactic vaccination, the immune system is stimulated with a vaccine before the individual has come into contact with the pathogen. Thus, immunity can be acquired e.g. by the generation of neutralizing ABs which effectively prevent an infection with the pathogen (Murphy *et al.*, 2016). Prophylactic vaccinations are among the most effective medical interventions and have saved millions of lives since their invention and broad availability (Nabel, 2013). In contrast, a therapeutic vaccination is administered after the infection with the pathogen and mostly works via the induction of antigen-specific T cells. Due to the highly specific targeting system of T cells, therapeutic vaccines can also be applied as a therapy for neoplastic malignancies since T cells are able to discriminate healthy from malignant cells.

Depending on the immune response that is required to either prevent (mostly humoral immune responses, i.e. ABs) or to treat an infection (mostly cellular immune responses, i.e. cytotoxic T cells), the vaccine formulation has to be chosen accordingly. In general, the response to a vaccination follows the same pattern as a natural initiation of an immune response by activation of APCs and subsequent clonal expansion of specific lymphocytes. The vast majority of vaccines approved today are prophylactic vaccines that often use attenuated strains of the pathogen or inactivated pathogens. These pathogen-based vaccines have good intrinsic immunostimulatory capabilities due to the presence of microbial or viral components. However, other forms of vaccine delivery (e.g. subunit vaccines like synthetic peptides) do not include the pathogen-associated molecular patterns (PAMP) that activate DCs and are therefore poorly immunogenic (Foged, 2011). In these cases, DC-activation signals have to be supplied by different means. To this end, adjuvants, which unspecifically stimulate the immune system, are included in the vaccine formulation. Examples of adjuvants are aluminum salts (alum), oil emulsions (Bonhoure and Gaucheron, 2006) and various natural or synthetic TLR agonists such as monophosphoryl lipid A (MPLA) (TLR4), polyinosinic:polycytidylic acid (poly I:C or pIC) (TLR3) or CpG (TLR9) (Adams, 2009). The mechanism of action of these adjuvants, however, is different and has not yet been

elucidated for many adjuvants (Ghimire, 2015). While the TLR agonists directly engage PRRs on DCs, alum and oil emulsions mostly work by binding the antigen and generating an antigen-rich depot at the injection site accompanied by general inflammation (Reinhardt *et al.*, 2003; Redmond and Sherman, 2005; Ghimire, 2015). While alum is an adjuvant broadly used for the induction of protective immunity via ABs, this adjuvant does not induce $CD8^+$ T cell responses that can mediate anti-tumor effects. The water-in-oil emulsion incomplete Freund's adjuvant (IFA) has for a long time been the gold standard adjuvant for induction of $CD8^+$ T cell responses. However, despite the induction of antigen-specific T cells, this emulsion-based vaccine formulation induces the sequestration of the specific T cells to the subcutaneous antigen depot and thus renders them dysfunctional (Hailemichael *et al.*, 2013). Newer subunit vaccines featuring peptides overcome this problem by making use of non-persistent formulations that, for example, can also target peptides to lymph nodes where they are taken up and processed by professional APCs such as DCs (Cho *et al.*, 2013; Liu *et al.*, 2014). These formulations are used in conjunction with TLR agonists, such as CpG or pIC, which mimic an acute infection by engaging TLRs on APCs. Thus, the activation of specific T cells is induced. Some studies give backing to the theory that MHC class II epitopes should be included in the vaccine formulation since this would lead to $CD4^+$-mediated help for the activation of $CD8^+$ T cells (BenMohamed *et al.*, 2000; Wiesel and Oxenius, 2012; Grabowska, Kaufmann and Riemer, 2014). However, there is abundant evidence for successful anti-tumor vaccines not containing MHC class II molecules (Cho *et al.*, 2013; Liu *et al.*, 2014).

Another strategy to improve immune responses is to target the antigens contained in the vaccine to DCs (reviewed in (Macri *et al.*, 2016)). This can be achieved by ABs specific for surface molecules expressed on DCs or by specific formulations and application routes e.g. for mRNA vaccines that induce mRNA expression almost exclusively in professional APCs (Kranz *et al.*, 2016). The latter approach offers the additional benefit that the mRNA at the same time encodes the antigen and serves as the TLR agonist. It has been shown that it is beneficial for vaccination success to deliver both components to the same DC (Blander and Medzhitov, 2006; Yarovinsky *et al.*, 2006).

1.2 Human papillomavirus

Papillomaviruses are strictly host specific and infect mammals, birds and reptiles (Bravo, de Sanjosé and Gottschling, 2010). Around 300 types of papillomavirus are known, around 200 of which infect humans (Van Doorslaer *et al.*, 2013, 2017). In groundbreaking research Harald zur Hausen and his team demonstrated that human papillomaviruses (HPV) are the most important causative agents for cervical cancer development (Dürst *et al.*, 1983; Boshart *et al.*, 1984).

HPVs are small double stranded non-enveloped DNA viruses with a genome size of approximately 8 kb (Doorbar *et al.*, 2015) (Figure 3). They contain six early genes (E1, E2, E4, E5, E6, E7) and two late genes (L1 and L2). The latter are coding for the proteins forming the virion particles (Doorbar *et al.*, 2015) (Figure 3). The missing member of the E1-E7 sequence, E3, was misidentified due to an error in the initial sequencing of a bovine papillomavirus (Doorbar *et al.*, 2015).

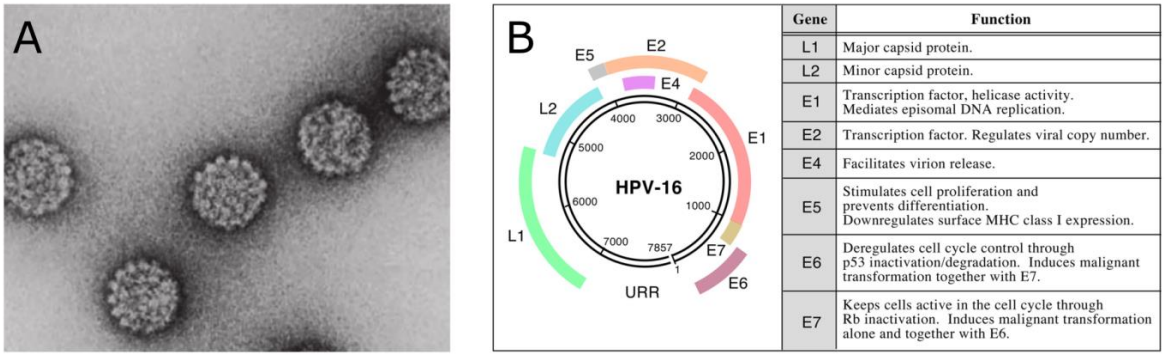

Gene	Function
L1	Major capsid protein.
L2	Minor capsid protein.
E1	Transcription factor, helicase activity. Mediates episomal DNA replication.
E2	Transcription factor. Regulates viral copy number.
E4	Facilitates virion release.
E5	Stimulates cell proliferation and prevents differentiation. Downregulates surface MHC class I expression.
E6	Deregulates cell cycle control through p53 inactivation/degradation. Induces malignant transformation together with E7.
E7	Keeps cells active in the cell cycle through Rb inactivation. Induces malignant transformation alone and together with E6.

Figure 3. A) HPV virions and B) HPV genes and their functions

The virions of HPVs are 52-55 nm in size (IARC Working Group on the Evaluation of Carcinogenic Risk to Humans, 2007) and made up by the two proteins L1 and L2. The circular DNA genome of HPV contains the genes for 8 proteins and an upstream regulatory region (URR). A) modified from (Schiffman *et al.*, 2016), B) modified from (Riemer *et al.*, 2010).

HPVs are categorized into 5 genera (alpha-, beta-, γ-, nu- and mu-papillomaviruses), species and types (Bernard *et al.*, 2010). An isolate is defined as a new type when the gene sequence of the capsid protein L1 differs more than 10 % from other known types (Bernard *et al.*, 2010). The types are numbered according to the sequence of their first discovery (De Villiers *et al.*, 2004). The alpha-papillomaviruses, which are highly relevant for overall disease

burden in humans, can further be classified into low-risk cutaneous, low-risk mucosal or high-risk with regard to their connection to cancers (Doorbar *et al.*, 2015) (Figure 4). High-risk types are carcinogenic and low-risk types can cause warts. 13 high risk types which are carcinogenic have been found so far (16, 18, 31, 33, 35, 39, 45, 51, 52, 56, 58, 59, 68) and 11 types that are probably carcinogenic (26, 30, 34, 53, 66, 67, 69, 70, 73, 82, 85) (IARC Working Group on the Evaluation of Carcinogenic Risk to Humans, 2007; Geraets *et al.*, 2012; Doorbar *et al.*, 2015).

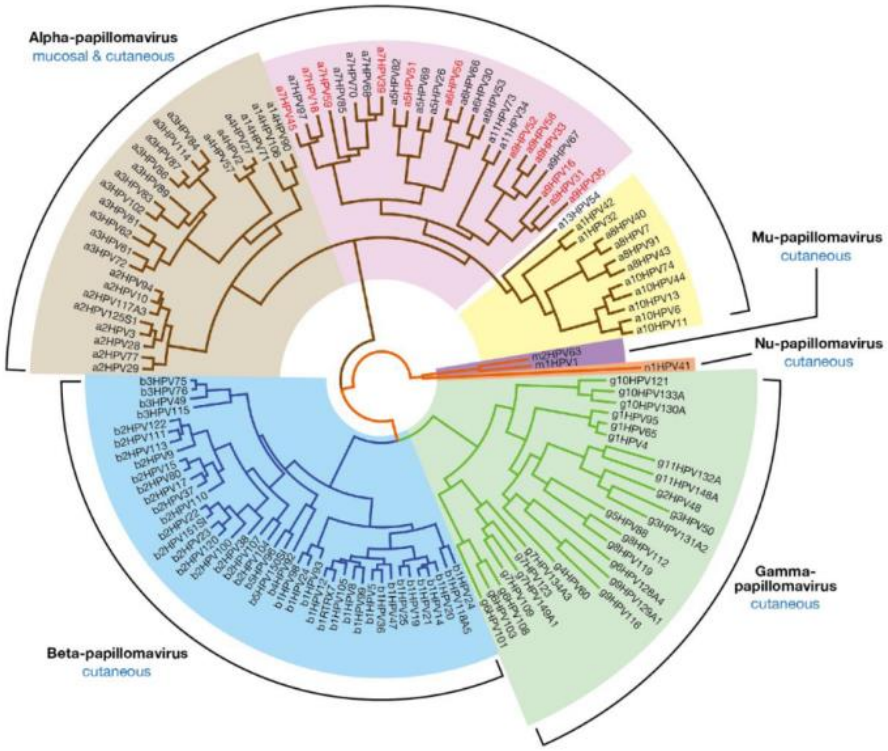

Figure 4. Phylogenetic tree of HPV

The phylogenetic tree was generated by sequence comparison of E1, E2, L1 and L2. The alpha-papillomavirus types are categorized according to their anatomical site preference and their association with cancer: low-risk cutaneous (light brown); low-risk mucosal (yellow); or high-risk (pink). Taken from (Egawa *et al.*, 2015).

In addition to cervical cancer, HPVs cause oropharyngeal and anogenital cancers in both sexes and penile cancer in men (Walboomers *et al.*, 1999; Moody and Laimins, 2010). In total, approximately 5 % of all cancer cases are caused by HPV (Plummer *et al.*, 2016). Worldwide, virtually 100 % of the annual 530.000 cervical cancer cases are the result of the

previous infection with a high-risk HPV (Walboomers *et al.*, 1999; Moody and Laimins, 2010). In 2012, 270.000 women died from cervical cancer (WHO, 2018), making cervical cancer the fourth most common cause of death from cancer in women (World Health Organization, 2014). The majority of cervical cancer cases is dependent on infection with only two of the high-risk HPV types, namely HPV16 (61 %) and HPV18 (10 %) (Serrano *et al.*, 2015). The contribution of these two high risk types to the number of HPV-induced head and neck cancers is even larger, since 85 % of all HPV-induced head and neck cancers are caused by HPV16 and HPV18 (de Martel *et al.*, 2017).

1.2.1 HPV infection, replication cycle and cancer induction

The HPV replication cycle starts with a HPV virion reaching the basement membrane of an epithelium (e.g. cervical epithelium) laid open by a microabrasion induced by local trauma (Figure 5) (Mirkovic *et al.*, 2015). Here, the capsid protein L1 binds to heparan sulfate proteoglycans, causing a conformational change in L2, which exposes its amino terminus to the extracellular protease furin. Furin cleaves L2, which can then bind to basal keratinocytes and thus induces the endosomal uptake of the virion by the target cell (Day *et al.*, 2010). While the L1 proteins are degraded, L2 together with the genome hitchhike on retromer processes to the nucleus (Day *et al.*, 2013; Lipovsky *et al.*, 2013). The HPV life cycle is absolutely dependent on cell cycle progression during the first instances of infection (Pyeon *et al.*, 2009). Only during mitosis the nuclear membrane integrity is partly compromised, which is used by the L2/genome complex to enter the nucleus, upon which transcription of the viral early 1 (E1) gene is initiated (Pyeon *et al.*, 2009). Expression of the viral proteins E1 and E2 drives a multiplication of the viral genome to approximately 50-100 episomal copies per cell (Day *et al.*, 2004). By making use of the high fidelity of the host's replication machinery, the virus achieves a low error rate resulting also in a smaller rate of evolution (Pastrana *et al.*, 2001).

In a healthy epithelium, cells divide only in the basal layers and differentiate during their migration to the top layer. HPV is dependent on this ordered differentiation of the epithelium in the generation of new virions but it is also dependent on cell cycle progression to replicate the viral genome (zur Hausen, 2002). The virus ensures continued cell cycling by expression of the three proteins E5, E6 and E7 (reviewed in (zur Hausen, 2002)). This progression enables the virus to switch to a high copy state (more than 1000 genome

copies/cell) (Roden and Stern, 2018). The three proteins drive the induction of S-phase by manipulating cellular processes, such as e.g. E5 triggering epidermal growth factor receptor (EGFR) signaling (Fehrmann, Klumpp and Laimins, 2003; Genther *et al.*, 2003).

The main function of E6 is to induce degradation of the cell cycle arrest protein p53. This is achieved by binding the E3-ligase E6-AP which in turn leads to increased ubiquitination of p53 and subsequent proteasomal p53 degradation (Werness, Levine and Howley, 1990). Thus, cell cycle arrest due to the accumulation of p53 is prevented. Furthermore, E6 decreases telomere shortening in the host cell's genome by the induction of telomerase expression, thus hampering cell cycle arrest due to shortened telomeres (Klingelhutz, Foster and McDougall, 1996; Galloway *et al.*, 2005). E7 binds to the retinoblastoma protein (pRb), targeting it for degradation and thus activates the transcription factor E2F1 (Dyson *et al.*, 1989). Importantly, this process also leads to the strong upregulation of $p16^{INK4A}$ (Kiyono *et al.*, 1998). Due to this strong upregulation, $p16^{INK4A}$ is used as a surrogate marker for HPV infection (Klaes *et al.*, 2001). Finally, in the terminally differentiated cells of the uppermost epithelial layers, the capsid proteins L1 and L2 are expressed (Doorbar *et al.*, 2015). The virions are assembled from capsomeres consisting of L1 (80 %) and L2 (20 %) (Modis, Trus and Harrison, 2002) and the viral genome is packaged. Several studies suggest that the E4 protein facilitates virion release but this has not been formally proven (reviewed in (Doorbar, 2013)). However, it has been shown that virion production does not lead to cell lysis but that the virions are released by physiological shedding of epithelial squamae.

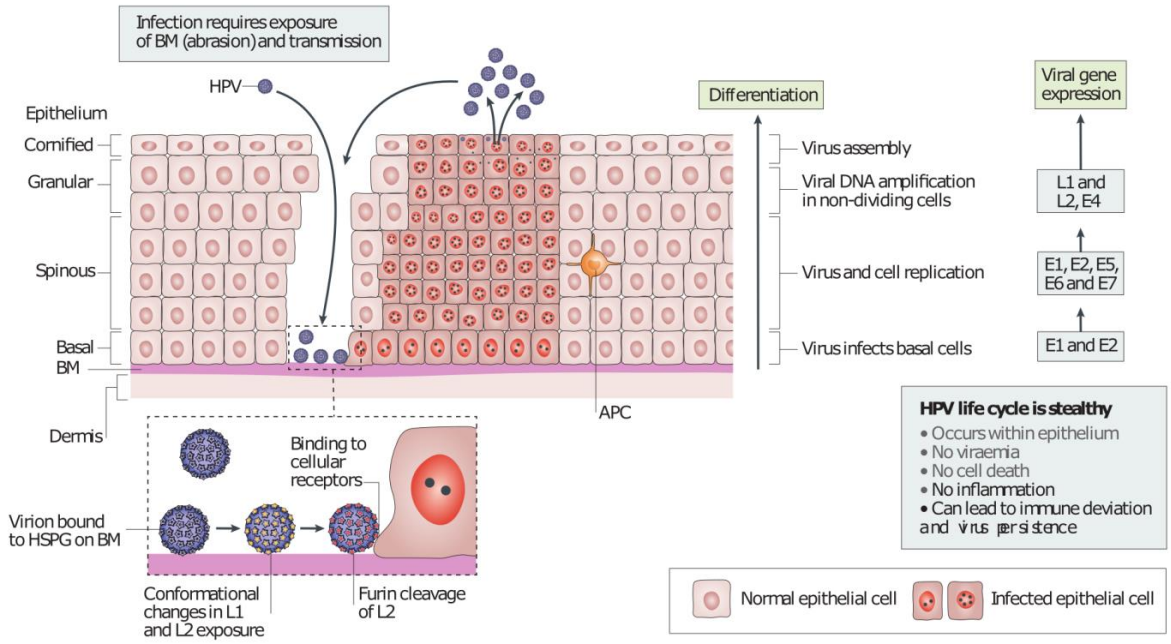

Figure 5. HPV replication cycle

The replication cycle of HPV starts when a HPV virion attaches to the basement membrane which is exposed by a microabrasion. After conformational changes induced by the binding to the basement membrane and protease cleavage, basal epithelial cells take up the virion. In this early stage of the infection, the virus uses the cellular replication machinery to establish 50-100 viral genome copies in the basal cells, controlled by E1 and E2. In suprabasal layers, the expression of the viral proteins E5, E6 and E7 keeps the cells in the cell cycle, allowing continuous viral gene replication. The virus-infected epithelial cells migrate towards the outer layers of the epithelium and along the way they differentiate into cornified keratinocytes. Here, the viral proteins L1 and L2 are expressed, assemble with the viral genomes and form new virions. The virion release, which is likely facilitated by E4-dependent effects, occurs during the physiological process of shedding the outermost layer of the epithelium. Taken from (Roden and Stern, 2018).

Infection with high-risk HPV and the resulting expression of viral proteins has many effects on the host cell that can lead to cancer (Figure 6). Apart from the uncontrolled cell replication induced by the combined effects of E6 and E7, an especially important event in the process of carcinogenesis is the integration of the viral DNA into the host cell's genome. This event often leads to the disruption of the E2 gene, which is a repressor of E6/E7 expression, and results in high levels of E6/E7 (zur Hausen, 2002; Isaacson Wechsler *et al.*, 2012; McBride and Warburton, 2017). This leads to an increase in genetic errors since both E6 and E7 disturb cellular processes that normally prevent mutations and genetic abnormalities (Isaacson Wechsler *et al.*, 2012). These processes do not immediately lead to cancer but first to dysplasia of increasing severity. In general, carcinogenesis occurs as an undesired byproduct

of the viral replication cycle, resulting from the viral protein effects as well as from the ensuing genomic instability. The induction of cancer offers no evolutionary benefit for the virus since it does not improve but actually diminishes virus production.

In the cervical area, which is highly susceptible to HPV infection, dysplasias are graded from CIN-I to CIN-III (cervical intraepithelial neoplasia). Dysplasias can resolve spontaneously but high grade dysplasias have a higher risk to develop into cancer than low grade dysplasias (McCredie *et al.*, 2008; Roden and Stern, 2018). For example, while 50 % of CIN-III develop into cancer, the development of CIN-I into malignant disease is much lower (McCredie *et al.*, 2008). Large screening programs, using the cytological Papanicolaou-tests (Pap-tests) and HPV DNA tests that allow the detection of abnormal and HPV-positive cells, are undertaken in the developed world to find CIN patients. If a CIN lesion is discovered, it is monitored and in - case of progression - surgical intervention is performed.

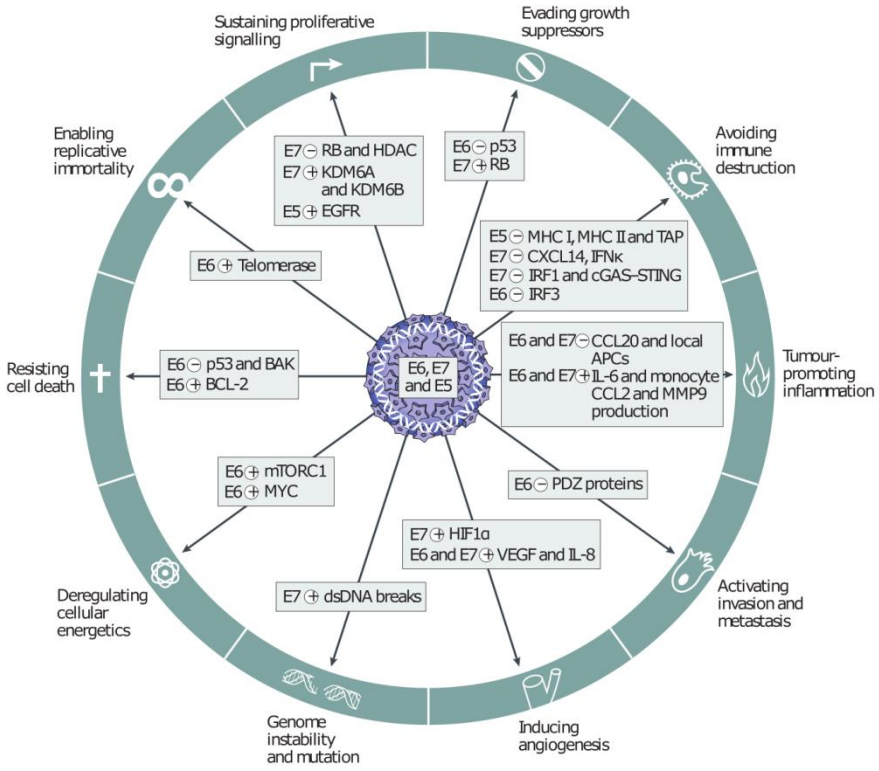

Figure 6. High-risk HPV E6/E7 induce hallmarks of cancer

After the integration of the viral genome, E2-mediated repression of E6/E7 expression is often abrogated. These two oncogenic proteins influence a variety of cellular processes, thus leading to carcinogenesis. One of the carcinogenic actions of the E6 protein is the induction of telomerase, leading to immortalization of the host cells. Furthermore, E6 prevents the p53-mediated stop of cell cycle progression, which stops the cell's ability to respond adequately to genomic damage. Therefore, mutations accumulate, further reducing physiological cellular behavior. One of the main carcinogenic functions of E7 is the binding to pRB, which induces unrestricted cell cycle progression, another hallmark of cancer. Taken from (Roden and Stern, 2018).

Usually, (in more than 90 % of the cases (Plummer *et al.*, 2007)) the HPV infection is cleared by the combined action of the innate and adaptive immune system (Trimble *et al.*, 2010) within less than 2 years (Rosa *et al.*, 2008; Bosch *et al.*, 2013). Virus clearance is achieved by T cells that recognize E2-, E6- and E7-derived epitopes and kill infected cells (de Jong *et al.*, 2004). The importance of the immune system in resolving HPV infections is also underlined by the finding that immunocompromised individuals (e.g. organ transplant recipients or HIV-infected patients) have a higher likelihood to develop HPV-induced cancers than fully immunocompetent people (Denny *et al.*, 2012; Wieland, Kreuter and Pfister, 2014).

On the other hand, HPVs employ several strategies in their replication cycle to evade detection by the immune system. First, HPVs do not infect cells below the basement membrane where immune cells are more abundant (Grabowska and Riemer, 2012). Additionally, HPV protein expression drives skin-resident DCs, Langerhans cells, out of the infected areas and thus impairs their sentinel function (Laurson *et al.*, 2010; Jemon *et al.*, 2016). After infection, the expression of the non-secreted viral proteins is kept at low levels which makes the detection of infected cells by T cells difficult since only few copies of immunogenic epitopes can be presented on MHC by infected cells (Crum *et al.*, 1986; Stoler *et al.*, 1992; Kanodia, Fahey and Kast, 2007). Even potentiating this effect is the fact that HPVs alter the antigen processing machinery, for example by the overexpression of the aminopeptidase ERAP I, thus leading to the destruction of HPV epitopes (Steinbach *et al.*, 2017). Furthermore, HPVs do not induce viremia, which would expose virions to a systemic immune response (Doorbar, 2005). In the last stage of the replication cycle, HPVs do not induce cell death to release newly assembled virions, but rely on the physiological shedding of terminally differentiated keratinocytes, which also does not give rise to an immune response (Stanley, 2012).

1.2.2 Prophylactic HPV vaccination

After the connection between HPV infection and cervical cancer formation had been established (Dürst *et al.*, 1983; Boshart *et al.*, 1984; Muñoz *et al.*, 1992), efforts were undertaken to develop a vaccine preventing the infection with high-risk HPV types. Vaccine development was made possible by the finding that recombinantly produced L1 protein can assemble into virus-like particles (VLPs), which, when injected, induce strong neutralizing AB responses (Deschuyteneer *et al.*, 2010). Two vaccines were brought to the market: Cervarix in 2007, which contains VLPs of HPV 16 and HPV 18 adjuvanted with aluminum hydroxide and MPLA, and Gardasil in 2006, which contains VLPs of HPV-6, HPV-11, HPV-16 and HPV-18 adjuvanted with aluminum hydroxyphosphate sulfate (AHSS) (Einstein *et al.*, 2014). VLPs of the two low-risk HPV types HPV-6 and HPV-11 were included in the Gardasil vaccine since they are the HPV types causing more than 90 % of genital warts (Roden and Stern, 2018). Both vaccines were shown to be very effective in preventing CIN-III lesions (Arbyn *et al.*, 2018). In general, the VLPs induce type-specific immunity but a cross-protection effect could be observed with the stronger adjuvanted Cervarix vaccine (Lehtinen *et al.*, 2012; Kuhs *et*

al., 2014). After vaccination, vaccinated individuals were protected against 93 % of all CIN-III lesions although only 52 % of CIN-III lesions are caused by HPV-16 and HPV-18. Both vaccines induce higher titers of neutralizing ABs than a natural infection (Einstein *et al.*, 2014). This is necessary to induce sterilizing immunity since the anti-L1/L2 ABs cannot alter the process of infection after virion uptake by the host cells anymore. Thus, to prevent infection, it is necessary to scavenge all virions before they reach host cells.

Another formulation of Gardasil (Gardasil 9) is now available, which covers HPV-6, HPV-11 and the seven most prevalent high-risk HPV types (Joura *et al.*, 2015), thus also preventing >90 % of cervical cancers. More vaccines are currently being developed, with one of the major development goals being the decrease of vaccine cost. Additional goals are to increase the number of virus types covered by the vaccine and to develop a vaccine that has prophylactic as well as therapeutic effects by inducing AB responses and cellular responses (reviewed in (Schiller and Müller, 2015)).

Prophylactic HPV vaccination is now recommended in several countries for girls and in some countries for girls and boys. However, vaccination rates are still low when compared to the rate of infected people, since it is estimated that almost every sexually-active individual will contract a high-risk HPV type at least once in their lifetime (Woodman, Collins and Young, 2007). In the USA, 49.5 % of 13-17 year old girls (boys: 37.5 %) received at least two injections of the vaccine (Walker *et al.*, 2017). In Germany, 44.6 % of 17-year old females received at least two injections (Robert Koch Institut, 2018a). A vaccination recommendation for boys has been issued in Germany only in June 2018 (Robert Koch Institut, 2018b), therefore the vaccination coverage in boys currently is assumed to be negligible. Worldwide, overall vaccination coverage is still very low, especially in low-middle income countries. In developed regions, 33.6 % of females 10-20 years of age received the recommended number of vaccinations, in contrast, the same holds true only for 2.7 % of females of the same age range in less developed countries (Bruni *et al.*, 2016). Epidemiologically, this is of particular importance, since in less developed countries no effective screening programs for precancerous lesions are in place, which leads to the fact that the vast majority of HPV-attributable cancer cases (86 %) are observed in these countries (Formana *et al.*, 2012; Bruni *et al.*, 2016; Plummer *et al.*, 2016; de Martel *et al.*, 2017). Importantly, not only vaccinated people benefit from high vaccination coverage, but also non-vaccinated individuals are

protected from HPV infection by the effect of herd immunity. In Australia, a reduction of HPV lesions could be observed also in heterosexual men after the implementation of large-scale vaccination programs targeting women (Chow *et al.*, 2017).

1.2.3 Therapeutic HPV vaccination

Vaccination against cancer or cancer precursor lesions represents an attractive treatment option due to long term immune surveillance and low side effects compared to conventional cancer treatments like surgery, chemotherapy and radiation therapy (Gulley, 2013). Side effects of conventional treatments of HPV-induced cancers range from lesion site-specific problems, such as premature deliveries after surgery to treat cervical HPV lesions (Albrechtsen *et al.*, 2008), significant loss of quality of life after surgery for oral (Rathod *et al.*, 2015) or anal lesions to the general side effects of chemotherapy as cancer treatment. Prevention of HPV infection by prophylactic vaccination against HPV will likely be a major contributor in reducing the number of new cases. However, since vaccination coverage to date is still low in most countries (Bruni *et al.*, 2016) and the latency period from HPV infection to development of lesions is long (McCredie *et al.*, 2008), only a small portion of HPV-induced cancers will be prevented by the prophylactic vaccinations performed so far. 530.000 cases of cervical cancer alone occur every year and since the current worldwide vaccination coverage is only 1.4 %, this number is not expected to decrease drastically in the next decades (Bruni *et al.*, 2016). This bad prognosis despite effective prophylactic vaccines is based on the fact that the prophylactic vaccines targeting capsid proteins are not effective against established infections (Hildesheim *et al.*, 2007, 2016). Cellular immune responses against the L1 protein can be detected (Steele *et al.*, 2002) but this protein is not expressed in the cells close to the basement membrane since only early genes are expressed in these layers (Stern *et al.*, 2012; van der Burg *et al.*, 2016).

Among all therapeutic anti-cancer vaccinations, HPV-induced malignancies represent an ideal target for two reasons (Cheever *et al.*, 2009; Chabeda *et al.*, 2018). First, the two oncoproteins E6 and E7 are obligatory for the malignant phenotype. Thus, immune escape by abrogating expression of these proteins is not an option for the cancer cell. Second, since E6 and E7 are viral proteins, they are not subject to central immune tolerance, and high-affinity cytotoxic T cells should therefore be present. Despite these positive characteristics,

therapeutic vaccination against HPV infections has proven to be challenging due to the viral immune evasion mechanisms.

There has been a plethora of tested immunotherapy approaches including vaccinations with recombinantly produced protein, subunit vaccines (minimal epitopes, synthetic long peptides (SLP)), virus-based and bacteria-based vaccines as well as nucleic acid-based (DNA and RNA) and cell-based (DC-based and adoptive T cell transfer) approaches (reviewed in (Khallouf, Grabowska and Riemer, 2014; Vici *et al.*, 2016; Yang *et al.*, 2016; Kim and Kim, 2017; Chabeda *et al.*, 2018; Hancock, Hellner and Dorrell, 2018)). Most therapeutic HPV vaccination approaches focus on HPV16 E6 and E7, since the other early proteins are not expressed in cancer or are not necessary for tumor cell malignancy (Stern *et al.*, 2012; van der Burg *et al.*, 2016).

Despite the multitude of favorable preclinical data, results from clinical trials have not met the high expectations of researchers. No therapeutic anti-HPV vaccines against either HPV infections or HPV-induced cancers have been approved by regulatory agencies so far (Chabeda *et al.*, 2018). One of the most successful studies to date was a randomized, double blind, placebo-controlled phase IIb trial using the DNA vaccine VGX-3100, which induced histopathological regression in 49.6 % of CIN-II/-III patients (30.6 % in the placebo group) (Trimble *et al.*, 2015). A study with the subunit vaccine ISA101 (E6/E7 SLPs emulsified in ISA51) led to complete response 12 months after treatment in 47 % of high-grade vulvar intraepithelial (VIN) neoplasia patients (Kenter *et al.*, 2009). Importantly, spontaneous regression in this disease stage occurs in only 1.5 % of the cases within 10 months after diagnosis. However, the positive results of this study in VIN patients could not be reproduced - neither in patients with advanced or recurrent HPV16-induced gynecological carcinoma (van Poelgeest *et al.*, 2013), nor in patients with high-grade CIN (de Vos van Steenwijk *et al.*, 2012) nor with low-grade pre-malignant disorders of the cervix (de Vos van Steenwijk *et al.*, 2014). Interestingly, in all studies HPV16-specific T cell responses could be detected but apparently did not lead to clinical benefits.

SLPs are peptides with a length of 15-36 amino acids and belong to the class of subunit vaccines, which is why they require additional immune stimulation by adjuvants like IFA. The advantage of SLP vaccines is, next to safety and ease of production, that mixtures of SLPs can

be administered that contain epitopes for all MHC types. A disadvantage connected to SLPs is that they do not focus the immune response on specific epitopes. Focusing the immune response induced by a therapeutic anti-HPV vaccine could be highly beneficial since due to the immune evasion mechanisms employed by HPVs (such as e.g. ERAP I-mediated destruction of HPV epitopes (Steinbach *et al.*, 2017) or other effects on the antigen processing machinery), not all possible HPV epitopes are indeed presented on the surface of infected or transformed cells. Therefore, inducing immune responses with SLPs against epitopes that are not presented on infected cells or tumor cells would lead to unproductive immune responses, since these T cells could not recognize their targets. This disadvantage also holds true for all other vaccination approaches that do not use defined epitopes. This problem could be overcome by using synthetic short peptides (SSP), which have a length of 8-11 amino acids. The SSPs included into a vaccine have to be matched to the patient's HLA-type to make sure that the vaccine contains epitopes binding to the patient's MHC class I molecules. Developing vaccines suitable for MHC class I alleles with a high frequency in the human population, such as HLA-A*0201, allows a broader applicability of these vaccines. However, HLA types can be grouped into supertypes, which have similar peptide binding characteristics (Sidney *et al.*, 2008). By combining SSPs to a vaccine that contains peptides binding to the 5 major supertypes, a population coverage of >95 % could be achieved. Another requirement for successful application of this technology is that the HPV E6/E7 epitopes presented by tumor cells have to be known for the MHC alleles with the highest frequency in the population. A first indication of which peptides are presented on tumor cells can be derived from analyzing the E6/E7 protein sequences with algorithms that predict the potential affinity of peptides contained in the analyzed sequences to a given HLA type. However, these algorithms do not take into account altered epitope-processing patterns induced by the expression of HPV proteins. Ever more sensitive technology has allowed to directly verify the MHC-mediated presentation of epitopes on the cell surface with mass spectrometry (MS) (Di Marco, Peper and Rammensee, 2017). The detection of HPV epitopes on cells of HPV-induced cancers is particularly challenging since these epitopes are presented at low abundance on the cell surface (Kanodia, Fahey and Kast, 2007). Nevertheless, two studies report the detection of HPV epitopes on cell lines of cervical cancer by mass spectrometry (Riemer *et al.*, 2010; Blatnik *et al.*, 2018).

Another challenge for developing effective therapeutic HPV vaccines is the mucosal location of many HPV-induced tumors, since the mucosae are continuously in contact with the exterior and therefore have a more tolerogenic milieu. Additionally, only T cells carrying a certain molecular signature migrate into these specific tissues. Therefore, systemically-induced T cells do not readily migrate into mucosal areas (reviewed in (Nardelli-Haefliger, Dudda and Romero, 2013)). Therefore, efforts have been undertaken to specifically target virus-specific T cells to the mucosal tumor site e.g. via induction of mucosal T cells (Sun *et al.*, 2015) or via prime-pull approaches (Domingos-Pereira *et al.*, 2013; Soong *et al.*, 2014; Tan *et al.*, 2017). For example, oral vaccination targeting HPV E7 was shown to elicit E7-specific mucosal immunity in the cervix of CIN-III patients (Kawana *et al.*, 2014).

In summary, HPV infection and the resulting malignancies represent a major global health burden. Improvement of prophylactic vaccination coverage and the development of better treatment alternatives, of which a therapeutic vaccine is the most attractive option, are expected to decrease the prevalence of HPV-induced morbidity and mortality in the near future.

1.3 Mouse models used in HPV research and HPV16 E6/E7-positive tumor models

Mice are by far the most commonly used mammals in medical research, since 99 % of their genes have counterparts in humans (Gunter, 2002), they can be bred as inbred lines, can be genetically altered and can be kept in a cost-effective way (The Jackson Laboratory, 2018b). Additionally, mice have a much shorter life span than many other mammals, thus allowing life cycle studies and tumor experiments in a shorter time frame (The Jackson Laboratory, 2018b). These characteristics also make mouse models indispensable tools for HPV research and in particular for research for anti-HPV immunotherapies.

1.3.1 Wildtype mice

Mice have been kept as inbred lines since the beginning of the 20th century and many different lines have been established, among these the lines C57BL/6 and C3H. Wildtype mice express murine MHC class I and MHC class II molecules. The genes encoding for murine MHC molecules are called H-2, with the MHC class I subclasses H-2K, H-2D and H-2L. The

subclasses of MHC class II molecules are H-2A and H-2E, which are also called IA and IE (from immune response (Ir)) (Murphy *et al.*, 2016) (Figure 7).

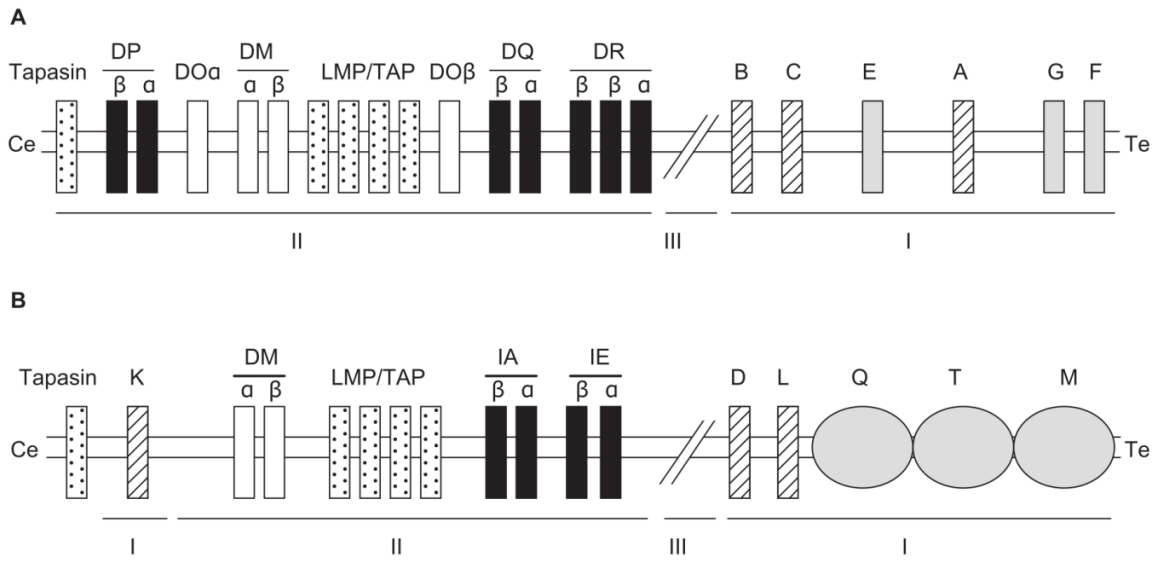

Figure 7. Human (A) and murine (B) MHC locus

A & B, The direct comparison of the human and murine MHC locus reveals the shared features. H-2K, H-2D and H-2L are MHC class I subclasses (B, striped boxes), their equivalents in the human genome are HLA-A, HLA-B and HLA-C (A). Spotted boxes represent genes involved in antigen processing for the MHC class I pathway. Genes for MHC class II molecules (IA and IE in mice; DP, DQ and DR in humans) are presented as black boxes and the respective antigen processing for MHC class II is done by genes depicted as white boxes. Gray ovals (B) represent three genes in the mouse MHC locus coding for non-classical MHC class I heavy chains. Figure adapted from (Pascolo 2005).

1.3.1.1 C57BL/6

Of the many mouse strains used in medical research, the C57BL/6 strain is the most common one. This strain and the various congenic substrains are used in all fields of medical and biological research, among them cardiovascular, diabetes, obesity and immunological research (The Jackson Laboratory, 2018a).

Since the H-2L gene is deleted in C57BL/6 mice (Pascolo 2005), these mice only express H-2K and H-2D as MHC class I molecules on the cell surface of their nucleated cells. In addition, the MHC class II protein IA is expressed on professional APCs. Complete IE molecules cannot be detected on the cell surface since the IEα gene is a pseudogene in C57BL/6 mice (Pajot, Michel, *et al.*, 2004). Like all other inbred strains, C57BL/6 only express one allele of each

expressed subclass. This characteristic is called the haplotype. The haplotype of C57BL/6 is b. Therefore, the MHCs are named as the gene (H-2K) with the haplotype in superscript (e.g. H-2K^b). The MHC expression of a C57BL/6 APC is depicted in Figure 8.

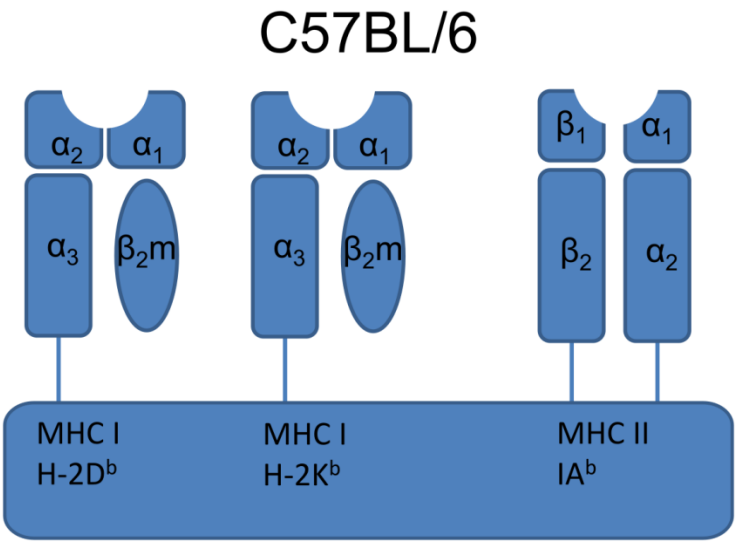

Figure 8. C57BL/6: Expression of MHC class I and class II

C57BL/6 mice express the two MHC class I subclasses H-2D and H-2K, both in the b haplotype. Furthermore, these mice express the MHC class II molecule IA^b. Many other mouse strains additionally express the MHC class II molecule IE but since the IEα gene is a pseudogene in C57BL/6, no IE molecules can be found on the cells of the C57BL/6 strain.

To be able to study anti-tumor responses directed against HPV16 E6/E7 epitopes in C57BL/6 mice, TC-1 tumor cells were generated by transducing C57BL/6 lung cells with a constitutively activated version of h-ras and with HPV16 E6 and E7 (Lin *et al.*, 1996). Most anti-HPV16 immunotherapy studies so far have been conducted with this model. Another HPV16 E6/E7-positive tumor model derived from C57BL/6 mice is the C3 cell line that was generated from embryonic cells by transfection with h-ras (EJ-ras) and HPV16 E6/E7 (Feltkamp *et al.*, 1993). Finally, the EL4 E7 cell line (Tindle *et al.*, 1995; Fernando *et al.*, 1998) is a H-2^b-positive thymoma cell line that was transfected with HPV16 E7. Initially, all of the transplantable tumor models mentioned above were used as subcutaneous or as pulmonary metastases models (Ji *et al.*, 1998) but in the last years, especially the TC-1 model was also used in orthotopic settings (Decrausaz *et al.*, 2011; Sandoval *et al.*, 2013). This means that the tumor cells are implanted at the sites HPV-related tumors naturally occur, in these cases

the oropharyngeal area (Sandoval *et al.*, 2013) and the female vaginal area (Decrausaz *et al.*, 2011). The orthotopic localization offers the advantage that the immune response in these areas against HPV-related cancers can be studied in a setting that more closely resembles the natural situation. This is necessary since the immune environment in mucosal areas such as the genital tract has special properties regarding immune responses (Mestecky, Moldoveanu and Russell, 2005). T cells that have been primed in non-mucosal regions often do not readily migrate into mucosal areas since T cells need special homing signals to do so (also see 1.2.3). To be able to monitor the tumor growth of these orthotopic models it is necessary to engineer the tumor cells to express markers such as luciferase so that the tumor size can be inferred from the intensity of light radiating from the tumor cells after injection of luciferin.

Transplantable tumor models like TC-1 or C3 offer many advantages such as fast availability, reliable tumor induction and relatively fast tumor growth (depending on the injected cell number). However, some characteristics of tumors that are important for studies of immunotherapeutic approaches, such as gradual induction of an immunosuppressive tumor microenvironment, are lost with transplantable models. Furthermore, the injection of cells always induces tissue destruction and thus also some inflammation at the injection site. All these characteristics reduce the translatability of results generated in a transplantable tumor model to the clinical setting in which a tumor gradually developed from healthy cells, which are always in contact and in communication with the cells and especially immune cells surrounding them.

In addition to transplantable HPV tumor models, there are also transgenic HPV mouse models available (reviewed in (Santos *et al.*, 2017)) such as the K14E6 and K14E7 strains (Brake *et al.*, 2003). The process of carcinogenesis in these models very closely resembles the one observed after natural infection. Therefore, it is believed, that these models can more closely mimic the clinical situation. However, the slow process of carcinogenesis offers experimental hurdles that make these models less attractive than transplantable models. Although some of the models express HPV oncogenes in relevant sites, the expression of the oncogenes is widespread, thus inducing immune tolerance, rendering these models not useful for the testing of immunotherapeutic interventions (Trimble and Frazer, 2009).

All of the above-mentioned transplantable tumor models have in common that the cells express the HPV16 oncogene E7 on a H-2D^b background. Therefore, all the tumor models present the immunodominant E7-derived H-2D^b-restricted epitope E7/49-57 (RAHYNIVTF). This epitope has an outstanding role in immunotherapeutic interventions since it has been shown that apart from being very immunogenic, it is immunodominant in the H-2D^b background. It has been observed that high frequencies of CD8$^+$ T cells specific for this epitope can be induced by various vaccination approaches and that TC-1 tumors can be effectively killed by these vaccination-induced T cells (Berraondo *et al.*, 2007; Cho *et al.*, 2013; Liu *et al.*, 2014; Kranz *et al.*, 2016). E7/49-57 is the only H-2D^b-restricted epitope derived from E7 and there seem to be no E6-derived H-2D^b-restricted epitopes (Peng *et al.*, 2004). However, since C57BL/6 mice also express H-2K^b, T cells of these mice can also respond to the H-2K^b-restricted HPV16 E6 epitope, E6/50-57 (YDFAFRDL) (Peng *et al.*, 2004).

1.3.1.2 C3H

The C3H mouse strain, which expresses H-2K^k, H-2D^k, IA^k and IE^k (Charles River, 2018), was the first mouse strain in which a orthotopic model for HPV16-associated head and neck cancers was generated. The cell line AT-84 was isolated from a naturally-occurring oral squamous cell carcinoma and then transfected with HPV16 E7 and luciferase to generate AT-84 E7 (Paolini *et al.*, 2013).

1.3.2 MHC-humanized mice

MHC-humanized mice are mice that carry one or several genetic modifications that result in an immune system that partly resembles the human immune system. This can be achieved by the expression of one or several human MHC molecules and this strategy is, in newer models, also expanded by knocking out the respective murine genes. The transgenes used are most often MHC alleles (e.g. HLA-A*0201) with a high frequency in the human population to allow generation of results relevant for a maximal number of people. Therefore, these mice are attractive tools to study immune responses specific for the human immune system *in vivo* (Pascolo 2005). MHC-humanized mice are used as animal models for diseases like arthritis (Kuon *et al.*, 1997, 2004; Kollnberger *et al.*, 2004), for the identification of epitopes from viruses (Drexler *et al.*, 2003; Gallez-Hawkins *et al.*, 2003) and malignant cells (Theobald *et al.*, 1997; Berard *et al.*, 2000; Carmon *et al.*, 2000), but the most important utilization of

HLA-transgenic mice is the evaluation of vaccination approaches using human epitopes (Pascolo, 2005).

In general, three generations of MHC class I-humanized mice are distinguished (reviewed in (Pascolo, 2005)). The mice of the first generation were transgenic for fully human MHC class I molecules. In these mouse models, there was only little evidence of murine T cells recognizing epitopes on HLA class I. After the discovery that the α3 domain of the human MHC class I heavy chain is not well recognized by murine CD8 co-receptor molecules (Irwin, Heath and Sherman, 1989), the chimeric HHM molecule (α1 human, α2 human, α3 murine, see Figure 9) was developed, with epitope-binding regions from different HLA-types (Kalinke, Arnold and Hämmerling, 1990; Vitiello *et al.*, 1991; Alexander *et al.*, 1997; Borenstein *et al.*, 2000). Mice of this second generation were able to successfully mount immune responses against epitopes presented on these modified HLA molecules. However, it was shown that there is a preferential induction of immune responses against murine epitopes (Firat *et al.*, 1999; Ureta-Vidal *et al.*, 1999; Pajot, Pancré, *et al.*, 2004) if the murine MHCs are still present. To overcome this problem, the third generation of HLA class I transgenic mice was developed. In these mice, immune responses are necessarily restricted by HLA class I since murine H-2 molecules are absent. The first attempts to generate mice without H-2 expression focused on the knockout of β2m since most MHC class I molecules are only stable on the cell surface when they are in a complex with β2m and a peptide with affinity for the respective MHC binding groove (Williams *et al.*, 1989; Murphy *et al.*, 2016). Thus, the knockout of β2m led to the virtual absence of H-2K and H-2D on these cells (Koller *et al.*, 1990; Zijlstra *et al.*, 1990). However, some researchers found that despite the lack of murine β2m, residual amounts of H-2D^{b} could be detected on the cell surface (Allen *et al.*, 1986; Bix and Raulet, 1992). After a knockout of the H-2D^{b} gene, no protein could be detected on the cell surface (Pascolo, 2005). The H-2D$^{b-/-}$ β2m$^{-/-}$ mice were crossed with mice expressing the HHD molecule, giving rise to the HHD mouse strain (Pascolo *et al.*, 1997). The HHD molecule is an HHM molecule with the α1 and α2 domain from HLA-A*0201 and the α3 from H-2D^{b}, hence its name (α1 **h**uman, α2 **h**uman, α3 H-2**D**^{b}) (Pajot, Michel, *et al.*, 2004). To allow surface expression of this chimeric MHC class I molecule in the absence of endogenous murine β2m, Pascolo *et al.* made use of the results of Mage *et al.* (Mage *et al.*, 1992) who had shown that a single chain MHC class I molecule containing the β2m represented a

functional MHC molecule. Therefore, the HHD molecule contains β2m that is covalently bound to the α1 domain of the MHC class I heavy chain via a 15 amino acid-long linker thus allowing the surface presentation of this chimeric HLA class I molecule independently of the endogenous murine β2m. The covalent linkage holds special importance since it prevents re-expression of endogenous H-2 molecules.

In recent days, Harada *et al.* generated further strains of 3rd generation HLA class I transgenic mice by introducing different chimeric monochain HLA molecules into the endogenous murine β2m locus. Reportedly, this led to HLA monochain expression concomitant with the disruption of the β2m gene resulting in abrogated surface expression of H-2D^b and H-2K^b. This strategy abolishes the need for time-consuming cross-breeding with H-2D^b and β2m KO mice and was used to generate four single knock-in (HLA-A*0201, HLA-A*0301, HLA-A*2402,and HLA-A*3101) and one double knock-in mouse strain (HLA-A*2402/HLA-A*0301) (Harada *et al.*, 2017).

1.3.2.1 AAD mice

AAD mice were bred on the C57BL/6 background and belong to the 2nd generation of humanized mice since they express a chimeric MHC class I heavy chain consisting of α1 and α2 (epitope binding regions) of HLA-A*0201 and the α3 domain of H-2D^d (Newberg *et al.*, 1996) (see Figure 9). The difference between these mice and 3rd generation transgenic mice is that AAD mice express the full set of H-2 molecules (class I and class II). Therefore, AAD mice can also mount immune responses against epitopes restricted by H-2D^b, H-2K^b and IA^b.

Two different HPV16 tumor models have been developed for AAD mice: TC-1/A2 cells (Peng *et al.*, 2006) and the HLF16 cell line (Eiben *et al.*, 2002; Daftarian *et al.*, 2007). TC-1/A2 cells are C57BL/6-derived TC-1 cells that were transduced with a vector encoding for a HHM (D^d) molecule (Newberg *et al.*, 1996; Peng *et al.*, 2006). In this MHC-humanized model, immune responses against the strongly immunogenic H-2D^b-restricted E7/49-57 epitope are preferentially induced (Peng *et al.*, 2006). Researchers tried to avoid this problem by excluding this epitope from their vaccine (Peng *et al.*, 2006) but it cannot be excluded that T cells against E7/49-57 or against E6-derived epitopes such as E6/50-57 are generated by antigen spreading.

In contrast, HLF16 cells were generated by transducing heart fibroblasts of AAD mice (Newberg *et al.*, 1996; Eiben *et al.*, 2002) with HPV16 E6/E7 (with E7 lacking the E7/49-57 epitope) and a constitutively activated version of h-ras to make the cells tumorigenic. The deletion of the immunodominant epitope was performed to make anti-tumor immune responses against this epitope impossible. Since the E6/E7 sequences do not contain any more H-2D^b-restricted epitopes, immune responses against HPV16 epitopes cannot be mediated by this MHC allele in this tumor model. However, H-2K^b-restricted anti-HPV16 immune responses (Peng *et al.*, 2004), cannot be excluded by this approach.

In addition, both models allow for H-2D^b and H-2K^b-restricted immune responses against neoepitopes. At least the parental TC-1 cell line was found to have mutations resulting in H-2D^b-restricted neoepitopes (Zottnick, 2017).

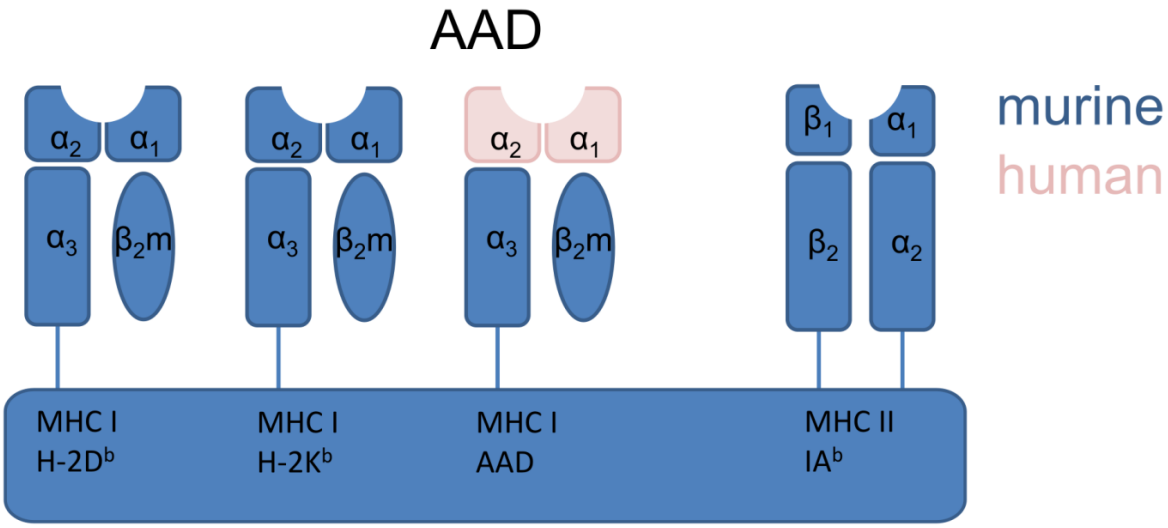

Figure 9. AAD: Expression of MHC class I and class II

AAD mice express all murine MHC molecules and, in addition, a HHM molecule (in this case called AAD) in which the epitope-binding regions are derived from the human HLA-A2 molecule. Therefore, immune responses in this mouse model can be restricted by murine MHCs and by HLA-A2.

1.3.2.2 A2.DR1 mice

A2.DR1 mice (Altmann *et al.*, 1995; Madsen *et al.*, 1999; Pajot, Michel, *et al.*, 2004) were also generated on the C57BL/6 background. These mice belong to a new class of humanized mice since they combine the advantages of 3rd generation HLA class I-humanized mice with the ones offered by MHC class II-humanized mice. A2.DR1 mice carry the transgene for the HHD molecule (antigen-binding domains of HLA-A*0201, α3-domain from H-2D^{b}, covalently bound β2m, cf. Figure 10) as a MHC class I molecule. In addition, these mice express one of the most common MHC class II molecules in the human population, HLA-DR1, which consists of HLA-DRA1*0101 and HLA-DRB1*0101 (Altmann *et al.*, 1995; Klitz *et al.*, 2003). In A2.DR1 mice, the gene coding for murine β2m was knocked out by the insertion of a neomycin resistance cassette and also the expression of H-2D^{b} was abrogated by a direct knockout. Furthermore, the whole MHC class II locus is also knocked out (Madsen *et al.*, 1999). Due to these sophisticated modifications, A2.DR1 mice only express MHC molecules that bind epitopes for two of the most common types of HLA class I and class II. Therefore, any immune responses are necessarily restricted by HLA-A2 or HLA-DR1.

Experimental evaluation demonstrated that indeed fully functional immune responses (AB responses, CD4^{+} T cells, CD8^{+} T cells) against the same epitopes as in humans could be induced in A2.DR1 mice upon vaccination with a DNA vaccine (Pajot, Michel, *et al.*, 2004).

Two versions of A2.DR1 mice are available. In the older of the two versions (named in this thesis "A2.DR1^{old}") the absence of the murine MHC class II molecules is achieved by inactivation of the IAβ^{b} gene. However, it could be shown that unconventional HLA-DRα/H-2IEβ^{b} hybrid molecules may form at least in the absence of HLA-DRβ (Lawrance *et al.*, 1989). In addition, in these mice only β2m but not H-2D^{b} is knocked out. Therefore, the newer version of A2.DR1 mice was generated (in this work referred to simply as "A2.DR1") in which the murine β2m, H-2D^{b} and the whole MHC class II locus are knocked out. If not specifically stated otherwise, all work in this thesis was performed with the new version of A2.DR1 mice (A2.DR1).

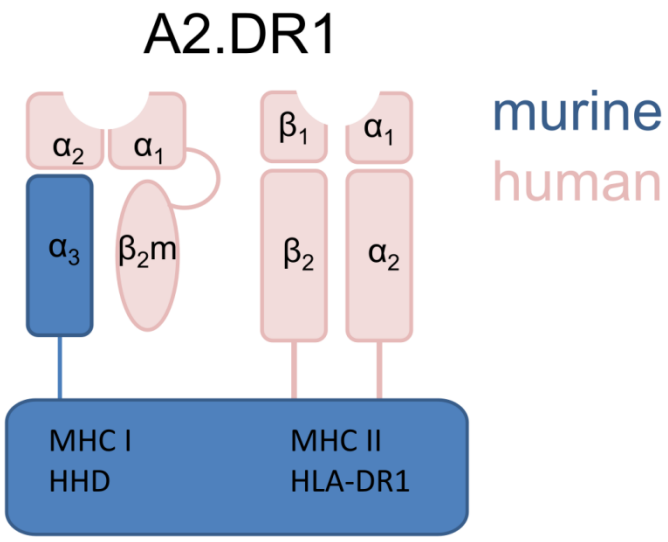

Figure 10. A2.DR1: Expression of MHC class I and class II

A2.DR1 mice express only two MHC molecules: The HHD molecule (MHC class I), which has the epitope-binding domains α1 and α2 of HLA-A*0201 and the α3 domain of the murine H-2D^{b}, covalently linked to human β2m. In addition, APCs express the fully human HLA-DR1 heterodimeric molecule (MHC class II). No murine MHC class I and MHC class II molecules are present on cells of these mice. Therefore, all immune responses are necessarily restricted by HLA-A2 and HLA-DR1.

To date, there are only two syngeneic tumor models published for this mouse model. One model is the 2277NS cell line, a chemically induced sarcoma derived from A2.DR1^{old} mice (Quandt, 2012). This cell line was transfected with a gene coding for an IDH1 mutation variant (Schumacher *et al.*, 2014) or a gene for a histone mutation variant (Ochs *et al.*, 2017), giving rise to two cell lines used for the validation of immunotherapeutic targets and immunotherapy approaches. The other cell line, SARC-L1, was generated by several *in vivo* passages of a naturally occurring sarcoma in A2.DR1^{old} mice (Rangan *et al.*, 2017).

However, to date, no HPV16 tumor model has been published that is suitable for A2.DR1 mice, which is a prerequisite for studying anti-tumor responses directed against HPV16 antigens in this advanced and sophisticated mouse model of human immune responses.

2 Aims of the study

The immunogenicity of human HPV16 E6/E7-derived, HLA-A2-binding epitopes can only be studied in genetically modified mice, such as the A2.DR1 mouse model. To improve translatability of our findings to the human setting, we chose this mouse model as a tool for the development of a therapeutic HPV16 vaccine.

2.1 Genotyping for A2.DR1 mice

A2.DR1 mice are a highly sophisticated mouse model since they underwent a multitude of genetic alterations to exhibit the HLA-$A2^+$/HLA-$DR1^+$, H-2^- phenotype. To guarantee the genetic identity of our A2.DR1 breeding colony, the implementation of reliable genotyping methods was the first aim of this work.

2.2 Generation of a HPV16 E6/E7-positive tumor model suitable for A2.DR1 mice

Prior to this study, no HPV16 tumor model was available that allows the exclusive investigation of HLA-restricted anti-tumor responses. Therefore, the second aim of this work was the development of such a HPV16 tumor model that is suitable for A2.DR1 mice. This tumor model should be established on the basis of the syngeneic 2277NS tumor cell line by transduction with the HPV16 proteins E6 and E7.

2.3 Epitope-specific vaccination against HPV16 E6/E7-positive tumors

Due to HPV16 immune evasion mechanisms, focusing the immune response on epitopes actually presented by $HPV16^+$ tumor cells is important to increase vaccine efficacy. Only some of the therapeutic vaccination approaches used so far allow the usage of selected epitopes. The third aim of this work was therefore to adapt the most promising vaccination approaches, which allow the use of defined epitopes, for the use with selected HPV16 epitopes and compare them for immunogenicity and anti-tumor effects in the A2.DR1 mouse model.

3 Materials and Methods

3.1 Materials

3.1.1 Mice

Strain	Specifications	Source
A2.DR1	Described in detail in 1.3.2.2. Mice were kept in individually ventilated cages in the mouse facility of the DKFZ	Initial breeding stock kindly provided by the Institut Pasteur (Paris, France)

3.1.2 Reagents

Name	Specifications	Manufacturer
Agarose NEEO		Roth, Karlsruhe
Ammonium chloride		Merck, Darmstadt
Carboxyfluorescein succinimidyl ester (CFSE)	#C1157	Thermo Fisher Scientific, Waltham, USA
$CD8^+$ isolation AB beads (untouched)	#130-104-075	Miltenyi Biotech, Bergisch Gladbach
CellTrace Far Red (FR)	#C34564	Thermo Fisher Scientific, Waltham, USA
Complete mini protease inhibitor cocktail	#11 836 153 001	Roche, Basel, Switzerland
CpG	ODN1826 TLR grade	Enzo Biochem, Farmingdale, USA
DMSO (dimethylsulfoxide)		Sigma-Aldrich, Taufkirchen
DNA ladder, 50 bp	#SM1133	Thermo Fisher Scientific, Waltham, USA
DNA-primers		Sigma-Aldrich, Taufkirchen

Name	Specifications	Manufacturer
DSPE-NHS	COATSOME® FE-8080SU5	NOF America Corporation, New York, USA
DSPE-PEG2000-maleimide	(1,2-distearoyl-3-sn-phosphatidylethanolamine)-PEG-maleimide	Laysan Bio Inc., Arab, USA
Ethanol		Sigma-Aldrich, Taufkirchen
Ethylenediaminetetraacetic acid (EDTA)		Roth, Karlsruhe
Formaldehyde	37 %	Avantor Performance Materials, Center Valley, USA
G418		Roth, Karlsruhe
GelRed		Biotium, Fremont, USA
Glycine		Sigma-Aldrich, Taufkirchen
Ionomycin	#10634	Sigma-Aldrich, Taufkirchen
ISA51	Montanide ISA51 VG	Seppic, Paris, France
Methanol		Sigma-Aldrich, Taufkirchen
OneComp eBeads	#01-1111-42	Thermo Fisher Scientific Ltd., Loughborgh, UK
XS15	Synthetic variant of Pam3Cys	Kindly supplied by Prof. Hans-Georg Rammensee, University of Tübingen
Phorbol myristate acetate (PMA)	#P8139	Sigma-Aldrich, Taufkirchen
Polyinosinic:polycytidylic acid (poly I:C)	High molecular weight poly I:C, #vac-pic, used as stock solution of 1 mg/ml	Thermo Fisher Scientific, Waltham, USA

Name	Specifications	Manufacturer
Potassium bicarbonate ($KHCO_3$)		Roth, Karlsruhe
RNA for vaccination	*In vitro* transcribed	Kindly supplied by BioNTech, Mainz
RNase-free water	#T143.3	Roth, Karlsruhe
RNase-free NaCl	5 M, #AM9760G	Thermo Fisher Scientific, Waltham, USA
Skim milk powder		Gerbu, Heidelberg
Sodium acetate		Roth, Karlsruhe
Sodium azide		AppliChem, Darmstadt
Sodium chloride		Sigma-Aldrich, Taufkirchen
Sodium dodecyl sulfate (SDS)	#13904	Gerbu, Heidelberg
Tris(hydroxymethyl)amino-methane (TRIS)		AppliChem, Darmstadt
Trypan blue	#T10282	Sigma-Aldrich, Taufkirchen
Tween20		Gerbu, Heidelberg
Zombie Aqua dead cell dye	used 1:200, #423101	Biolegend, San Diego, USA
β-mercaptoethanol	#11528926	Thermo Fisher Scientific, Waltham, USA

3.1.3 Solutions

Name	Composition/specification	Manufacturer
ACK buffer	155 mM NH_4Cl 10 mM $KHCO_3$ 0.1 mM EDTA pH 7.2 – 7.4	Self-produced
Blocking solution WB	5 % (w/v) milk powder 1 % bovine serum albumin (BSA)	Self-produced
Enhanced chemiluminescence (ECL) solution	#32209	Thermo Fisher Scientific, Waltham, USA
High sensitivity ECL solution	#RPN2232	GE Healthcare, Chalfont St Giles, UK
Laemmli buffer (4x sample buffer)	222 mM Tris (pH 6.8) 3.5 % (w/v) SDS 35 % (w/v) glycerol 0.016 % (w/v) bromophenol blue 10 % (v/v) β-mercaptoethanol	Self-produced
Lysis buffer	10 mM Tris-HCL (pH 7.5) 50 mM KCl 2 mM $MgCl_2$ 1 % (v/v) Triton X-100 14.3 % (v/v) of protease inhibitor cocktail (1 tablet in 750 µl H_2O)	Self-produced
MACS buffer	0.5 % BSA 2 mM EDTA in PBS	Self-produced

Name	Composition/specification	Manufacturer
Matrigel	#734-0270	BD, Franklin Lakes, USA
Flow cytometry fix buffer	1 % FCS 2.5 % Formaldehyde in PBS	Self-produced
Running buffer for SDS-PAGE	0.303 % (w/v) Tris 1.44 % (w/v) glycine 0.1 % SDS	Self-produced
Staining buffer	0.1 % BSA 0.1 % sodium azide in PBS	Self-produced
TAE buffer (50x)	24.2 % (w/v) Tris 2.05 % (w/v) $C_2H_3NaO_2$ 1.85 % (w/v) EDTA pH 7.8	Self-produced
Transfer (semidry blot) buffer	0.36 % (w/v) Tris 1.728 % (w/v) glycine 20 % (v/v) methanol	Self-produced
Water (double distilled)		Self-produced

3.1.4 Cell lines

Name	Specifications	Source
2277NS cell line	Chemically (MCA) induced sarcoma cell line derived from A2.DR1 mice (Schumacher *et al.*, 2014)	Kindly provided by Dr. Theresa Bunse (DKFZ)

Name	Specifications	Source
PAP-A2 cell line	2277NS cells transduced with HPV16 E6 (flag-tagged) and HPV16 E7 (strep-tagged)	Generated in the course of this PhD project (3.2.6 Generation of the PAP-A2 cell line)
CaSki cell line	$HPV16^+$ cell line derived from a cervical carcinoma (Pattillo *et al.*, 1977)	Purchased from ATCC

3.1.5 Cell culture solutions

Name	Specifications	Source
2277NS medium (for PAP-A2 medium add 2 µg/ml puromycin)	85 % (v/v) DMEM 10 % (v/v) FCS 1 % (v/v) HEPES 0.1 % (v/v) β-mercaptoethanol (50 mM) 1 % (v/v) gentamicin (10 mg/ml) 2 % (v/v) glutamine (200 mM) 1 % (v/v) sodium pyruvate (100 mM) For 2 µg/ml puromycin add: 0.02 % (v/v) puromycin (10 mg/ml)	Self-produced
CaSki medium	DMEM 10 % (v/v) FCS	Self-produced
Dulbecco's Modified Eagle Medium (DMEM)	#D5671	Sigma-Aldrich, Taufkirchen
Fetal calf serum (FCS)	#10270	Thermo Fisher Scientific, Waltham, USA
Gentamicin	#4-07F00-H	Bioconcept, Allschwil, Switzerland

Name	Specifications	Source
HEPES	#15630080	Thermo Fisher Scientific, Waltham, USA
L-glutamine	#MT25005CI	Corning, Corning, USA
Phosphate buffered saline (PBS)	137 mM NaCl 2.7 mM KCl 12 mM PO_4 pH 7.2-7.4	Self-produced
Puromycin	P9620-10ML	Sigma-Aldrich, Taufkirchen
Roswell Park Memorial Institute medium (RPMI 1640)	#R0883	Sigma-Aldrich, Taufkirchen
Sodium pyruvate	#MT25000CI	Corning, Corning, USA
T cell medium	90 % (v/v) αMEM 10 % (v/v) FCS 1 % (v/v) glutamine (200 mM) 0.1 % (v/v) β-mercaptoethanol (50 mM)	Self-produced
Trypsin-EDTA	#T3924	Sigma-Aldrich, Taufkirchen
αMEM	#M4526	Sigma-Aldrich, Taufkirchen
β-mercaptoethanol (cell culture)	#31350-010	Thermo Fisher Scientific, Waltham, USA

3.1.6 Kits

Name	Specification	Manufacturer
BD Cytofix/Cytoperm™ kit	#554714	BD, Franklin Lakes, USA
Detergent compatible (DC) protein assay kit	#5000116	Biorad, Hercules, USA
DirectPCR Lysis Reagent Tail kit	#31-101-T	VWR, Darmstadt
peqGold Gel Extraction kit	#732-2777	VWR, Darmstadt
QIAmp DNA Mini kit	#51304	Qiagen, Hilden
REDTaq kit	#D4309	Sigma-Aldrich, Taufkirchen

3.1.7 Proteins

Name	Specifications	Manufacturer
Bovine serum albumin (BSA)		GE Healthcare, Chalfont St Giles, UK
BSA standard		BioRad, Hercules, USA
Murine interferon-γ (IFN-γ)	#34-8311-82	Thermo Fisher Scientific, Waltham, USA
Protein marker	Precision plus Protein™ standards kaleidoscope (10-250 kDa)	BioRad, Hercules, USA
Proteinase K	20 mg/ml, #1014023	Qiagen, Hilden

3.1.8 Peptides

Peptide	Sequence	Supplier
E7/7-15	TLHEYMLDL	DKFZ peptide production facility
E7/11-19	YMLDLQPET	DKFZ peptide production facility
E7/82-90	LLMGTLGIV	DKFZ peptide production facility
E6/25-33	ELQTTIHDI	DKFZ peptide production facility
SLHEYMLDL	SLHEYMLDL	DKFZ peptide production facility
$Survivin_{96-104}$ (Surv)	LMLGEFLKL	DKFZ peptide production facility
PADRE	AK-Cha-VAAWTLKAAA (Cha = Cyclohexylalanin)	DKFZ peptide production facility
E7 pool	pool of 22 peptides (15mers with 11 aa overlap)	JPT Peptide Technologies GmbH, Berlin
Pam2KFVM-E7/11-19	see Figure 27	Peptide Specialty Laboratories GmbH, Heidelberg
Pam1KFVM-E7/11-19		Department of Nuclear Medicine, Heidelberg University Hospital, Heidelberg

Peptide	Sequence	Supplier
Stea2KFVM-E7/11-19		Department of Nuclear Medicine, Heidelberg University Hospital, Heidelberg
Lipo-PEG-peptides (LPPs)	see Figure 29	Department of Nuclear Medicine, Heidelberg University Hospital, Heidelberg; Peptides & elephants, Hennigsdorf

3.1.9 Antibodies

Name	Clone/specification	Dilution	Provider
α-alpha-tubulin	#T6074	1:5000	Sigma-Aldrich, Taufkirchen
αCD19-PE-Cy5.5	#RM7718	1:100	Thermo Fisher Scientific, Waltham, USA
αCD3-PE-Cy7	#552774	1:100	BD, Franklin Lakes, USA
αCD4-FITC	#553047	1:200	BD, Franklin Lakes, USA
αCD8-PE	#sc-53473 PE	1:100	BD, Franklin Lakes, USA
αE6 (HPV16)	E6-6F4	1:1000	Euromedex, Souffelweyersheim, France

Name	Clone/specification	Dilution	Provider
αE7 (HPV16)	NM2	1:1000	Kindly provided by Prof. M. Müller, DKFZ
αHLA-A2-FITC	BB7.2, #551285	1:100	BD, Franklin Lakes, USA
αIFN-γ-APC	#562018	1:200	BD, Franklin Lakes, USA
α-mouse-HRP	#62-6520	1:5000	Thermo Fisher Scientific, Waltham, USA
αTNF-α-eFluor450	#48-7321-82	1:100	Thermo Fisher Scientific, Waltham, USA

3.1.10 Plastics and consumables

Name	Specifications	Manufacturer
Cell culture flasks	25 cm^2, 75 cm^2, 150 cm^2	TPP, Trasadingen, Switzerland
Cell culture plates	96-well	TPP, Trasadingen, Switzerland
Cell strainer	70 µm	Merck, Darmstadt
Eppendorf tubes	0.5 ml, 1.5 ml, 2 ml	Eppendorf, Hamburg
Eppendorf tubes (low DNA-binding)	#30108078	Eppendorf, Hamburg
FACS tubes	round bottom	BD, Franklin Lakes, USA
Falcon tubes	15 ml, 50 ml	BD, Franklin Lakes, USA
Hollow needle	20G, 26G, 27G	Braun, Melsungen

Name	Specifications	Manufacturer
LS+ Positive MACS column	#130-042-401	Miltenyi Biotech, Bergisch Gladbach
MACS SmartStrainer, 70 µM	#130-098-462	Miltenyi Biotech, Bergisch Gladbach
Mini-protean TGX AnykD™ polyacrylamide gel	#4569036	BioRad, Hercules, USA
Pipette tips	small, medium, big	Starlab, Hamburg
Scalpel	No. 20	Feather, Osaka, Japan
Sterile filter	low binding, 0.22 µm	Merck, Darmstadt
Syringe connector	#MX494P1	Smiths Medical, Minneapolis, USA
Syringes	1 ml, 3 ml	Braun, Melsungen
Whatman chromatography paper	#88600	GE Healthcare, Chalfont St Giles, UK

3.1.11 Laboratory equipment, machines & instruments

Name	Specifications	Manufacturer
Anesthesia device (isoflurane)	Isoflurane Vet. Med. Vapor	Dräger Medizintechnik GmbH, Lübeck
Analytical balance		Ohaus, Nänikon, Switzerland
Automated cell counter	Countess® Automated Cell Counter	Thermo Fisher Scientific, Waltham, USA
Centrifuge	(table top), #5418	Eppendorf, Hamburg
Centrifuge	(table top), #5407	Eppendorf, Hamburg

Name	Specifications	Manufacturer
Centrifuge	(falcons, plates), Multifuge® 16R	Heraeus, Hanau
Chemiluminescence reader	INTAS ECL Chemocam Imager	Intas Science Imaging Instruments, Göttingen
Digital calipers		Hogetex, Nieder-Olm
Electrophoresis chamber (agarose gels)	Owl Easycast B2	Owl Separation Systems, Portsmouth, USA
Electrophoresis chamber (SDS-PAGE)	Mini-PROTEAN® Tetra Cell	Biorad, Hercules, USA
Flow Cytometer	FACS Canto II	BD, Franklin Lakes, USA
Gel analyzer (agarose gels)	Gel Jet Imager 2006	Intas, Göttingen
Heating shaker	Eppendorf Thermomixer	Eppendorf, Hamburg
Incubator (cell culture)	Heracell 150i	Thermo Fisher Scientific, Waltham, USA
Laminar flow hood	SterilGard® Class II Typ A B3	The Baker Company, Sanford, USA
Light microscope	Wilovert Standard 30 microscope	Hund Wetzlar, Wetzlar
Liquid nitrogen tank	Locator 8 plus ARPEGE110 NU	Barnstead/Thermolyne, Dubuque, USA Cryopal, Bussy-Saint-Georges, France
MACS magnet	Quadro MACS	Miltenyi Biotech, Bergisch Gladbach
Magnetic stirrer	MR-Hel Standard	Heidolph Instruments, Schwabach
Mr. Frosty freezing container	#9400945	Faust, Klettgau

Name	Specifications	Manufacturer
Multilable plate reader	Multiskan™ FC microplate photometer	Thermo Fisher Scientific, Waltham, USA
Nano Drop	ND-1000	VWR, Darmstadt
PCR cycler	PTC-200 TProfessional Trio48	MJ Research, Canada Biometra, Göttingen
pH Meter	MP220 InLab Microelectrode	Mettler Toledo, Glostrup, Denmark
Pipetboy	Pipetboy acu	Integra Biosciences, Biebertal
Pipettes	2 µl, 10 µl, 20 µl, 200 µl, 1,000 µl	Gilson, Middleton, USA
Platform shaker	STR6 Rotamax 3013	Stuart Bibby Scientific, Staffordshire, UK Heidolph Instruments, Schwabach GFL, Burgwedel
Power supply for electrophoresis	EPS500-400, EPS3500 MP 250V PowerPac300	Pharmacia, Uppsala, Sweden MS Major Science, Saratoga, USA BioRad, Hercules, USA
Rolling shaker	CAT RM5	Zipperer, Staufen
Surgical tweezers and scissors		Dimeda, Tuttlingen
Thermomixer	Thermomixer compact	Eppendorf, Hamburg
Trans-blot semidry transfer cell		Biorad, Hercules, USA
Vortexer	Vortex-Genie 2	Scientific Industries, Bohemia, USA
Water bath		GFL, Burgwedel

3.1.12 Software

Software	Manufacturer
FACSDIVA v6.1.2	BD, Franklin Lakes, USA
Flowjo 10	Treestar, Ashland, USA
Graph Pad Prism 5	GraphPad Software Inc., La Jolla, USA
ImageJ	(Schneider, Rasband and Eliceiri, 2012)
Inkscape 0.91	The Inkscape Team, www.inkscape.org
Mendeley	Elsevier B.V., Amsterdam, Netherlands
Microsoft Office 2010	Microsoft Corporation, Redmond, USA
SnapGene	GSL Biotech LLC, Chicago, USA

3.2 Methods

3.2.1 Polymerase chain reaction (PCR)

The polymerase chain reaction allows the multiplication of a given stretch of DNA by using parts of the cellular replication machinery (Saiki *et al.*, 1985; Mullis *et al.*, 1986). The components of a PCR reaction are: Template DNA, nucleotides, primers and heat-stable DNA polymerase (often from thermophilic bacteria such as Thermus aquaticus, abbreviated as Taq) in a buffer solution providing suitable conditions for the DNA polymerase. The primers are short fragments of DNA that bind to their complementary DNA stretch on the template DNA. To amplify specific template DNA sequences, one primer that binds upstream (forward (F) primer) and one that binds downstream (reverse (R) primer) of the sequence of interest is used.

PCR reactions follow steps with defined temperatures: Denaturation of the double-stranded DNA into single-strands at 94 °C, primer annealing at a primer-specific temperature and elongation at a polymerase-specific temperature (for the Taq polymerase 72 °C). One series of denaturation, annealing and elongation completes one cycle. Often, an initial denaturation step for 7 min at 94 °C ensuring complete initial denaturation and a terminal elongation step for 7 min at 72 °C ensuring complete synthesis of all fragments are included in the PCR program.

In the elongation step, the DNA polymerase elongates the primers by adding nucleotides to the 3’ end of the primer. After one cycle, the number of DNA copies has doubled. Therefore, the number of DNA fragments increases exponentially with the number of cycles, thus allowing also the detection of minuscule amounts of DNA. For the detection of the amplified fragments, the fragments are first separated by size during an electrophoretic migration through an agarose gel. Smaller fragments migrate faster through the pores of the gel than larger fragments. DNA migrates to the plus pole due to its negatively charged phosphate backbone.

Usually the agarose gel is supplemented with ethidium bromide. Ethidium bromide intercalates in DNA (Waring, 1965) which induces a change in its fluorescence spectrum upon exposure to UV light (Le Pecq and Paoletti, 1966). This allows the detection of the DNA bands under UV light.

3.2.2 A2.DR1 genotyping by PCR

Animals used for breeding were routinely genotyped by PCR to monitor the genetic identity of the breeding colony. Specific primers were used to either verify the existence of a transgene in the genomic DNA or the absence of a gene that was knocked out. Mice were tailed at weaning and the tails were lysed with the DirectPCR Lysis Reagent Tail kit (with proteinase K (0.2 mg/ml)) for 3-16 h at 55 °C in a rotating heater. Proteinase K was inactivated for 45 min at 85 °C and the lysate was subsequently used as a template for the genotyping PCR reactions using REDTaq® ready mix, which contains nucleotides, buffer solutions and the REDTaq® DNA polymerase. PCR reactions were carried out according to the manufacturer's instructions with 6.75 µl REDTaq® mix, 0.5 µl template, and 0.125 µl of each primer, topped up to 12.75 µl with DNase free water supplied with the REDTaq® Ready mix.

Primers and PCR programs are depicted in Table 1. PCR products were analyzed for correct size by visualizing them in agarose gels after gel electrophoresis. TAE buffer-based 2 % agarose gels were used for all analyses except for the H-2D^b WT PCR product, which was analyzed in 1 % gels due to the longer fragments amplified by this PCR. The agarose gels were supplemented with 10 µl/100 ml GelRed as a safer and more sensitive replacement for ethidium bromide.

Table 1. PCR programs and primers for A2.DR1 genotyping

PCR name	PCR product	Primers	Primer sequences	PCR program
HHD	400 bp	HHD F	CAT TGA GAC AGA GCG CTT GGC ACA GAA GCA G	94° 7 min 94° 0.5 min 66° 0.5 min 72° 1 min x 40 72° 4 min 4° ∞
		HHD R	GGA TGA CGT GAG TAA ACC TGA ATC TTT GGA GTA CGC	
HLA-DRA1	153 bp	HLA DRA 1 F	CTC CAA GCC CTC TCC CAG AG	94° 7 min 94° 0.5 min 66° 0.5 min 72° 1 min x 40 72° 4 min 4° ∞
		HLA DRA 1 R	ATG TGC CTT ACA GAG GCC CC	
HLA-DRB1	228 bp	HLA DRB 1 F	TTC TTC AAC GGG ACG GAG CGG GTG	94 ° 5 min 94 ° 1 min 57 ° 1 min 72 ° 2 min x 40 72 ° 5 min 4 ° ∞
		HLA DRB 1 R	CTG CAC TGT GAA GCT CTC ACC AAC	
β2 microglobulin	KO: 600 bp WT: 270 bp	ß2m0	CTG AGC TCT GTT TTC GTC TG	94 ° 5 min 94 ° 1 min 57 ° 1 min 72 ° 2 min x 40 72 ° 5 min 4 ° ∞
		ß2m4	CTT AAC TCT GCA GGC GTA TG	
		Neo 55 A	CCT GCC GAG AAA GTA TCC A	

PCR name	PCR product	Primers	Primer sequences	PCR program
H-2D^b KO	340 bp	H2 DB KO F	CAG CAG AAA CAT ACA AGC TGT C	94 ° 7 min 94 ° 1 min 60 ° 2 min 72 ° 2 min 72 ° 7 min 4 ° ∞ x 40
		H2 DB KO R	AAC GAT CAC CAT GTA AGA GTC AGT	
H-2D^b WT	1600 bp	Db-WT-F SMO 130	ATT GGG AGC GGG AAA CAC AG	95 ° 5 min 95 ° 30 sec 64 ° 40 sec 72 ° 70 sec 72 ° 10 min 4 ° ∞ x 35
		Db-WT-R SMO 131	TCC GAC CCC AAG TCA CAG	
MHC class II	KO: 209 bp WT: 178 bp	oIMR1020 Mutant	CGG AAG TGC TTG ACA TTG G	94 ° 3 min 94 ° 30 sec 61 ° 45 sec 72 ° 1 min 72 ° 3 min 4 ° ∞ x 35
		oIMR1021 Mutant	GTA TTG ACC GAT TCC TTG CG	
		oIMR1273 WT	AAC CTT CAG GAT CTG TGA TCC	
		oIMR1274 WT	GTG GCT GTT GCC TTA AGA CC	

3.2.3 Mouse experiments

Mice were kept in individually ventilated cages in the DKFZ animal facility. Prior to an experiment, age-matched groups of female mice (7-15 weeks old) were selected and pooled in experimental cages. Group sizes ranged from 3 mice for the testing of individual tumor cell clones, to usually 6 mice for the comparison of vaccine formulations to up to 15 mice in anti-tumor vaccination experiments.

3.2.4 Cell culture

Newly acquired cell lines were tested for mycoplasma contamination and cell line authentication (done by Multiplexion, Immenstaad) was performed. Cell culture was

performed in a laminar flow hood. Cells were cultured at 37 °C, 95 % relative humidity and 5 % CO_2 in an incubator. CaSki, 2277NS and PAP-A2 cell lines exhibit adherent growth. To subculture these cell lines, cells have to be detached by incubation with Trypsin-EDTA. Trypsin enzymatically digests cell adhesion molecules and EDTA chelates Ca^{2+}, thus weakening Ca^{2+}-dependent cell-cell and cell-matrix interactions. For this, the medium was taken off and cells were washed once with phosphate buffered saline (PBS) to remove residual medium containing large quantities of proteins. This was done because the proteins in the medium slow down the enzymatic digestion of cell adhesion molecules after addition of a trypsin solution. Sufficient amounts of Trypsin-EDTA to cover the growth area were added to the cells. After all cells were detached, medium containing fetal calf serum (FCS) was added to provide excess protein and thus to slow down the enzymatic digestion of cellular components. Cells were resuspended, counted with a Countess® automated cell counter, transferred to a tube and spun down (422 g, 4 min, RT). Subsequently, the medium containing the trypsin solution was decanted and cells were taken up in fresh medium and subcultured or used in experiments.

3.2.4.1 Freezing and thawing of cells

For freezing, cells were harvested by trypsin detachment and taken up in the respective medium for the cell line supplemented with 50 % FCS and 10 % DMSO as a cryoprotectant that reduces the formation of harmful ice crystals (freezing medium). The medium containing the cells was transferred to cryovials. Cryovials were collected in a freezing container (Mr. Frosty) that ensures a constant cooling rate of 1 °C per minute when stored at -80 °C. The slow rate of temperature reduction also decreases the generation of ice crystals in the cells. After 1 day at -80 °C, cells were transferred from -80 °C to liquid nitrogen for long term storage.

For thawing of cells, a cryovial was taken out of the liquid nitrogen storage and thawed in a water bath, which was preheated to 37 °C. Once the ice was thawed, the medium containing the cells was transferred to a tube containing 20 ml of the respective medium and inverted once. Cells were immediately spun down (422 g, 4 min, RT) and the medium containing DMSO was decanted. Cells were taken up in the respective medium and seeded in cell culture flasks or plates.

3.2.4.2 Treatment of cells with IFN-γ

Cells upregulate the expression of MHC class I molecules upon stimulation with IFN-γ. To test the ability of the 2277NS cell line to respond adequately to this stimulus, cells were cultured to a density of 60-70 %. Subsequently, the medium was taken off and replaced with 2277NS medium containing 100 ng/ml murine IFN-γ. The cells were cultured for 48 h, harvested and stained with fluorophore-coupled ABs specific for HLA-A2.

3.2.5 Flow cytometry

Flow cytometry allows the rapid analysis of a large number of single cells. In this technique, cells are passed by a laser as single cells in a liquid stream. The laser beam is scattered when hitting the cell and cellular characteristics such as cell size and granularity can be inferred from the scatter pattern. Additionally, fluorophore-coupled ABs can be used to stain live or dead cells for surface markers or permeabilized cells for intracellular molecules. Unstained cells and cells stained with a suitable isotype control were used to assess autofluorescence and background AB-binding of the examined cells and to adjust the sensitivity of the detectors.

3.2.5.1 Staining of adherent cells for assessment of HLA-A2 surface expression by flow cytometry

Cells were harvested by trypsin detachment, washed once in PBS and taken up in 50 µl staining buffer (1 % FCS in PBS). 0.5 µl of FITC-coupled anti-HLA-A2 AB were added and the cells were incubated at 4 °C for 20 min in the dark. After incubation, cells were washed three times with 200 µl staining buffer and were taken up in 200 µl staining buffer for direct analysis by flow cytometry. Analysis was performed using a FACS Canto II which was provided and maintained by the DKFZ flow cytometry core facility.

3.2.5.2 Staining of non-adherent cells for flow cytometry analysis

Non-adherent cells were stained for surface and intracellular protein expression and subsequently analyzed by flow cytometry as described in 3.2.17.

3.2.6 Generation of the PAP-A2 cell line

2277NS cells (Quandt, 2012; Schumacher *et al.*, 2014) were cultured in 2277NS medium and transduced with the lentiviral vector pWPI HPV16 E6/E7 (Figure 16) by Ruwen Yang (DKFZ). Successfully transduced cells were selected with 2277NS medium containing 2 µg/ml

puromycin. Surviving cells were stained for HLA-A2, and HLA-A2-high cells were single cell-sorted in 96-well flat bottom plates. Clones were tested for E6, E7 and HLA-A2 expression (for detailed results see 4.2). Subsequently, clonal cell lines were each injected into three or four A2.DR1 mice ($0.75x10^6$ - $1x10^6$). Only one of the cell injections resulted in tumor growth. The respective clone, IVA2, exhibited medium expression of HLA-A2, medium E6 and medium E7 expression compared to the other clonal cell lines. The IVA2-derived tumor was excised aseptically, mashed with the help of a metal sieve and taken up in 2277NS medium supplemented with 2 µg/ml puromycin. The cell line growing from this outgrowing tumor was called PAP-A2. The HPV16 E6/E7 sequence identity in PAP-A2 cells was confirmed by DNA sequencing (performed by GATC-Biotech, Konstanz). For this, genomic DNA of PAP-A2 cells was isolated with the QIAmp DNA Mini kit from a cell pellet. To generate genomic DNA, cells were lysed, the DNA was precipitated and bound to a silica gel matrix. After washing, the DNA was eluted from the matrix by the addition of water. The E6/E7 DNA was PCR-amplified with the PCR programs and primers depicted in Table 2. After confirming the correct length of the PCR products through agarose gel (2 %) electrophoresis, the gel bands containing the fragments of interest were cut out and the DNA was extracted from the agarose gel. For this, the gel piece was dissolved by heating and the DNA was bound to a silica column. After washing, DNA was eluted with water. This DNA was sent to GATC Biotech and served as a template for the sequencing reaction with the primers depicted in Table 2. The sequence of the pWPI HPV16 E6/E7 vector was compared to the sequencing results with the help of the SnapGene® software. Both sequences were found to be identical.

Table 2. PCR programs and primers for HPV16 E6/E7 sequence authentication

PCR name	PCR product	Primers	Primer sequences	PCR Program
HPV16 E6	932 bp	3Flag-P2A-pWPI-F	TAAGCAACGCGTGATTACAA GGATGACGACGAT	94° 5 min 94° 1 min 54.3° 0.5 min 72° 2 min x 40 72° 5 min 4° ∞
		IRES rev	CCGCCTTTGCAGGTGTATCT	
HPV16 E7	640 bp	Human elongation factor-1a promoter (EF1a F)	TCAAGCCTCAGACAGTGGTT C	94° 5 min 94° 1 min 66° 0.5 min 72° 1 min x 40 72° 5 min 4° ∞
		Strep-P2A-pWPI-R4	TTTTTCGAACTGCGGGTGGCT CCACGATCCACCTCCCGATCC	

3.2.7 SDS-PAGE and Western blot

SDS (sodium dodecyl sulfate) polyacrylamide gel electrophoresis (PAGE) (Laemmli, 1970) allows the separation of proteins according to their size in a polyacrylamide gel. In a SDS-PAGE, the migration distance in the polyacrylamide gel is dependent on the size of the respective protein since negatively charged SDS is bound to all amino acids of a protein and thus masks the natural charge of the amino acids.

3.2.7.1 Preparation of cell extracts for SDS-PAGE

For the preparation of cell extracts suitable for SDS-PAGE, cultured cells were detached by trypsin treatment, washed and lysed with lysis buffer (80 µl/10^6 cells). For protein samples from tumor tissue, a tumor was excised and homogenized in lysis buffer (20 µl/µg of tumor tissue). The samples were kept on ice and vortexed shortly every 2 minutes for 20 min. Subsequently, lysates were cleared of cell debris by centrifugation (20.817 g, 10 min, 4 °C). The protein-containing supernatant was mixed with 4 x Laemmli buffer containing β-mercaptoethanol as a reducing agent, which is breaking up disulfide bonds, and was heated

for 5 min at 95 °C to fully denature all proteins. Subsequently, protein samples were stored at -80 °C or directly used for SDS-PAGE.

3.2.7.2 Detergent compatible (DC) protein assay

To determine the protein concentration in a sample before the addition of Laemmli buffer, the DC protein assay kit was used. In this assay, the protein concentration is derived from a color change induced by the reactions of the amino acids tyrosine, tryptophan, cysteine and histidine with copper tartrate and Folin reagent. The color intensity induced by the proteins in the samples to be analyzed is compared to that of a standard curve generated with BSA samples of known concentration.

3.2.7.3 SDS-PAGE and Western blot

In this study, the SDS-PAGE system according to Laemmli (Laemmli, 1970) with a Tris-glycine buffer was used. Usually, 15 µg of protein were loaded into the pockets of the polyacrylamide gels and the gel was run at 300 V with maximal current for 15-20 minutes. 5 µl of a protein molecular weight marker were used for every gel. After separation of the protein bands via SDS-PAGE, the proteins were immobilized on a methanol-activated PVDF membrane by Western blot. For this process, the proteins were electrophoretically transferred to the PVDF membrane in a semidry blot chamber for 25 min at 150 mA and maximal voltage. The proteins were thus fixed to the membrane via dipole and hydrophobic interactions.

Subsequently, detection of proteins via specific ABs was performed. To saturate protein binding sites on the membrane, the membrane was blocked for 45 min in blocking solution (5 % low-fat milk powder/1 % BSA/0.2 % Tween-20 in PBS). For the detection of proteins immobilized on the PVDF membrane, the membrane was incubated with the respective specific primary AB in blocking solution for 1 h at RT or overnight at 4 °C on a rocking shaker. After washing three times for 5 min on a rocking shaker with 0.2 % Tween-20 in PBS (PBS-T), the secondary ABs coupled to horseradish peroxidase diluted in blocking solution was added and incubated for 1 h at RT on a rocking shaker. After 3 subsequent washes for 5 min at RT with PBS-T, the Western blot was developed. For this, the membranes were shortly washed in PBS, excess PBS was taken off by dabbing the membrane's edges on tissue paper and 500 µl of ECL solution were spread on the membrane. To allow the visualization of the low

protein levels of E6 and E7 bands, high sensitive ECL solution was used for these Western blots. Since the expression levels of the loading control protein α-tubulin is much higher, normal ECL solution gave rise to sufficient chemiluminescent reaction to allow detection of the emitted light signal. The light signal was detected with a chemiluminescence reader. Quantification of band intensities was performed with ImageJ software.

3.2.8 Peptide and peptide conjugate synthesis

Reference sequences for HPV16 E6 (NCBI Reference Sequence: NC_001526.2) and E7 (NCBI Reference Sequence: NC_001526.2) were used as shown in (8 Annex).

3.2.8.1 Peptide synthesis

Peptides were produced by the DKFZ Peptide Production Unit (Prof. Stefan Eichmüller, GMP & T Cell Therapy Unit, DKFZ, Heidelberg) with a purity of > 95 %. The peptides were synthesized by solid phase synthesis using the Fmoc strategy (Merrifield, 1963; Carpino and Han, 1972). For this, preloaded Wang-Resins and 2-(1H-Benzotriazole-1-yl)-1,1,3,3-tetramethyluronium hexafluorophosphate (HBTU) as a coupling agent were used with a fully automated multiple Syro II synthesizer (MultiSyn Tech, Germany). Purification took place by preparative high-performance liquid chromatography (HPLC) with 0.1 % trifluoroacetic acid in water (A) and 80 % acetonitrile in water (B). Elution was achieved by a successive linear gradient of 25 % B to 80 % B in 30 min at a flow rate of 10 ml/min. The purified peptides were lyophilized and taken up in DMSO to a final concentration of 50 mM.

3.2.8.2 Synthesis of Pam2-E7/11-19

For the synthesis of Pam2-E7/11-19 (done by Peptide Specialty Laboratories GmbH, Heidelberg), the lysine in the peptide KFVMYMLDLQPET was palmitoylated on its amino-groups. The linker KFVM was selected since this linker had already been successfully used by Cho *et al.* (Cho *et al.*, 2013). The resulting product was difficult to purify, therefore its final purity was only estimated to be approximately 20 %.

3.2.8.3 Synthesis of Pam1-E7/11-19

The synthesis of Pam1-E7/11-19 was done by Dr. Max Sauter (Department of Nuclear Medicine, Heidelberg University Hospital, Heidelberg, Germany). For this synthesis, the lysine in the peptide KFVMYMLDLQPET was palmitoylated on one of its amino groups. The

product was lyophilized and subsequently purified by preparative HPLC. The purity of this compound was calculated on the basis of HPLC analysis to be approximately 95 %.

3.2.8.4 Synthesis of Stea2-E7/11-19

The amphiphilic peptide Stea2-E7/11-19 was synthesized by Dr. Philipp Uhl and Dr. Max Sauter (Department of Nuclear Medicine, Heidelberg University Hospital, Heidelberg, Germany) by coupling DSPE-NHS (N-(Succinimidyloxy-glutaryl)-L-α-phosphatidylethanolamine, distearoyl) to the N-terminal lysine of KFVMYMLDLQPET. For this, DSPE-NHS and the peptide were dissolved in a 3:1 (v/v) mixture of DMSO/PBS pH 8.16. Both compounds were mixed in the stoichiometric ratio of 1:2 and stirred overnight at RT for coupling. The product was lyophilized and subsequently purified by preparative HPLC. The purity of this compound was calculated on the basis of HPLC analysis to be approximately 70 %.

3.2.8.5 Synthesis of LPPs

The synthesis of the lipo-PEG-peptides (LPPs) was performed by Dr. Philipp Uhl and Dr. Max Sauter and the company peptides & elephants (Hennigsdorf, Germany). N-terminally cysteinylated peptides were dissolved in a 2:1 (v/v) mixture of PBS pH 5.5 and acetonitrile. DSPE-PEG-maleimide ((1,2-distearoyl-3-sn-phosphatidylethanolamine)-PEG-maleimide) was dissolved in a 1:1 mixture of DMSO/PBS pH 5.5. Coupling of peptides to DSPE-PEG-maleimide was done by mixing both solutions in a stoichiometric ratio of 2:1 (peptide/DSPE-PEG-maleimide) and stirring overnight at RT. The product was lyophilized and subsequently purified by preparative HPLC. The purity of the final compound was assessed by HPLC and HPLC-MS and was usually higher than 70 %. LPPs were dissolved in DMSO to a final concentration of 25 mM and stored in aliquots at -80 °C.

3.2.9 mRNA production

In vitro transcribed mRNA was produced by the company BioNTech (Mainz, Germany) as described in (Kreiter *et al.*, 2007). In brief, “pST1-A120 based plasmids were linearized behind the poly(A) tail, purified by phenol chloroform extraction and sodium acetate precipitation and used as templates for *in vitro* transcription (IVT) with Message-Machine Kit (Ambion, Austin, USA). The RNA concentration and quality were assessed by spectrophotometry and agarose/formaldehyde gel electrophoresis” (Kreiter *et al.*, 2007).

3.2.10 Vaccination with emulsion-based formulations

To generate incomplete Freund's adjuvant (IFA) vaccine emulsions, ISA51 mineral oil was used in conjunction with PBS and peptides with or without TLR-agonists. 1 ml of ISA51 was taken up in a 3 ml syringe and 1 ml of PBS containing the peptide (100 nmol E7/11-19/mouse and 100 nmol PADRE/mouse) and the TLR-agonists (20 µg MPLA/mouse or 40 µg XS15/mouse) in another 3-ml syringe. Both syringes were connected with an i-connector after removal of any air in the syringes and the connector. ISA51 was pressed through the connector into the other syringe where both liquids were thus mixed. Subsequently, the mixture was pressed into the first syringe again. With this, the first cycle of mixing was completed. To complete the first stage of mixing, 19 more slow cycles with 1 cycle per 8 seconds were performed, followed by the second stage with 40 fast cycles in approximately 20 seconds. The resulting emulsion was dropped onto a water surface for quality control. A good emulsion forms a stable ball of emulsion that does not disperse on the water surface.

100 µl of the emulsion were injected subcutaneously into the flank of each mouse. 12 days after the injection, mice were sacrificed for analysis of vaccination-induced T cells by intracellular IFN-γ staining.

3.2.11 Vaccination with mRNA-lipoplexes (mRNA-LPX)

To generate mRNA lipoplexes, 40 µg of *in vitro* transcribed RNA per mouse were mixed with RNase-free water in low-DNA binding Eppendorf tubes and vortexed. Subsequently, RNase-free 5 M NaCl solution was added and the solution was vortexed. Finally, liposomes (liposome composition is proprietary knowledge of BioNTech) were added, the resulting solution was inverted four times and incubated at RT for 10 min. A correctly prepared mRNA lipoplex solution is slightly opaque and does not contain any precipitates. For injection, mice were anesthetized by isoflurane inhalation and 200 µl of RNA-LPX were injected retro-orbitally into the bloodstream. A prime immunization at day 0, and booster immunizations on days 7, 14 and 21 were performed. Mice were sacrificed on day 28 for analysis of vaccination-induced T cells by intracellular IFN-γ staining.

3.2.12 Vaccination with free E7/11-19 peptide

Per mouse, 100 nmol of E7/11-19 peptide were mixed with PBS and 50 µg pIC. The volume of PBS was adjusted so that the volume of the peptide plus pIC and PBS reached 100 µl. 100 µl of the resulting solution were injected on day 0 and day 6 subcutaneously into the flank of the mice. Mice were sacrificed on day 19 for analysis of vaccination-induced T cells by intracellular IFN-γ staining.

3.2.13 Vaccination with Pam2-E7/11-19 and Pam1-E7/11-19

Per mouse, approximately 30 nmol of Pam2-E7/11-19 (for 1x Pam2-E7/11-19) or approximately 60 nmol of Pam2-E7/11-19 (for 2x Pam2-E7/11-19) or 100 nmol of Pam1-E7/11-19 were mixed with PBS and 50 µg pIC. The volume of PBS was adjusted so that the volume of the peptide compound plus pIC and PBS reached 100 µl. 100 µl of the resulting solution were injected on day 0 and day 14 subcutaneously into the flank of the mice. Mice were sacrificed on day 21 for analysis of vaccination-induced T cells by intracellular IFN-γ staining.

3.2.14 Vaccination with Stea2-E7/11-19

Per mouse, 33 nmol of Stea2-E7/11-19 were mixed with PBS and 50 µg pIC. The volume of the PBS was adjusted so that the volume of the peptide compound plus pIC and PBS reached 100 µl. 100 µl of the resulting solution were injected on days 0, 7 and 14 intravenously or subcutaneously into the flank of the mice. Mice were sacrificed on day 21 for analysis of vaccination-induced T cells by intracellular IFN-γ staining.

3.2.15 Vaccination with LPPs

Per mouse, 50 nmol of LPPs or DSPE-PEG-maleimide without peptide as a vehicle control were mixed with sterile PBS and 50 µg pIC or 1.24 nmol CpG. The volume of PBS was adjusted so that the volume of the peptide compound plus pIC and PBS reached 100 µl. 100 µl of the resulting solution were injected subcutaneously into the flank of the mice. In tumor bearing mice (see 3.2.21), injections were performed on the contralateral flank.

For the vaccination with combinations of LPPs, mice were injected with 50 nmol of each of the LPPs in separate sites on the left flank of the mice. Each mouse received a total amount of 50 µg pIC, which were distributed equally over all injections.

3.2.16 Isolation of splenocytes

Mice were sacrificed by CO_2 asphyxiation or cervical dislocation and the spleen was removed aseptically and stored in ice-cold PBS. In a laminar flow hood, the spleen was put into a 70 µm nylon cell strainer and minced with a scalpel. Subsequently, the piston of a disposable plastic syringe was used to press the splenocytes through the cell strainer. Splenocytes were washed out of the strainer with 5 ml ice-cold PBS into a 50 ml Falcon tube. The remaining spleen fragments were again mashed with the piston and leftover splenocytes were washed out with 5 ml ice-cold PBS and collected in the Falcon tube. The cells were spun down for 4 min at 422 g at 4 °C. The supernatant was discarded and incubation in 4 ml ACK-buffer for 50 seconds was used to osmotically disrupt red blood cells. After 50 seconds, 46 ml ice-cold PBS were added to the tube to restore physiological osmotic pressure. Cells were spun down for 4 min at 422 g at 4 °C, the supernatant was discarded and the cells were taken up in 50 ml ice-cold PBS. The cells were counted with a Countess® cell counter. Cells were spun down for 4 min at 422 g at 4 °C, the supernatant was discarded and cell concentration was adjusted to $2x10^6$/100 µl with RPMI/10% FCS.

3.2.17 Intracellular cytokine staining (IFN-γ/TNF-α)

$CD8^+$ T cells which recognize their specific peptide presented on MHC class I become activated and produce IFN-γ and/or TNF-α. This mechanism was used to quantify vaccination-induced $CD8^+$ T cells by restimulating splenocytes of vaccinated mice with the cognate peptide and control peptides in the presence of compounds (GolgiStop™ and GolgiPlug™) that inhibit Golgi apparatus-mediated cytokine secretion. IFN-γ and other cytokines are thus retained in the cell and can be rendered detectable by intracellular staining with specific fluorophore-coupled ABs. The frequency of IFN-γ^+ and/or TNF-α^+ and thus epitope-specific $CD8^+$ T cells was subsequently assessed by flow cytometry analysis.

For IFN-γ/TNF-α intracellular staining, $2x10^6$ splenocytes (see 3.2.16) were incubated in 200 µl RPMI/10 % FCS with GolgiStop™ (1,5 µl/ml) and Golgi Plug™ (1 µl/ml) in the presence of either PMA (10 ng/ml) + ionomycin (1000 ng/ml) as a positive control, cognate peptides (10 µM) or an irrelevant HLA-A2-binding peptide (Survivin/96-104, Surv, 10 µM) as a negative control in a round bottom 96-well plate. After 5 h of incubation at 37 °C, cells were spun down for 3 min at 568 g in a cooled centrifuge (4 °C), after which the supernatant was discarded. A mastermix of the respective ABs (CD3, CD4, CD8, CD19) and Zombie Aqua in

staining buffer was prepared and 50 µl were added to each well. The cells were incubated at 4 °C in the dark for 30 min. 150 µl staining buffer were added as the first washing step and cells were spun down for 3 min at 568 g at 4 °C. The supernatant was discarded and the cells were washed two additional times with 200 µl staining buffer. 100 µl of the fixation/permeabilization solution from the BD Cytofix/Cytoperm™ Kit were added to the cells. By incubating the cells in this buffer, the cellular proteins are crosslinked by formaldehyde and the cell membrane is disrupted by the detergents in the buffer. The cells are thus fixed and permeabilized. After 10 min of incubation in the dark at 4 °C, 100 µl 1x wash buffer from the BD Cytofix/Cytoperm™ Kit were added and the cells were spun down for 3 min at 568 g at 4 °C. The cells were washed two times more with 200 µl of 1x wash buffer. IFN-γ and TNF-α ABs were diluted in staining buffer. 50 µl of this mixture were added to each well, followed by incubation in the dark at 4 °C for 30 min. 150 µl 1x wash buffer were added to the cells and the cells were spun down for 3 min at 568 g at 4 °C. The cells were washed two times more with 200 µl of 1x wash buffer. Subsequently, the cells were taken up in 200 µl flow cytometry fix buffer.

3.2.18 *In vitro* T cell expansion from splenocytes

To expand specific T cells *in vitro*, splenocytes (containing $CD4^+$ T cells, $CD8^+$ T cells and professional APCs) isolated from vaccinated mice were cultured in upright standing flasks in T cell medium supplemented with the cognate epitope (100 nM). For harvesting of these non-adherent cells, cells were thoroughly resuspended in the culture medium and then used in further experiments.

3.2.19 Isolation of $CD8^+$ T cells

$CD8^+$ T cells were isolated according to the manual for the "untouched $CD8^+$ isolation kit" from BD. $1x10^7$ cultured splenocytes were taken up in 40 µl of MACS buffer and 10 µl of a cocktail of biotinylated ABs (CD4, CD11b, CD11c, CD19, CD45R (B220), CD49b (DX5), CD105, MHC-class II, Ter-119 and TCRγ/δ) were added. Cells were incubated for 5 min at 4 °C. Thus, all cell populations except $CD8^+$ T cells were bound by ABs. 30 µl of MACS buffer and 20 µl of streptavidinylated iron beads were added to the cells. Subsequently, cells were incubated at 4 °C for 10 min. The streptavidin on the iron beads binds strongly to the biotin coupled to the ABs. Thus, all non-$CD8^+$ T cells are attached to iron beads. After the incubation time, the volume of the solution was adjusted to 500 µl by the addition of MACS buffer. A LS MACS

column was placed in a MACS magnet and rinsed with 3 ml MACS buffer. Afterwards, the cell suspension was applied to the column. The column was washed two times with 1 ml MACS buffer. In this step, all $CD8^+$ T cells were washed out of the column while all other cells were magnetically retained in the column since they were coupled to iron micro beads. The unlabeled (untouched) $CD8^+$ T cells were collected and counted for subsequent experiments.

3.2.20 Cytotoxicity assay – Vital-FR

To assess the specific cytotoxicity of T cells, *in vitro* expanded T cells were magnetically isolated and used as effector cells in a flow cytometry-based cytotoxicity assay (Stanke *et al.*, 2010). The working principle of the Vital-FR assay is illustrated in Figure 36.

For this assay, PAP-A2 specific target cells were labeled with CFSE (in PBS with 2.5 µM CFSE), 2277NS unspecific target cells with FarRed dye (FR) (in PBS with 0.5 µM FR) for 15 min at 37 °C in an incubator. After the incubation period, cells were spun down (422 g, 4 min, RT), the supernatant was discarded and cells were washed three times with RPMI/10 % FCS. Subsequently, both specific target cells and unspecific target cells were cultured for 24 h, harvested by trypsinization and then mixed at a 1:1 ratio. 3,000 target cells (1,500 specific target cells plus 1,500 unspecific target cells) were seeded in triplicates into the wells of a 96-well plate.

For the comparison of specific peptide-loaded 2277NS/unspecific peptide-loaded 2277NS, cells were labeled and cultured for 24 h as described above. Subsequently, cells were loaded with the respective minimal epitope. For this, they were incubated for 1.5 h in an incubator in 1 ml RPMI/10 % FCS containing 10 µM of the respective peptide. After incubation, cells were washed three times with 1 ml RPMI/10 % FCS and spun down (422 g, 4 min, RT) before they were seeded in 96-well plates.

MACS-isolated $CD8^+$ T cells were added in different ratios to the wells containing the target cells. Ratios ranged from zero $CD8^+$ up to 20:1 (20 times more effector cells than target cells). After 48 h of co-incubation of target cells and T cells, the medium was taken off, the well was carefully washed once with PBS and the cells in the well were harvested by trypsinization. Cells were spun down for 4 min at 422 g, the supernatant was discarded, cells were taken up in flow cytometry fix buffer and stored at 4 °C in the dark until flow cytometry analysis. The

frequency of live $CFSE^+$ and live FR^+ cells was determined and specific killing was calculated using the formula depicted below.

$$\%\ specific\ killing = 100 - \frac{\left(\frac{\%\ specific\ target\ cells\ with\ T\ cells}{\%\ unspecific\ target\ cells\ with\ T\ cells}\right)}{\left(\frac{\%\ specific\ target\ cells\ without\ T}{\%\ unspecific\ target\ cells\ without\ T\ cells}\right)} x100$$

3.2.21 Tumor inoculation

A2.DR1 mice were housed under specific pathogen free conditions. Seven to 15-week-old animals were selected for experiments and pooled in age-matched groups at least seven days prior to experiments. For tumor challenges, PAP-A2 cells were harvested by trypsinization and subsequent stopping of the process by addition of 2277NS medium. Cells were spun down for 4 min at 422 g and the supernatant was discarded. Cells were taken up in 50 ml PBS and counted. The required number of cells was taken out, spun down again, taken up in PBS and transferred to 2 ml Eppendorf tubes. Cells were spun down again (194 g, 4 min, RT) and the supernatant was taken off completely with a pipette. Cells were taken up in PBS (for the injection of $1{,}5x10^6$ PAP-A2 cells: 50 µl PBS/$1{,}5x10^6$ cells) and put on ice. After the cell suspension had cooled down to 4 °C, an equal volume of matrigel was added. The mixture was resuspended thoroughly by pipetting. The mixture was kept on ice until injection. The subcutaneous injection into the flank of the mice was performed with precooled syringes and 27G needles. After tumor inoculation, tumor growth was monitored by measuring with digital calipers every 2-4 days. Animals were sacrificed when the tumor volume exceeded 1000 mm^3 or when the animals exhibited signs of distress such as extreme weight loss or apathy. The tumor volume was calculated using the formula below.

$$tumor\ volume = length\ x\ width^2\ x\ 0.6$$

3.2.22 Statistics

For calculation of statistical significance, GraphPad Prism 5 software was used. The used statistical tests are indicated in the legends for the respective figures.

4 Results

4.1 Establishment of genotyping PCRs for A2.DR1 mice

The genotypic background of all mice used for breeding was monitored throughout the work presented here to exclude breeding errors. To fully verify the genetic identity of A2.DR1 mice, seven genotyping PCRs are needed. Three different PCRs show the presence of the three transgenes: the HHD molecule (a chimeric molecule consisting of the α3 domain from H-2D^b and the α1 and α2 domains from HLA-A*0201, covalently linked to human β2m), HLA-DRA1 and HLA-DRB1. The presence of all three transgenes could be confirmed in our A2.DR1 mice (Figure 11). Unexpectedly, we sometimes observed weak bands in the PCR products generated from C57BL/6 negative controls migrating at the same level as the bands indicating the presence of the HLA-DR1 transgenes in A2.DR1 mice. To control for substrain-specific effects we included DNA samples from the two C57BL/6 substrains C57BL/6N and C57BL/6J in our analysis.

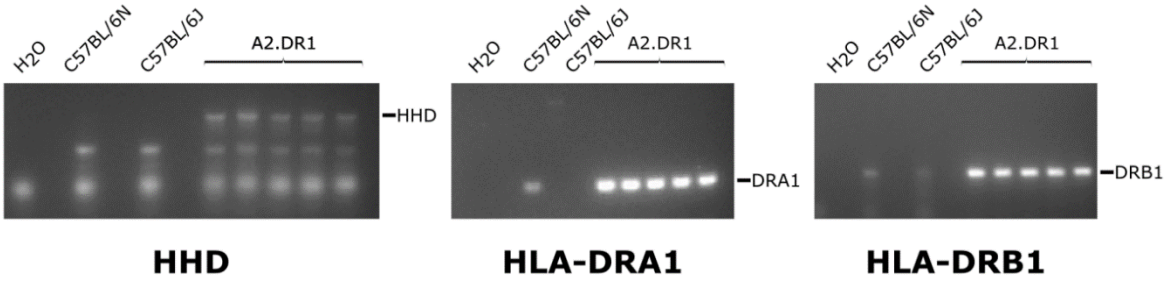

Figure 11. Genotyping PCRs confirm the presence of the HHD, HLA-DRA1 and HLA-DRB1 transgenes in the genome of A2.DR1 mice

The three PCRs (HHD, HLA-DRA1, HLA-DRB1) were performed with the primers and PCR programs as described in Table 1. The sizes of the PCR-amplified fragments are: HHD=400 bp, HLA-DRA1=153 bp, HLA-DRB1=228 bp. H_2O and DNA obtained from biopsies of C57BL/6 mice served as negative controls for DNA obtained from A2.DR1 breeding animals.

We hypothesized that the large degree of sequence similarity between HLA-DR1 and murine MHC class II sequences allowed the HLA-DR1 primers to bind to murine MHC class II genes, thus giving rise to the weak bands observed upon analysis of the PCR product. Therefore, we tested the same primer combinations also in an experiment with DNA from MHC class II KO mice as additional negative template controls. Interestingly, DNA templates from MHC

class II KO mice also induced some bands, but no bands migrating at the same level as the bands consisting of the amplified sequences of HLA-DRA1 and HLA-DRB1 (Figure 12).

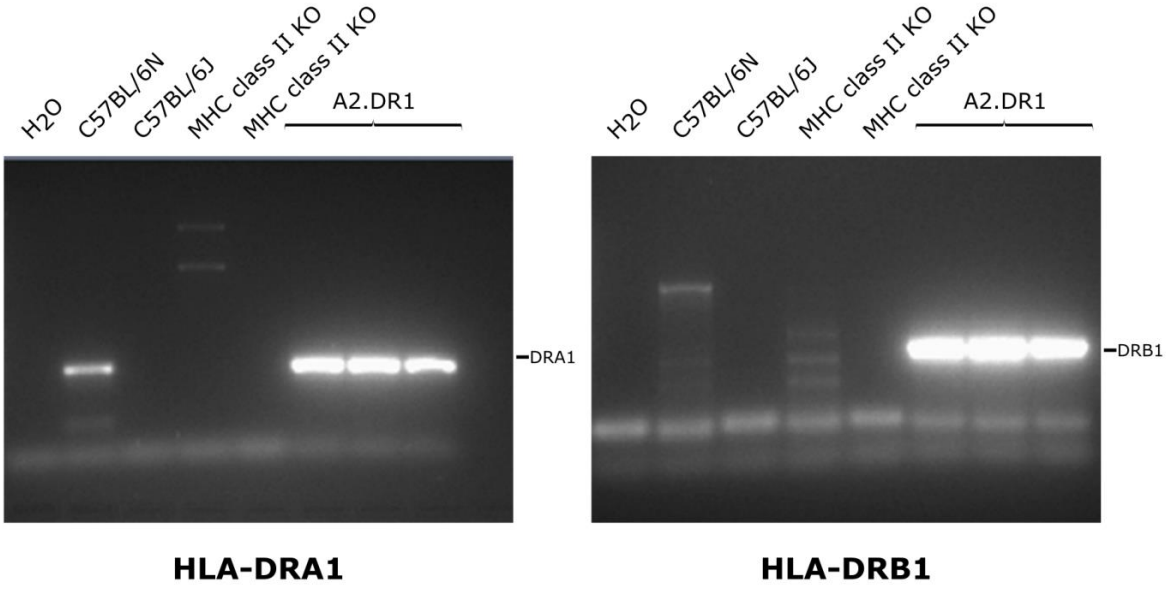

Figure 12. No amplification of a fragment resembling the HLA-DR1 PCR fragment from MHC class II KO mice template DNA

The PCRs for the detection of the transgenes HLA-DRA1 and HLA-DRB1 were performed with the primers and PCR programs as described in Table 1. H_2O and DNA obtained from biopsies of C57BL/6 mice served as negative controls for DNA obtained from A2.DR1 breeding animals. In contrast to the experiment shown in Figure 11, in this experiment, DNA obtained from biopsies of MHC class II KO mice were included as additional negative controls.

In addition to the presence of the transgenes, also the knockout of murine β2m, of H-2D^b and of the murine MHC class II locus needed to be assessed. Due to a mix of three primers, two different bands are generated in the β2m PCR depending on whether the template DNA was obtained from a C57BL/6 or an A2.DR1 sample (Figure 13, upper left panel) verifying the presence or KO of murine β2m, respectively. The same holds true for the MHC class II KO PCR with the only difference that this PCR reaction uses 4 primers (Figure 13, upper right panel). The KO of the H-2D^b gene in A2.DR1 is assessed via two different PCRs: one PCR (H-2D^b WT) amplifies the wildtype H-2D^b, resulting in no PCR product in A2.DR1 mice. The other PCR (H-2D^b KO) amplifies the resistance cassette used to interrupt the H-2D^b gene in A2.DR1 mice (Figure 13, lower panels). In all these PCRs, samples generated from A2.DR1 mice and

C57BL/6 control mice gave rise to the expected band patterns during the analysis of the PCR products.

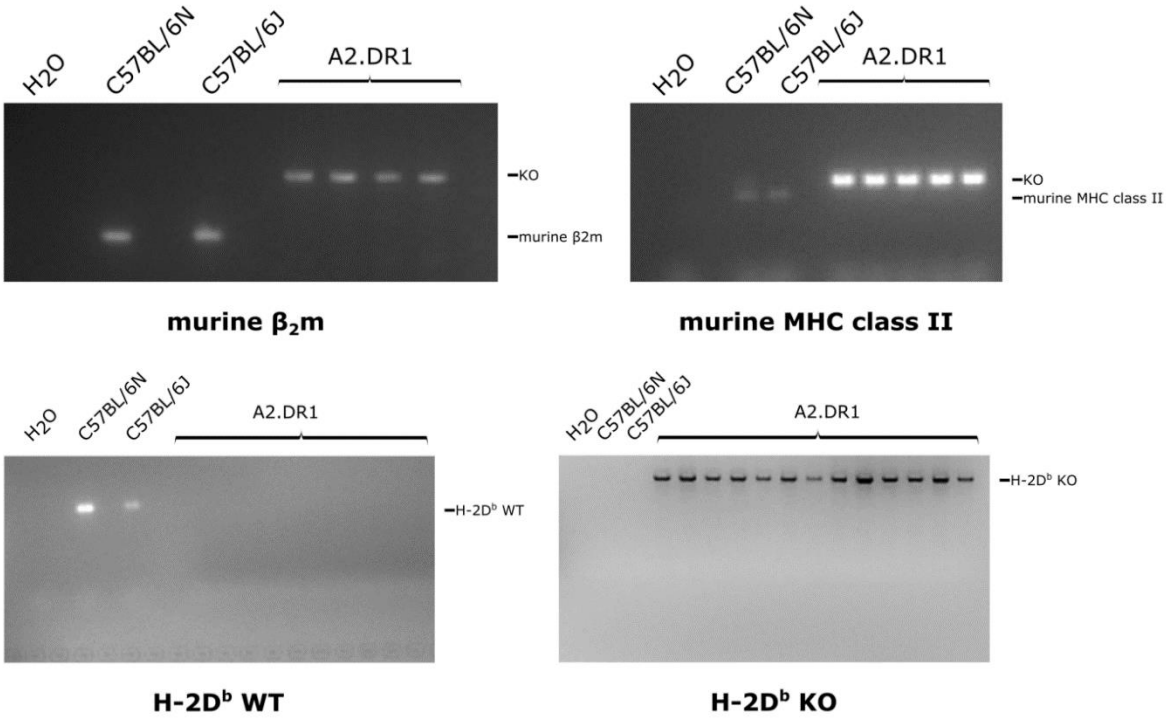

Figure 13. Genotyping PCRs show the KO of murine antigen presentation-related genes in A2.DR1 mice

The four PCRs (β2m, MHC class II KO, H-2Db KO and H-2Db WT) were performed with the primers and PCR programs as described in Table 1. The sizes of the PCR-amplified fragments are: β2m KO=600 bp, murine β2m=270 bp, MHC class II KO=209 bp, murine MHC class II=178 bp, H-2Db WT=1600 bp, H-2Db KO=340 bp. H_2O and DNA obtained from biopsies of C57BL/6 mice served as controls for DNA obtained from A2.DR1 breeding animals.

The exemplary results shown in Figure 11 - Figure 13 could be reproduced for all the A2.DR1 mice used for breeding in this study. This finding proves that the A2.DR1 breeding colony had the desired genotype.

4.2 Generation of the PAP-A2 cell line

The strategy to generate a HPV16 E6/E7-positive tumor model suitable for A2.DR1 mice was to transduce the chemically induced sarcoma cell line 2277NS with HPV16 E6/E7. However, since the 2277NS cell line is derived from A2.DR1^{old} mice, a slightly different version of the A2.DR1 mouse model than the one used in this study, the potential of 2277NS cells to form tumors in "our" A2.DR1 mice had to be established. Indeed, the injection of 0.8x10^6 2277NS cells induced tumor growth in 3 out of 3 mice (Figure 14).

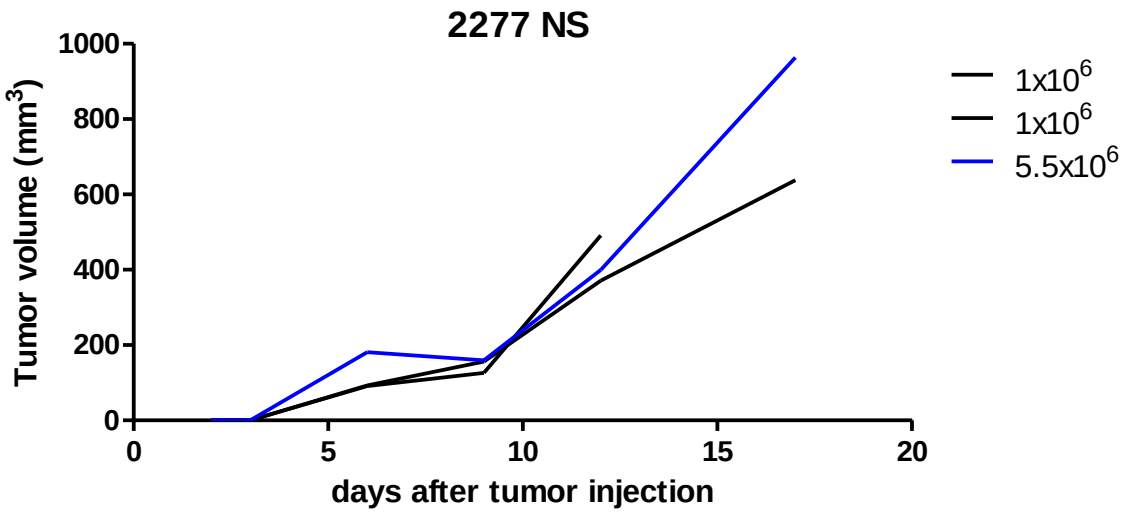

Figure 14. Growth of 2277NS cells in A2.DR1 mice

A2.DR1 mice were injected with 1x10^6 (n=2) or 5.5x10^6 (n=1) 2277NS cells in matrigel. Tumor size was measured with digital calipers and tumor volume was calculated with the formula *volume = length x width^2 x 0.6*.

After having validated the tumorigenicity of 2277NS cells in A2.DR1 mice, we assessed the expression of HLA-A2 in the form of the chimeric HHD molecule on the cell surface since only a model with sufficient expression of HLA-A2 can be targeted by antigen-specific immunotherapy. We found the expression of HLA-A2 on 2277NS cells to be low (example shown in Figure 15) but to be consistently detectable (data not shown). Healthy cells upregulate MHC class I expression upon exposure to IFN-γ. We tested if this was also true for 2277NS cells and could observe an upregulation of HLA-A2 after treatment with IFN-γ for 48 hours (Figure 15).

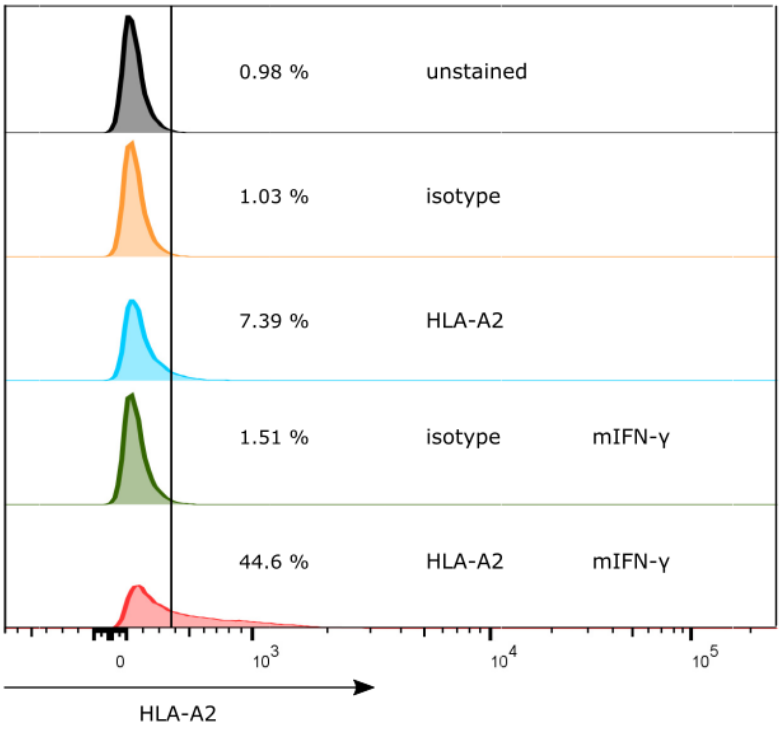

Figure 15. 2277NS cells upregulate HLA-A2 expression after exposure to IFN-γ

2277NS cells were either incubated with murine IFN-γ for 48 h or left untreated. Cells were subsequently stained with anti-HLA-A2 ABs coupled to FITC, with the respective FITC-coupled isotype control or left unstained. Intensity of staining was assessed by flow cytometry.

4.2.1 Transduction of 2277NS cells with pWPI E6/E7

Cell lines suitable as a tumor model for testing therapeutic vaccinations against HPV16-induced malignancies in the A2.DR1 mouse model should have three characteristics: First, tumorigenic growth in A2.DR1 mice, second, expression of HLA-A2 and third, expression of HPV16 E6/E7. After having established the adequacy of 2277NS cells for the characteristics of tumorigenic growth and HLA-A2 expression, HPV16 E6/E7 expression had to be induced in these cells. To this end, 2277NS were transduced with the lentiviral vector pWPI HPV16 E6/E7 (vector map shown in Figure 16) by Ruwen Yang (DKFZ). Also the vector was kindly supplied by R. Yang.

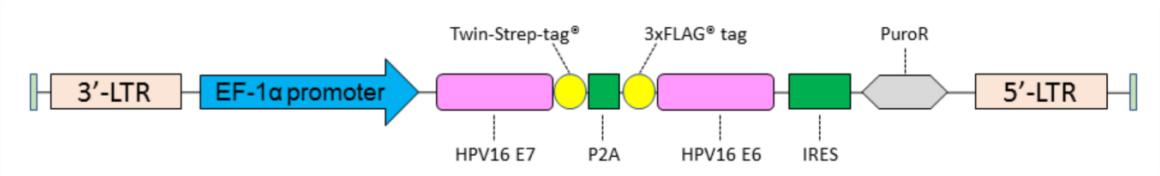

Figure 16. Vector map pWPI HPV16 E6/E7

The lentiviral pWPI vector used for the introduction of HPV16 E6 and E7 into 2277NS cells. The expression of strep-tagged E7, flag-tagged E6 and a puromycin resistance cassette are under the control of a single EF-1α promotor. The use of a P2A sequence and an IRES sequence allows the expression of three different proteins from one mRNA. Figure taken from Kruse *et al.*, provided by Ruwen Yang.

Successfully transduced 2277NS were puromycin-resistant and were called 2277NS (pWPI). These cells were analyzed by Western blot (WB) for E6 and E7 expression and were found to express the introduced tagged versions of E6 and E7. The expression levels of E6 and E7 were found to be higher than in CaSki cells, which are derived from a metastatic cervical carcinoma (Pattillo *et al.*, 1977) and express the natural untagged HPV16 E6/E7 proteins. Parental 2277NS cells, used as negative controls, did not give rise to E6 or E7 bands (Figure 17).

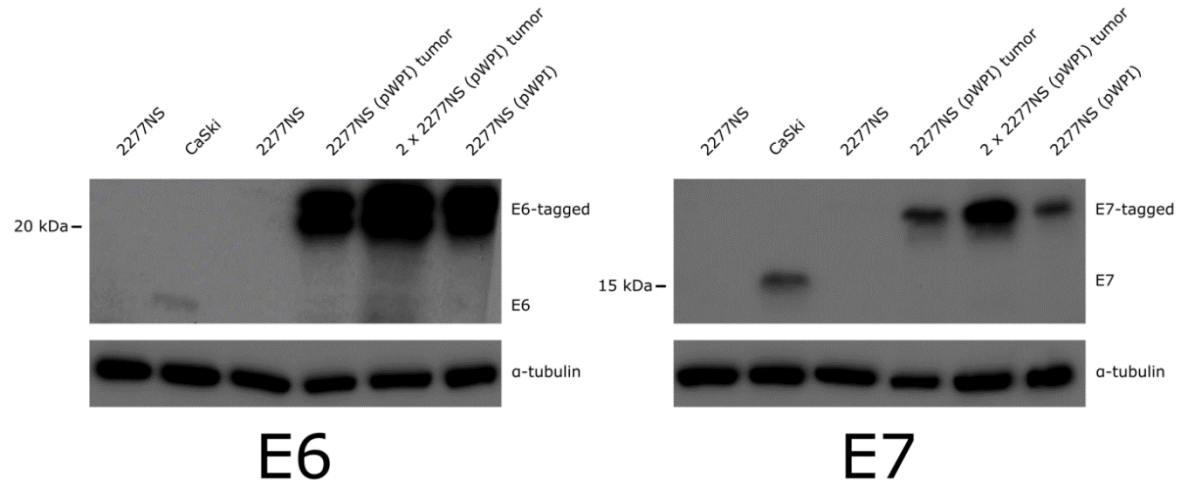

Figure 17. 2277NS cells transduced with pWPI HPV16 E6/E7 express HPV16 E6/E7

15 µg of lysates of the indicated cell lines and tumors (30 µg for 2 x 2277NS (pWPI) tumor) were separated by SDS-PAGE in an AnykD™ polyacrylamide gel and blotted subsequently onto a PVDF membrane. Membranes were incubated with primary ABs specific for E6 (left, clone E6-6F4) and E7 (right, clone NM2) and were subsequently incubated with suitable HRP-coupled secondary ABs. The membrane parts with the E6/E7 proteins were developed with high-sensitive ECL solution, the α-tubulin-containing membrane parts with normal ECL solution.

Next, we assessed if 2277NS (pWPI) cells were still able to form tumors in A2.DR1 mice. This was necessary since by the introduction of viral antigens, the immune system of the mice could recognize these cells as foreign or virus-infected and therefore reject them. Injection of 10^6 2277NS (pWPI) cells in three A2.DR1 mice proved that either no immune response was triggered or that the immune response induced against these cells was not strong enough to cause rejection since all three mice developed outgrowing tumors with growth kinetics similar to tumors induced by 2277NS cells (data not shown). The continued HPV16 E6/E7 expression of these tumors was confirmed by WB (Figure 17).

To obtain a homogenous cell line with the required characteristics, we generated clonal cell lines by single cell sorting. We sorted the top 1 % HLA-A2 expressing cells from the 2277NS (pWPI) polyclonal cell line into single wells of a 96-well plate, from which we expanded the clones to sufficient cell numbers for subsequent analysis (Figure 18).

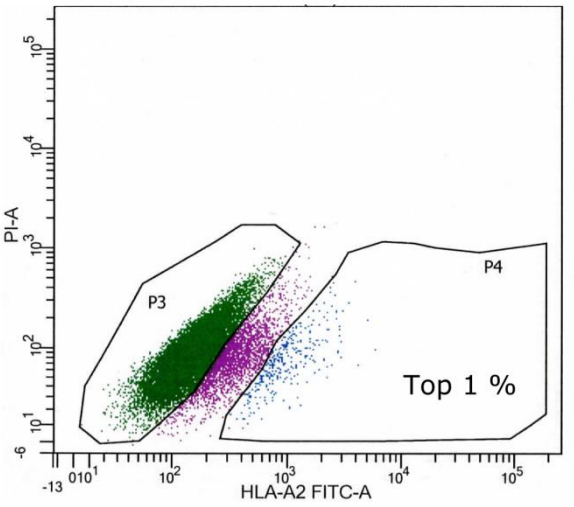

Figure 18. Single cell sorting of 2277NS (pWPI) for clones with high HLA-A2 expression

2277NS (pWPI) cells were stained with anti-HLA-A2 AB. The top 1 % of HLA-A2-expressing cells were sorted (1 cell per well) into 96-well plates to generate clonal cell lines.

The 2277NS (pWPI) clonal cell lines were examined for the three characteristics specified before. WB analysis revealed that not all clones expressed E6 and E7 (Figure 19), despite being puromycin resistant. Additionally, E6/E7 expression levels varied between clones. In general, clones expressing comparably high levels of E6 also expressed comparably high levels of E7. All clones expressed higher levels of E6 and E7 than the two cell lines acting as positive controls, TC-1 and CaSki. The TC-1 cell line was established by transducing C57BL/6-derived lung cells with HPV16 E6/E7. Interestingly, we failed to detect E6 protein in CaSki and E7 protein in TC-1 cells in these WBs.

Parts of the work concerning the analysis of the clonal cell lines were generated during the course of Philipp Scherer's bachelor thesis under the direct supervision of Sebastian Kruse. Therefore, some of the results shown here were also presented in Philipp Scherer's bachelor thesis.

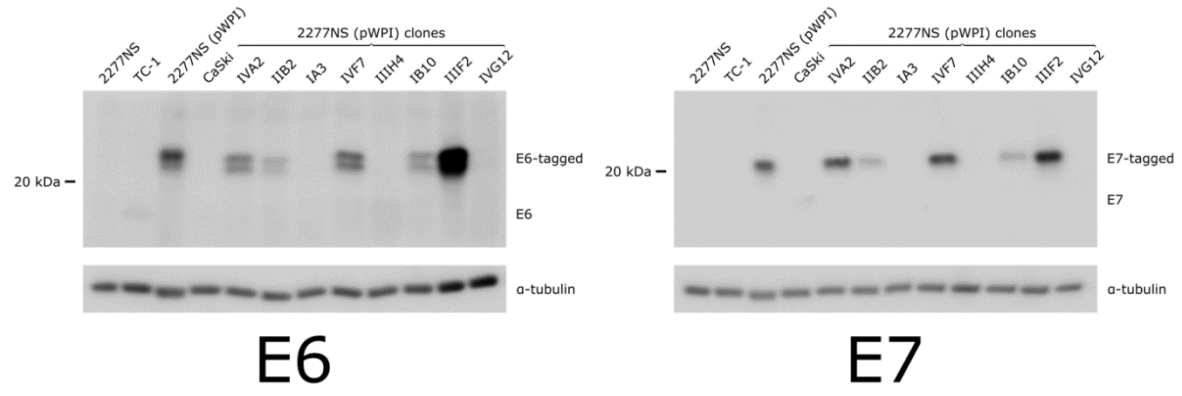

Figure 19. Clonal 2277NS (pWPI) cell lines show different E6/E7 expression patterns

15 µg of lysates of the indicated cell lines were separated by SDS-PAGE in an AnykD™ polyacrylamide gel and blotted subsequently onto a PVDF membrane. Membranes were incubated with primary ABs specific for E6 (left, clone E6-6F4) and E7 (right, clone NM2) and were subsequently incubated with suitable HRP-coupled secondary ABs. The membrane parts with the E6/E7 proteins were developed with high-sensitive ECL solution, the α-tubulin-containing membrane parts with normal ECL solution.

Since it could be shown before (Figure 15) that 2277NS cells express only low levels of HLA-A2, we also tested the HLA-A2 expression of the clonal cell lines. Figure 20 shows the quantification of HLA-A2, E6 and E7 expression of the clonal cell lines, each normalized to the value of the cell line with the highest expression levels. The differences in HLA-A2 expression are remarkably high, with the clone IIIF2 having approximately 20 times less surface HLA-A2 than the highest expressing clone IVF7. This is especially interesting considering the fact that all clonal cell lines were derived from clones that ranked among the top 1 % of HLA-A2 expressing cells in the polyclonal 2277NS (pWPI) cell line. Out of the eight tested clones, three did not express E6 or E7, which rendered them unusable as a tumor model. Therefore, the clones left to be tested for their tumorigenicity were clones IVA2, IIB2, IVF7, IB10 and IIIF2.

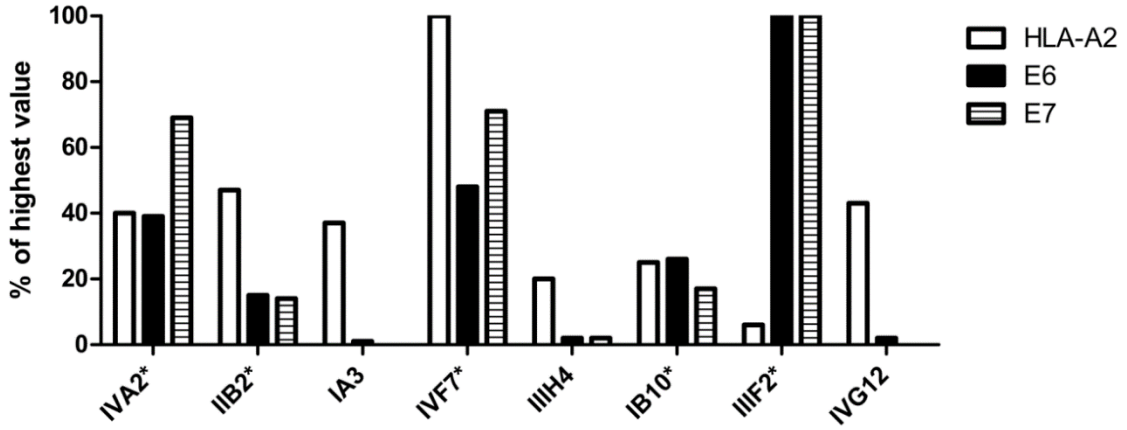

Figure 20. HLA-A2, E6 and E7 expression of clonal 2277NS (pWPI) cell lines

Values are normalized to the highest value. HLA-A2 expression (white bars) of the clonal cell lines was quantified by flow cytometry analysis. Data for E6/E7 expression levels (black/striped bars) are derived from the E6/E7 WBs shown in Figure 19. The optical density of the bands in these WBs was quantified with the software ImageJ. Clones marked with an asterisk exhibited E6/E7 expression and were later tested for tumorigenicity in *in vivo* experiments.

4.2.2 Reisolation of IVA2 cells after *in vivo* passage

To test the tumorigenicity of the E6/E7-expressing clones (IVA2, IIB2, IVF7, IB10 and IIIF2), three or four mice for each clone were injected with $0.75x10^6$ cells of the respective cell line. No sustained tumor growth could be observed for all clones (data not shown) except for one mouse injected with the IVA2 clone (Figure 21). This tumor was removed and transferred into *in vitro* cell culture. The resulting cell line was named PAP-A2 (for **pap**illomavirus HLA-**A2**). 6 master cryo-stock vials of PAP-A2 cells were generated and stored in liquid nitrogen. One of the master stocks was thawed to be expanded to generate 120 single-use cryo-stock vials of PAP-A2 cells that were also frozen and stored in liquid nitrogen. All following experiments presented in this thesis could therefore be conducted with PAP-A2 cells with a defined passage number, since a new single-use cryo-stock was thawed prior to the experiments.

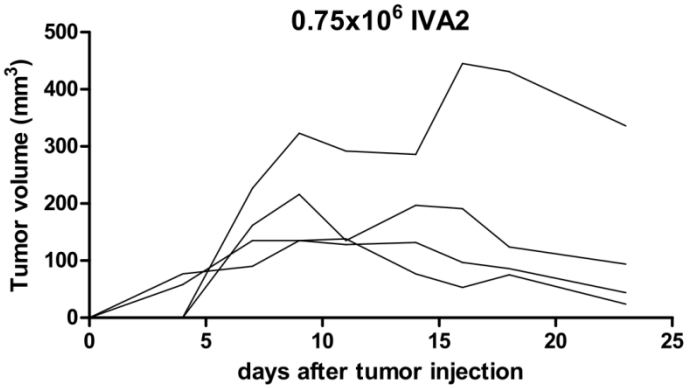

Figure 21. Clone IVA2 gives rise to tumor growth in one A2.DR1 mouse

Four A2.DR1 mice were injected with $0.75x10^6$ IVA2 cells in matrigel. Subsequently, mice were monitored for tumor growth. The only mouse exhibiting tumor growth was sacrificed at day 23 after tumor injection and the tumor cells were isolated for further *in vitro* culture.

4.2.3 Characterization of PAP-A2 cells

We tested the newly generated PAP-A2 cell line for E6/E7 sequence identity, HLA-A2-expression, E6/E7 expression and *in vivo* growth. The E6/E7 sequences found in PAP-A2 cells were found to be identical to the E6/E7 sequences in the pWPI HPV16 E6/E7 vector (data not shown). Flow cytometry-based assessment of HLA-A2 expression showed more HLA-A2-expression by PAP-A2 cells than was seen in 2277NS cells (Figure 15, Figure 22). Since it had been established in previous experiments that there is virtually no background binding of the FITC-coupled isotype control AB to 2277NS derived cells, this control was omitted in this experiment.

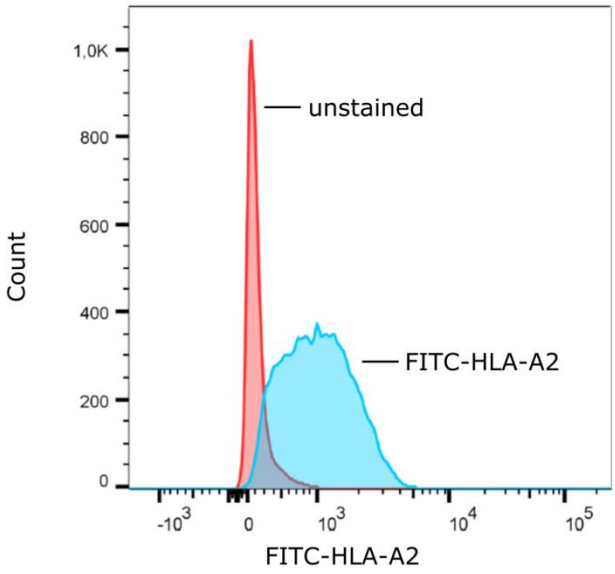

Figure 22. PAP-A2 cells express high levels of HLA-A2

PAP-A2 cells were stained with anti-HLA-A2 AB or left unstained. The intensity of the staining was assessed by flow cytometry.

WB analysis revealed that PAP-A2 cells express HPV16 E6 and E7 and still do so after having grown as a tumor in A2.DR1 mice (Figure 23). As already shown in Figure 17, the HPV16$^+$ cervical cancer-derived cell line CaSki expresses the natural HPV16 E6/E7 whereas the 2277NS (pWPI)-derived PAP-A2 cells express the tagged versions of E6/E7 that were introduced via the lentiviral construct pWPI HPV16 E6/E7. As expected, the parental 2277NS cells do not express the E6 and E7 proteins. Interestingly, the relative E6 expression level of CaSki is lower than the one for PAP-A2. In contrast, the relative E7 expression level of CaSki is higher than the one for PAP-A2.

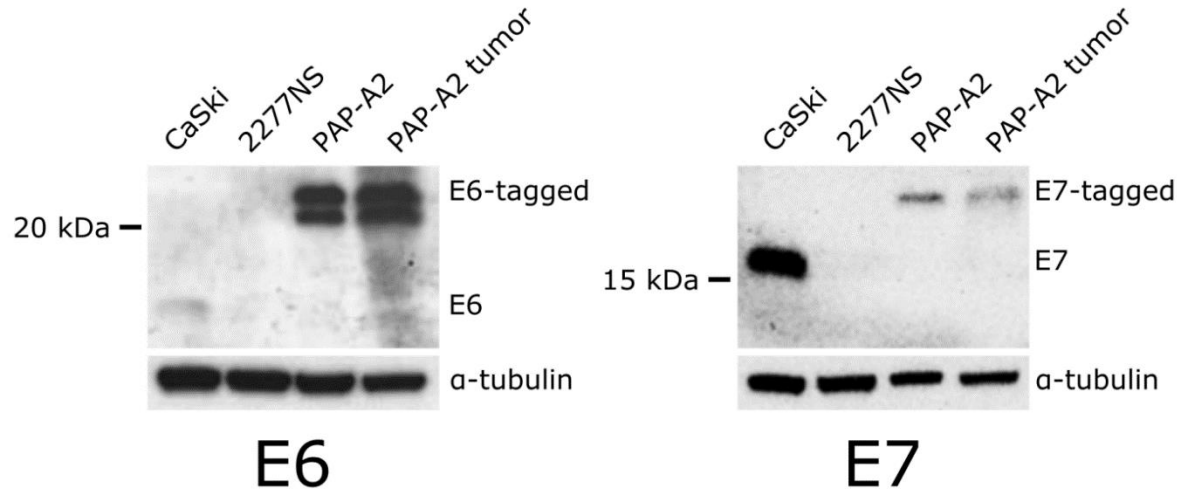

Figure 23. HPV16 E6/E7 expression of the PAP-A2 cell line

15 µg of lysates of the indicated cell lines and tumor were separated by SDS-PAGE in an AnykD™ polyacrylamide gel and blotted subsequently onto a PVDF membrane. Membranes were incubated with primary ABs specific for E6 (left, clone E6-6F4) and E7 (right, clone NM2) and were subsequently incubated with suitable HRP-coupled secondary ABs. The membrane parts with the E6/E7 proteins were developed with high-sensitive ECL solution, the α-tubulin-containing membrane parts with normal ECL solution.

Finally, the *in vivo* growth of PAP-A2 cells was assessed. Injection of $1x10^6$ PAP-A2 cells induced tumor growth in 60 % of mice, injection of $2.5x10^6$ and $5x10^6$ led to tumor growth in 100 % of the injected mice (Figure 24). To induce as high a tumor-take as possible and at the same time induce tumor growth slow enough to allow for therapeutic intervention, in all subsequent tumor experiments $1.5x10^6$ PAP-A2 were used for tumor inoculations.

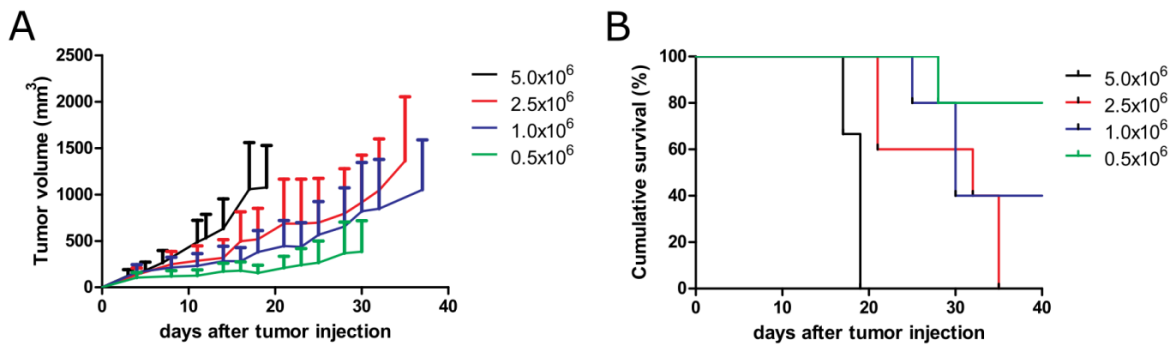

Figure 24. Cell number titrations with PAP-A2 cells

A2.DR1 mice were injected with different numbers of PAP-A2 cells and monitored for tumor growth. A, tumor growth curves and B, survival curves of groups. Groups consisted of n=3 for $5x10^6$ and n=5 for all other groups. In A, mean and error bars (standard deviation (SD)) are depicted.

4.3 Epitope-specific vaccination against HPV16 E6/E7-positive tumors

Various vaccine formulations have been developed for therapeutic anti-HPV16 vaccines, among them vaccines that contain the full protein sequences as well as vaccines containing only parts of the two main targets E6 and E7 (Khallouf, Grabowska and Riemer, 2014; Chabeda *et al.*, 2018; Hancock, Hellner and Dorrell, 2018). It was shown by mass spectrometry analysis that not all possible HLA-A2-restricted E6/E7 epitopes are presented by $HPV16^+$ cell lines derived from human cervical cancer (Riemer *et al.*, 2010; Blatnik *et al.*, 2018). Therefore, we hypothesized that it is important to select only E6/E7 epitopes for vaccination that are presented on $HPV16^+$ tumor cells since T cells specific for all other epitopes cannot contribute to anti-tumor effects. Consequently, we tested only vaccine formulations in our newly established A2.DR1 mouse model that allow the use of defined epitopes since only this ensures that the vaccination-induced immune response consists of T cells which can recognize tumor cells.

For first immunogenicity tests we selected the epitope E7/11-19 since this epitope was found to be presented on HLA-A2 on several cell lines of human cervical cancer at relatively high abundance (Riemer *et al.*, 2010; Blatnik *et al.*, 2018) and also T cells specific for this epitope were found in the blood of healthy donors (Blatnik *et al.*, 2018). In the latter study, 50 % of HPV16-reactive healthy donors responded strongly against E7/11-19.

4.3.1 Determination of the most suitable vaccine formulation for CD8+ T cell induction in A2.DR1 mice

4.3.1.1 Emulsion-based vaccines

Emulsion-based vaccines are generated from two different liquids, a hydrophobic and a hydrophilic phase, in which the hydrophilic phase contains the water-soluble antigens. The antigens used in this formulation are often minimal epitopes or SLPs that are only weakly immunogenic on their own. The mineral oil that is often used as the hydrophobic phase cannot be degraded physiologically and therefore ensures a depot effect at the injection site. For our experiments, we used the mineral oil formulation ISA51, since it is commercially available in a high quality that allows conducting experiments with an exactly defined compound. Furthermore, ISA51 has been previously used in clinical studies for the induction of anti-cancer immune responses (Pol *et al.*, 2015) and has a well-established safety profile (van Doorn *et al.*, 2016).

We tested this vaccination formulation with our lead epitope E7/11-19. We chose the emulsion-based formulation since it is known to reliably induce $CD8^+$ responses when containing minimal epitopes. Furthermore, this formulation is easily produced with different synthetic peptides. Additionally, since this formulation is considered the gold standard adjuvant for the induction of T cells, obtained results serve as a benchmark to compare the quality of the induced immune response with immune responses induced by other vaccine formulations.

We vaccinated A2.DR1 mice with E7/11-19 together with PADRE (pan HLA-DR epitope) in a water-in-oil emulsion (PBS in ISA51) and determined the frequency of E7/11-19-specific $CD8^+$ T cells 12 days after vaccination. PADRE was included to ensure $CD4^+$ T cell-mediated help for $CD8^+$ T cell activation. For all vaccination experiments, determination of frequencies of epitope-specific $CD8^+$ T cells was done by restimulation of splenocytes of vaccinated mice with either the cognate epitope (E7/11-19) or the irrelevant survivin-derived HLA-A2-binding epitope Surv/96-104 followed by intracellular IFN-γ staining. In all experiments, the frequencies of $CD8^+$ T cells producing IFN-γ after stimulation with the irrelevant epitope were negligible.

Figure 25 shows that low frequencies (in general lower than 0.5 % of $CD8^+$ T cells) were induced with this vaccination approach. To increase the frequency of antigen-specific $CD8^+$ T cells, we subsequently included two different TLR agonists in the formulation: either monophosphoryl lipid A (MPLA), a lipopolysaccharide (LPS) derivative and thus a TLR4 agonist, or XS15, a synthetic variant of the TLR2/3 agonist Pam3Cys. Indeed, the inclusion of MPLA into the vaccine formulation induced on average 0.65 % E7/11-19-specific $CD8^+$ T cells and thus three times more E7/11-19-specific $CD8^+$ T cells than the formulation without MPLA (mean frequency of 0.2 % E7/11-19-specific T $CD8^+$ cells). In the MPLA group, however, the mean frequency is strongly influenced by three animals that exhibited high frequencies of E7/11-19-specific $CD8^+$ T cells (1.4 %, 1.6 % and 3 %). The median frequency is a more robust measure when outliers occur. When comparing the median frequency of the two treatment groups, the inclusion of MPLA induces a median frequency that is twice as high as the median frequency in the group without TLR agonist (0.4 % compared to 0.2 %). Interestingly, the inclusion of XS15 did not induce higher frequencies of E7/11-19-specific $CD8^+$ T cells when compared with the formulation without TLR agonists.

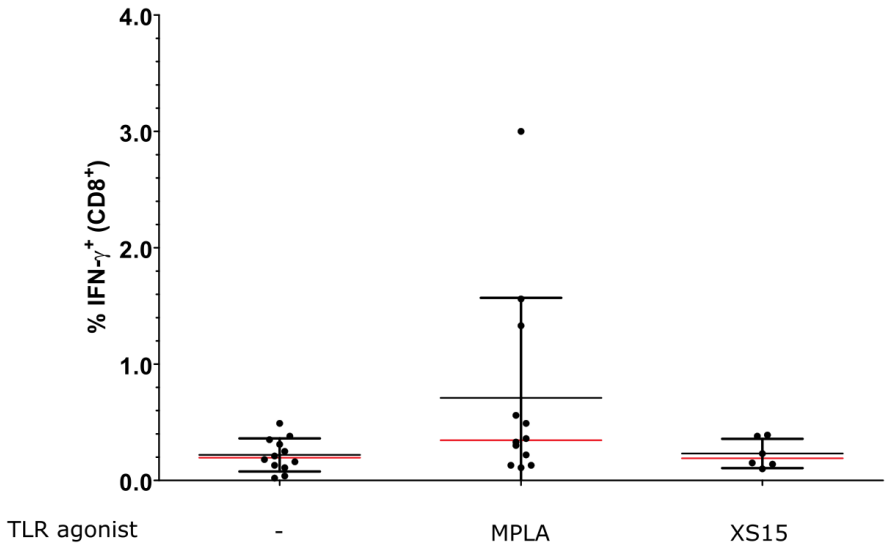

Figure 25. Induction of E7/11-19-specific CD8⁺ T cells with emulsion formulations

A2.DR1 mice were subcutaneously injected with 100 µl E7/11-19-containing ISA51 emulsion with the indicated TLR agonist (20 µg MPLA/mouse or 40 µg XS15/mouse). 12 days after the injection, mice were sacrificed, splenocytes were isolated and stimulated with E7/11-19 peptide in the presence of Golgi apparatus-transport inhibitors. After subsequent intracellular IFN-γ staining, the frequency of IFN-γ⁺ (E7/11-19-specific) CD8⁺ T cells was determined by flow cytometry. Results displayed for no TLR and MPLA are for n=12 mice each, for XS15 for n=6 mice. Data for no TLR and MPLA are from two independent experiments with each n=6. Mean (black bar), median (red bar) and SD are depicted.

4.3.1.2 mRNA vaccines

RNA vaccines offer several advantages over other vaccine formulations. For example, they are self-adjuvanting and allow fast and easy production (Kreiter *et al.*, 2015). Furthermore, the antigen presentation efficiency can be increased by designing mRNA constructs that couple antigens to MHC class I trafficking signals (Kreiter *et al.*, 2007). Additionally, the route of application and the formulation of the mRNA influences the sites and cell types in which the mRNA is expressed. It was shown that intravenous injection of mRNA-lipoplexes can target the RNA expression to professional antigen-presenting cells in spleen and lymph nodes and thus drastically increase vaccination-induced immune responses (Kranz *et al.*, 2016). In a preliminary experiment, we tested the HPV16 E7 full length (FL) mRNA produced by BioNTech (Mainz) for the induction of HPV16 E7-specific CD8⁺ T cells in A2.DR1 mice. Interestingly, in this test experiment, which was designed to screen several mRNA vaccines in small-scale experiments and that was therefore conducted with only one mouse, no

antigen-specific T cells could be found. mRNA encoding only for the minimal epitope E7/11-19 also did not give rise to specific T cells. However, this was an expected result, since earlier experiments performed by BioNTech (personal communication Dr. Christian Grunwitz) demonstrated that the elongation of a minimal epitope with three amino acids N- and C-terminally is necessary to ensure proper epitope processing. This finding was confirmed by our test of mRNA coding for E7/8-21, since both the version with and without the PADRE helper epitope induced $CD8^+$ T cells specific for E7/11-19. Sequence analysis with the epitope prediction server NetMHC 4.0 prior to the experiment showed that the mRNA sequences flanking E7/8-21 (proprietary information of BioNTech) together with E7/8-21 result in a new HLA-A2-binder (SLHEYMLDL). Therefore, we tested also for the induction of $CD8^+$ T cells against this peptide and indeed could find SLHEYMLDL-specific $CD8^+$ T cells in frequencies up to five-fold higher than the ones for E7/11-19. To generate mRNAs that do not induce a response against SLHEYMLDL, we exchanged the serine at position 1 in SLHEYMLDL to alanine, thus removing an anchor amino acid for HLA-A2. However, in mice injected with this mRNA, no E7/11-19 specific $CD8^+$ T cells could be found (data not shown), probably due to impaired antigen processing as a result of the amino acid exchange. The integrity of the mRNA used in this experiment and the general induction of an immune response could be confirmed by the detection of PADRE-specific $CD4^+$ T cells (data not shown).

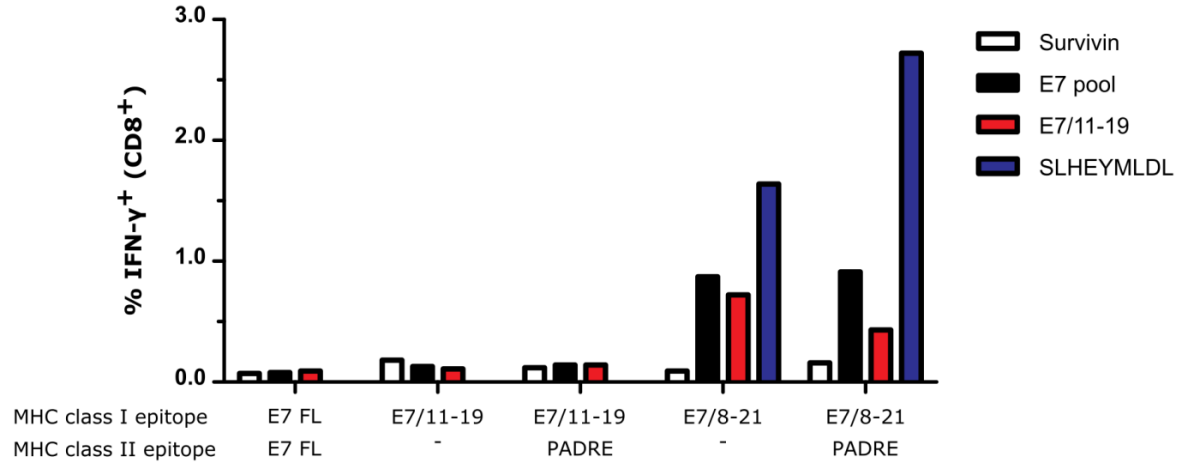

Figure 26. Antigen-specific CD8⁺ T cells after mRNA vaccination

A2.DR1 mice (n=1 per construct) were injected intravenously on days 0, 7, 14, 21 with 40 µg mRNA mixed with lipoplexes. On day 28, mice were sacrificed, splenocytes were isolated and restimulated with the peptides or the peptide pool indicated by the color code in the presence of Golgi apparatus-transport inhibitors. After subsequent intracellular IFN-γ staining, the frequency of IFN-γ⁺ (specific) CD8⁺ T cells was determined by flow cytometry. A survivin-derived epitope was used as an irrelevant HLA-A2-binding control epitope. SLHEYMLDL is an epitope that results from E7/8-21 and the flanking sequences of the mRNA that ensure correct intracellular targeting and epitope processing.

4.3.1.3 Amphiphilic vaccines

Coupling of peptide vaccines to fatty acids induces a strong T cell immune response (Cho *et al.*, 2013; Liu *et al.*, 2014). Since these antigen carriers do not have an inherent ability to activate antigen-presenting cells, they are used together with different TLR agonists such as poly I:C (pIC) or CpG. The study by Liu *et al.* demonstrated that the amphiphilic constructs bind to albumin and “hitchhike” on albumin to the lymph nodes where they are taken up by professional APCs. Subsequently, the activated professional APCs initiate a specific immune response by activating T cells.

We tested the two amphiphilic constructs developed by Liu *et al.* and Cho *et al.* for their compatibility with the minimal HPV16 epitope E7/11-19.

4.3.1.3.1 Pam2 and Stea2

In the amphiphilic construct developed by Cho *et al.*, the epitope of interest is coupled via a four amino acid linker (KFVM, structure in Figure 27) to two palmitic acids (Pam). The synthesis of this construct coupled to E7/11-19 turned out to be challenging since the

purification process was hampered by the fact that the palmitic acid chains attach to the columns that are used for peptide purification. The purity of the construct therefore was estimated to be only 20 %.

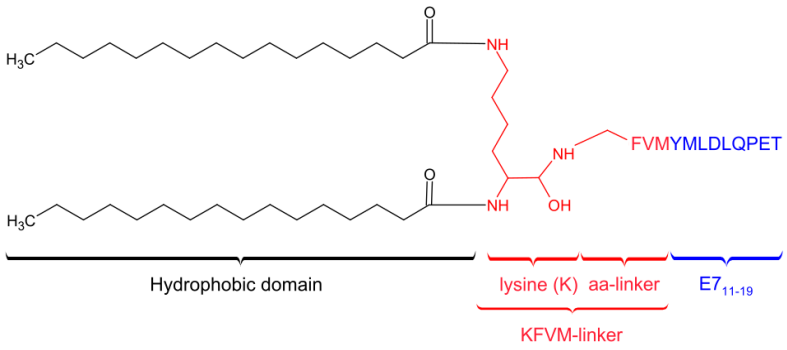

Figure 27. E7/11-19 in the Pam2 amphiphilic construct (Pam2-E7/11-19)

The Pam2-E7/11-19 construct has a hydrophobic domain (black) made up of two palmitic acid chains (C16 bodies). These fatty acid chains are coupled to the amino groups of a lysine, which is the first amino acid of the KFVM linker (red). The E7/11-19 epitope (blue) is coupled to the KFVM-linker via a peptide bond.

Nevertheless, a strong E7/11-19-specific $CD8^+$ T cell response was induced after intravenous injection of this compound together with the TLR3 agonist pIC (Figure 28). This result was even improved by injecting a Pam2-E7/11-19 dose that was twice as high (called Pam2-E7/11-19 2x) as the dose used in the first experiment. However, since this increase in vaccination response was mostly due to one strongly responding mouse (13.4 % E7/11-19-specific $CD8^+$ T cells), the median frequencies of E7/11-19-specific $CD8^+$ T cells were similar after vaccination with the low and the high Pam2-E7/11-19 dose. As a comparison, we injected the free minimal epitope E7/11-19 together with pIC intravenously. After this treatment, we did not observe any E7/11-19-specific $CD8^+$ T cells.

Interestingly, the addition of free PADRE peptide to the vaccine solution drastically reduced the E7/11-19-specific T cell response (data not shown). Therefore, we refrained from using amphiphilic peptides together with free PADRE peptide in subsequent vaccination experiments. Remarkably, the vaccine efficacy enhancing effect of palmitic acid could only be observed when two palmitic acid chains were coupled to the epitope, since the construct

Pam1-E7/11-19 only induced very low frequencies of epitope-specific CD8$^+$ T cells (Figure 28).

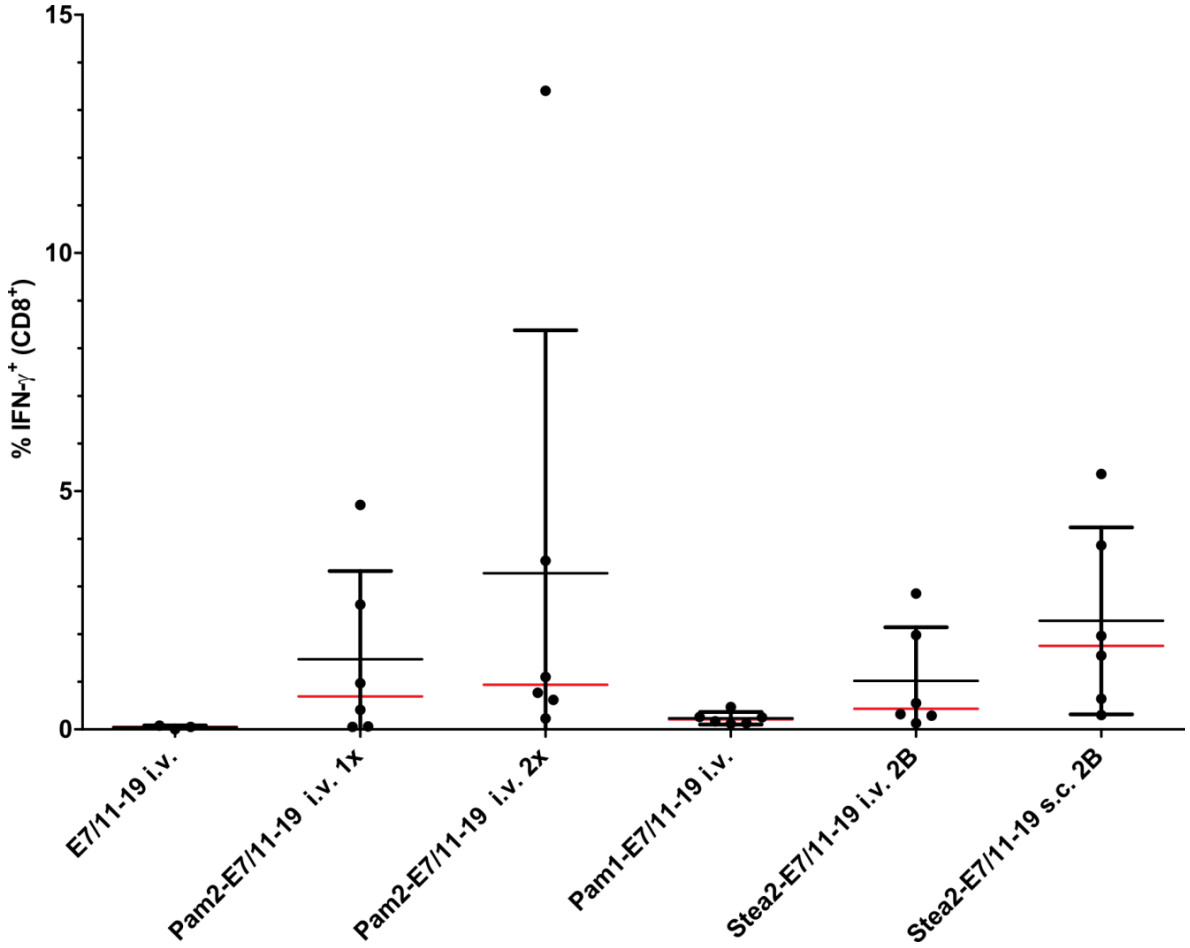

Figure 28. E7/11-19-specific CD8$^+$ T cells induced by Pam2-E7/11-19, Pam1-E7/11-19 and Stea2-E7/11-19 vaccination

A2.DR1 mice (n=3 for E7/11-19 i.v., n=6 per group for the other groups) were injected with the indicated peptide or amphiphilic construct together with 50 µg pIC via the indicated injection route. E7/11-19 i.v. were injected on days 0 and 6 and mice were sacrificed on day 19. Pam2-E7/11-19 1x, Pam2-E7/11-19 2x and Pam1-E7/11-19 were injected on days 0 and 7 and mice were sacrificed on day 21. Pam2-E7/11-19 1x signifies a low dose of Pam2-E7/11-19, Pam2-E7/11-19 2x signifies a double dose. Both Stea2 groups were injected on days 0, 7, 14 and sacrificed on day 21 (2B=2 boosts). Splenocytes of all treatment groups were isolated and stimulated with E7/11-19 peptide in the presence of Golgi apparatus-transport-inhibitors. After subsequent intracellular IFN-γ staining, the frequency of IFN-γ$^+$ (E7/11-19-specific) CD8$^+$ T cells was determined by flow cytometry. Mean (black bar), median (red bar) and SD are depicted.

To overcome the problem of the low purity of the Pam2-E7/11-19 compound, in cooperation with Dr. Max Sauter and Dr. Philipp Uhl from the Department of Nuclear Medicine,

Heidelberg University Hospital, we devised a strategy that allowed synthesizing a similar compound with 2 fatty acids with higher purity. To do so, a compound named Stea2-E7/11-19 was produced. The fatty acids (stearic acids) of this compound are 2 carbon atoms longer than the ones of Pam2 and it was reported that these slightly longer fatty acids induce even better albumin binding than palmitic acid chains (Liu *et al.*, 2014). This compound could be purified to 70 % purity (data not shown). We tested this newly developed compound first with intravenous injection, as performed before with the Pam2-E7/11-19 compound, but in a two-boost regimen. The two-boost regimen was introduced to further increase the frequency of specific T cells. The intraexperimental variance of E7/11-19-specific $CD8^+$ T cell frequencies was much lower with this compound when compared with the results of the vaccination with Pam2-E7/11-19 2x, likely due to the higher purity of Stea2-E7/11-19. However, when disregarding the one very strong responder in Pam2-E7/11-19 2x, frequencies of E7/11-19-specific $CD8^+$ T cells induced by intravenously injected Stea2-E7/11-19 were similar to the ones induced by intravenously injected Pam2-E7/11-19 (Figure 28). In the study by Liu *et al.*, a lipo-PEG-peptide (LPP) amphiphilic compound (see 4.3.1.3.2) was injected subcutaneously and induced high frequencies of epitope-specific $CD8^+$ T cells. Therefore, we also tested our Stea2-E7/11-19 construct with subcutaneous injection. This different route of administration increased the mean frequency of E7/11-19-specific $CD8^+$ T cells from 1 % induced by intravenous injection to 2.2 % (Figure 28).

4.3.1.3.2 LPP

Another amphiphilic minimal epitope construct that we tested to enhance the immunogenicity of E7/11-19 was called lipo-PEG-peptide (LPP), which was developed by Liu *et al.* (Liu *et al.*, 2014). The structure of LPP and the coupling process to E7/11-19 is depicted in Figure 29. The structure shows that two stearic acid chains (C18 bodies) are connected via phosphoethanolamine to a long polyethylene glycol (PEG) spacer, which is in turn connected to maleimide. Maleimide readily reacts with the sulfhydryl group of a cysteine. This mechanism is used during the modular synthesis because it allows coupling every minimal epitope to the maleimide as long as it is extended by an N-terminal cysteine. Using cysteine-extended E7/11-19 (CYMLDLQPET), LPP-E7/11-19 could be generated with a purity of more than 70 %.

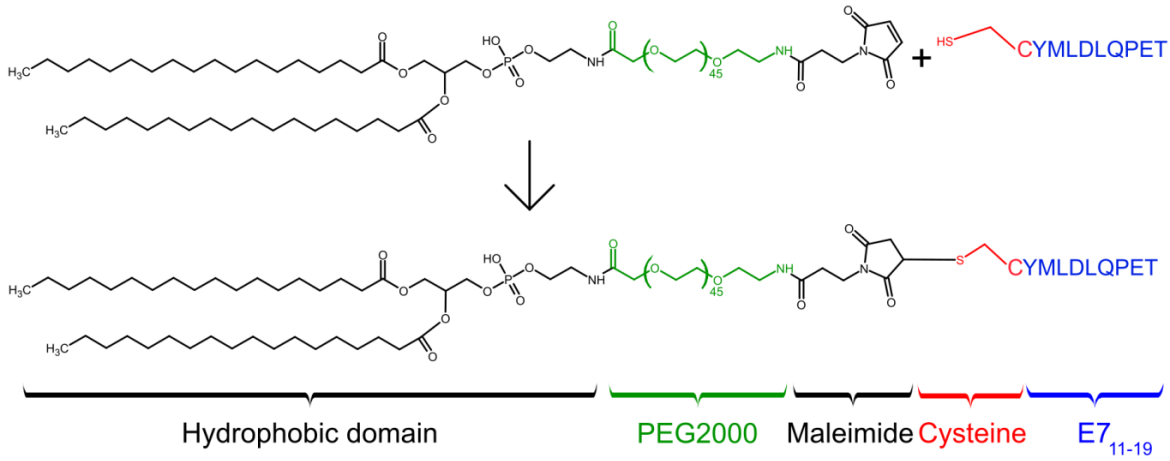

Figure 29. E7/11-19 in the LPP amphiphilic construct

Top row: the two components of LPP, DSPE-PEG-maleimide (1,2-distearoyl-3-sn-phosphatidylethanolamine)-PEG-maleimide) and an N-terminally cysteine-extended peptide (in this case E7/11-19) are mixed together and coupled through a spontaneous chemical reaction between the cysteine's sulfhydryl group and the maleimide. The coupled compound is referred to as LPP-E7/11-19 (lipo-PEG-E7/11-19).

Subcutaneous injection in a one-boost regimen together with pIC robustly induced E7/11-19-specific $CD8^+$ T cells in frequencies of up to 6.5 % (Figure 30). Remarkably, the intravenous injection of LPP-E7/11-19 together with pIC as a TLR agonist did not give rise to substantial frequencies of E7/11-19-specific $CD8^+$ T cells. Interestingly, an exchange of the TLR agonist from pIC to CpG in the vaccine formulation abrogated the induction of measurable $CD8^+$ T cell responses against E7/11-19. Using the same subcutaneous 2-boost vaccination regimen as for Stea2-E7/11-19, mean frequencies of approximately 6-9 % epitope-specific $CD8^+$ T cells could be reproducibly induced (Figure 30, Figure 33).

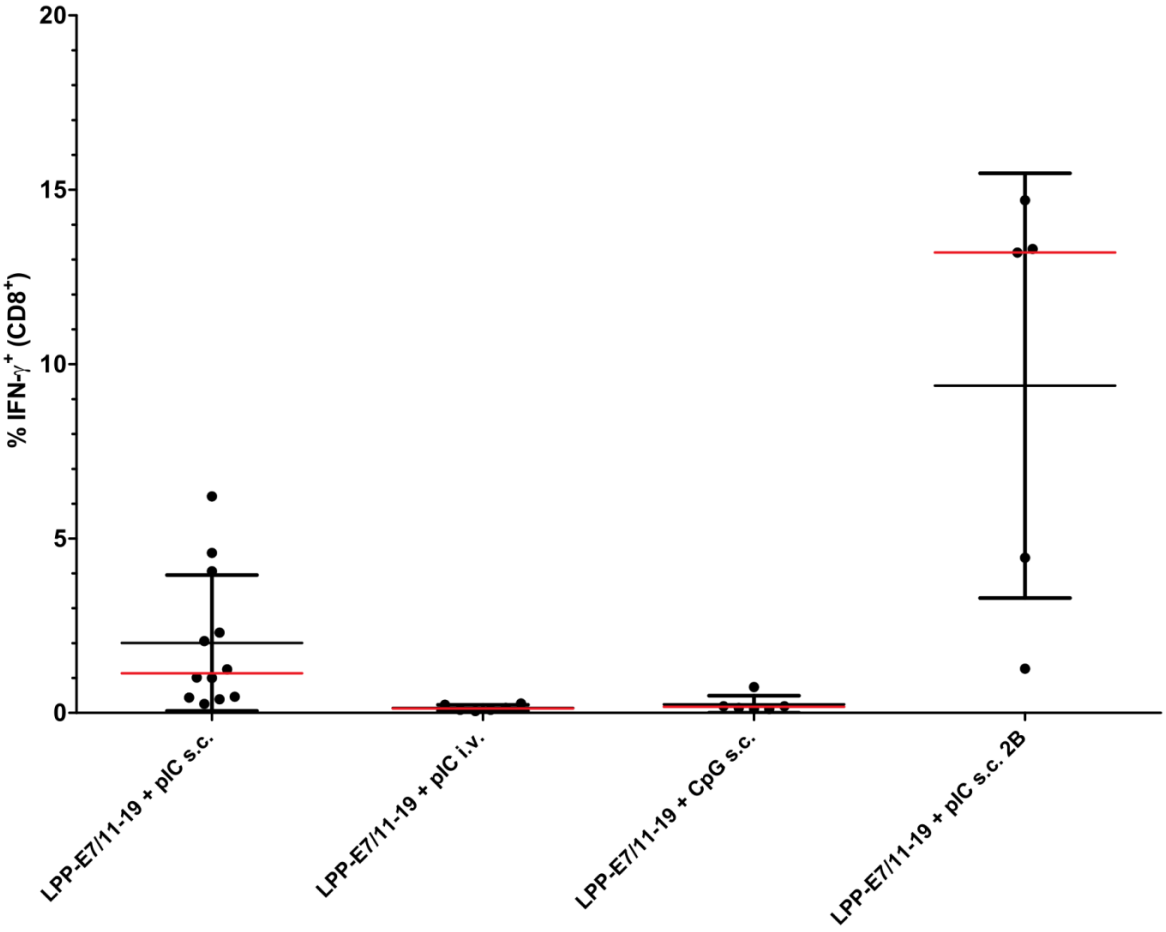

Figure 30. Comparison of vaccination routes and TLR agonists with LPP-E7/11-19

A2.DR1 mice (n=12 for LPP-E7/11-19 + pIC s.c., n=6 for all other groups) were injected with 50 nmol LPP-E7/11-19 mixed with either 50 µg pIC or 1.24 nmol CpG. The first three groups were injected on days 0 and 14, the LPP-E7/11-19 + pIC s.c. 2B group was injected on days 0, 7 and 14 (2B=2 boosts). Mice were sacrificed on day 21 and splenocytes were isolated and stimulated with E7/11-19 peptide in the presence of Golgi apparatus-transport inhibitors. After subsequent intracellular IFN-γ staining, the frequency of IFN-γ$^+$ (E7/11-19-specific) CD8$^+$ T cells was determined by flow cytometry. Each dot represents one mouse. Mean (black bar), median (red bar) and SD are depicted.

4.3.1.4 Overall comparison of the tested vaccine formulations

To appreciate the full extent of differences in induction of epitope-specific CD8$^+$ T cells it is insufficient to monitor only the frequencies of specific CD8$^+$ T cells, but it is also important to know the total number of specific CD8$^+$ cells in the individual. This number can be calculated if the frequency of specific CD8$^+$ T cells among the total CD8$^+$ T cells and the total number of CD8$^+$ T cells in an individual is known. Since it is experimentally not possible to quantify the total number of CD8$^+$ T cells in an individual mouse, the total number of CD8$^+$ T

cells in the spleen represents a potential surrogate measure. We quantified the numbers of splenocytes of each mouse by electronic counting with the Countess® cell counter. However, small differences in the settings of the machine, such as the focus, result in relatively large differences of cells counted for the same sample. To minimize this error, we used the same settings for every experiment. Nevertheless, the interexperimental variance due to this technical characteristic can be considerable. Due to these uncertainties, we chose not to include the total number of $CD8^+$ T cells in our analysis comparing the efficacy of the different vaccine formulations. Instead we decided to base our comparison on the frequencies of E7/11-19-specific $CD8^+$ T cells among $CD19^-$ splenocytes as these frequencies can be calculated from the frequency of E7/11-19-specific $CD8^+$ T cells among $CD8^+$ T cells and the frequency of total $CD8^+$ T cells among the $CD19^-$ splenocytes. Both data points can be reliably assessed by flow cytometry analysis.

The quantification of the $CD8^+$ T cells in the spleens of vaccinated mice showed large differences between the different treatments (Figure 31). The mean frequency of $CD8^+$ T cells in the spleen of naïve A2.DR1 mice is approximately 5 % of the $CD19^-$ splenocytes. This frequency is not changed when A2.DR1 mice are vaccinated with emulsion-based formulations with or without the TLR agonists MPLA and XS15. Vaccination with mRNA leads to a remarkable increase in the overall frequency of $CD8^+$ T cells. This increase to mean frequencies of 13 % is induced irrespective of the specificity of the mRNA, as also mRNAs that did not induce HPV16 E6/E7-specific T cells increased frequencies of $CD8^+$ T cells among the $CD19^-$ splenocytes. The intravenous injection of the free E7/11-19 peptide together with pIC did not give rise to increased frequencies of $CD8^+$ T cells. All amphiphilic vaccines increased the overall frequencies of $CD8^+$ T cells in the spleen to approximately 6-9 % of the $CD19^-$ cells. Interestingly, there seems to be a dose dependency in the case of Pam2-E7/11-19 since the small dose (Pam2-E7/11-19 1x) induced a lower frequency of $CD8^+$ T cells than the higher dose (Pam2-E7/11-19 2x). Furthermore, subcutaneous and intravenous injection of Stea2-E7/11-19 with pIC also induced an increase in $CD8^+$ T cell frequency, in this case to 7.5 % and 9.5 %, respectively. A remarkable finding was that a second booster injection in the subcutaneous LPP-E7/11-19 injection regimen did not further increase the frequency of $CD8^+$ T cells in the spleen compared to the one boost-regimen, as can be seen in the comparison of the two regimens LPP-E7/11-19 and LPP-E7/11-19 2B.

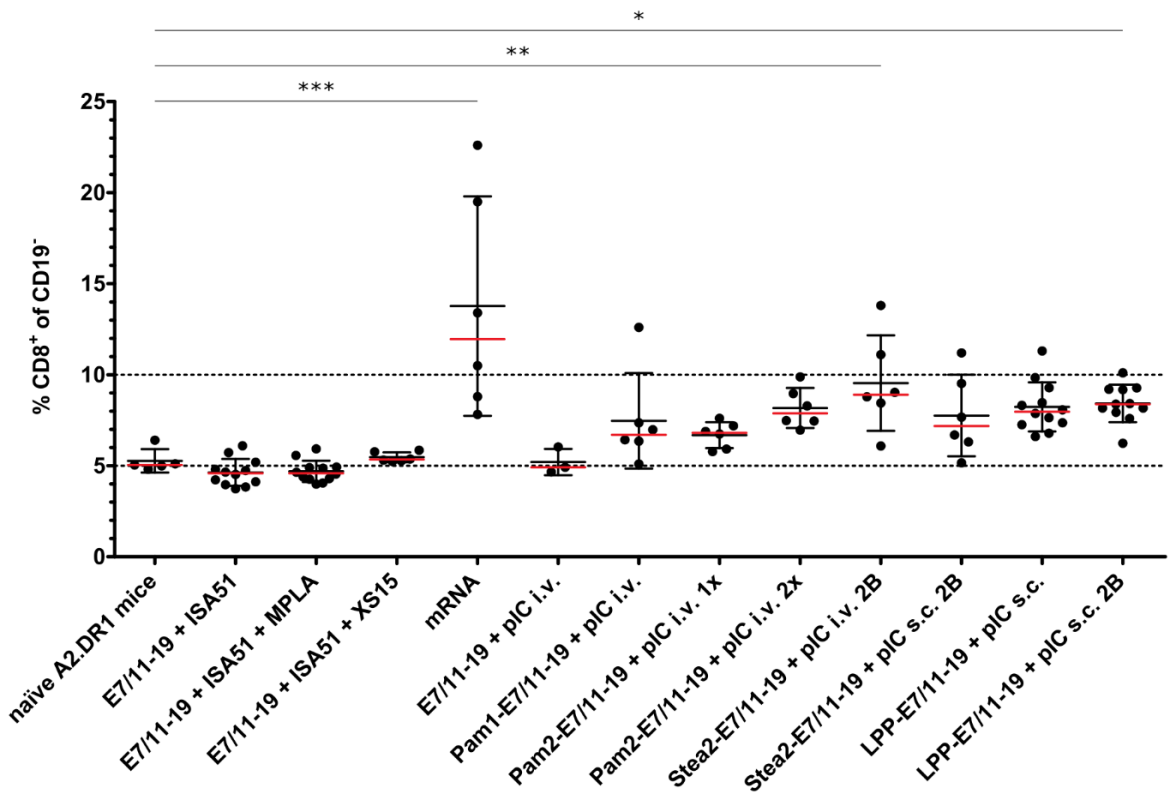

Figure 31. Frequency of total CD8⁺ T cells among CD19⁻ splenocytes after vaccination

A2.DR1 mice were treated as described before for the respective experiments (see Figure 25, Figure 26, Figure 28, Figure 30). The frequency of $CD8^+$ T cells among $CD19^-$ splenocytes was determined by flow cytometry. Each dot represents one mouse. Mean (black bar), median (red bar) and SD are depicted. *p≤0.05, **p≤0.01, ***p≤0.001 (ANOVA with Dunnett's multiple comparison test). All comparisons are made against naïve A2.DR1 mice.

To calculate the frequencies of E7/11-19-specific $CD8^+$ T cells among $CD19^-$ splenocytes, the product of E7/11-19-specific T cells among $CD8^+$ T cells (Figure 25, Figure 26, Figure 28, Figure 30) and total $CD8^+$ among the $CD19^-$ splenocytes (Figure 31) was formed (Figure 32). The comparison of these frequencies shows that the emulsion-based formulations induced the lowest overall numbers of E7/11-19-specific $CD8^+$ T cells (median frequency for ISA51: 0.007 % and for ISA51 + MPLA: 0.024 %). The two mRNA vaccines that induced E7/11-19-specific $CD8^+$ T cells (E7/8-21 and E7/8-21 + PADRE) showed better performance (median frequency: 0.065 %) than the emulsion-based formulations but still induced lower specific cell frequencies than the amphiphilic formulations. The amphiphilic formulations performed best since they induced high frequencies of E7/11-19-specific T cells among the $CD8^+$ T cells

and at the same time increased the frequencies of $CD8^+$ T cells among the $CD19^-$ splenocytes. In this analysis, the LPP construct used in a two boost-regimen, adjuvanted with pIC, exhibited the highest efficacy of all tested vaccine formulations. The induced frequencies were significantly higher than the ones induced by all other formulations. Only the comparison to the Pam2-E7/11-19 pIC i.v. group is not statistically significant, however, this is due to the outlying data point in this group as the medians are vastly different (0.07 % and 0.63 %).

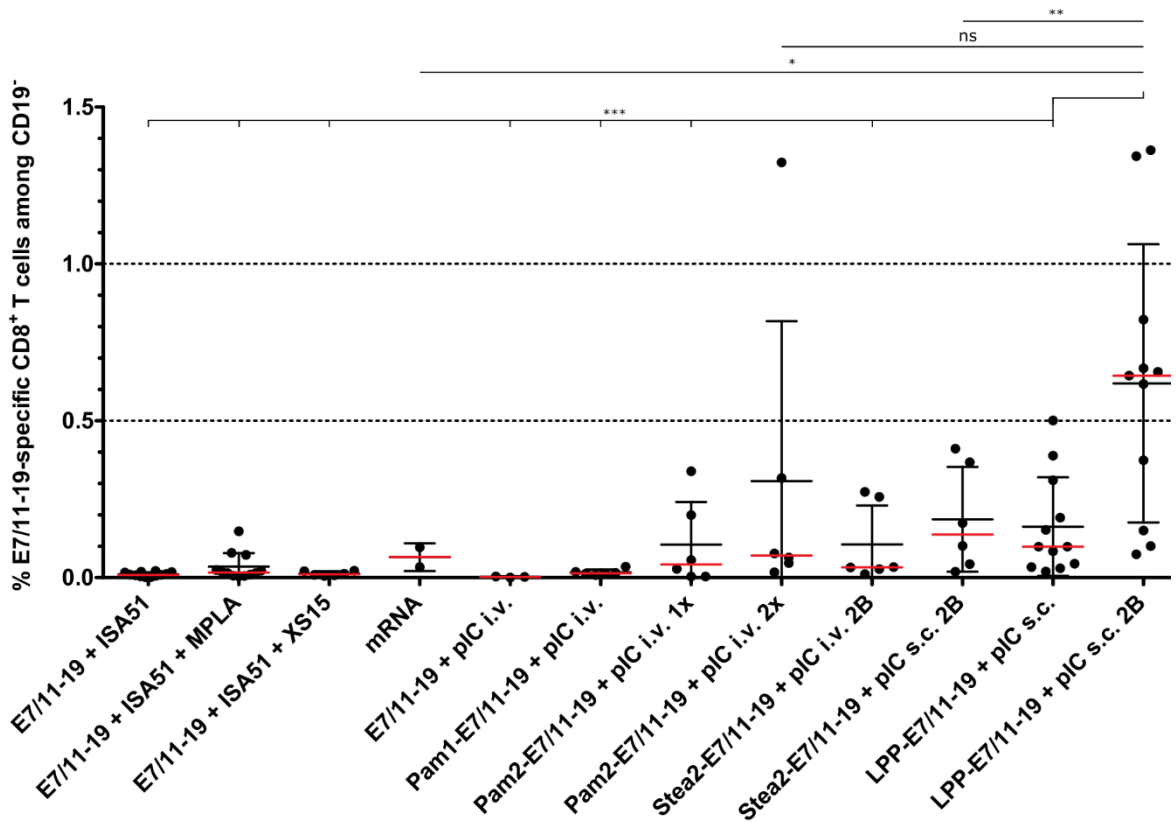

Figure 32. Frequency of E7/11-19-specific $CD8^+$ T cells among $CD19^-$ splenocytes after vaccination

The displayed frequencies are the product of the frequencies of E7/11-19-specific $CD8^+$ T cells among $CD8^+$ T cells (Figure 25, Figure 26, Figure 28, Figure 30) and the frequencies of $CD8^+$ T cells among $CD19^-$ splenocytes (Figure 31). Each dot represents one mouse. Mean (black bar), median (red bar) and SD are depicted. *p≤0.05, **p≤0.01, ***p≤0.001 (ANOVA with Dunnett's multiple comparison test). All comparisons are made against LPP-E7/11-19 + pIC s.c. 2B.

Due to the strong induction of E7/11-19-specific $CD8^+$ T cells by vaccination with the LPP-E7/11-19 compound, its easy synthesis and the high achievable purity, we continued to work with this compound and not with the Pam2-E7/11-19 or Stea2-E7/11-19 compounds.

4.3.2 In-depth analysis of LPP vaccination

4.3.2.1 Comparison of four HPV16 E6/E7 epitopes

Once we had established a vaccination approach that reliably induced E7/11-19-specific $CD8^+$ T cells, we used LPP constructs also with two other HPV16 E7 epitopes (E7/7-15 and E7/82-90) that were found to be presented on HLA-A2 on a human cervical cancer cell line and against which T cells could be found in the blood of healthy donors (Blatnik *et al.*, 2018). In addition, we used HPV16 E6/25-33 as an example of an E6-derived epitope. The use of these additional epitopes as LPP constructs was facilitated by the modular synthesis process of LPP.

The three additional LPP constructs were compared side by side with a new batch of LPP-E7/11-19 in their ability to induce epitope-specific $CD8^+$ T cells as assessed by intracellular IFN-γ staining after restimulation with the cognate peptide. All three newly tested epitopes were found to be immunogenic in A2.DR1 mice (Figure 33). Although LPP-E7/11-19 induced the highest mean frequencies of epitope-specific T cells, the frequencies induced by the other LPP constructs were comparable.

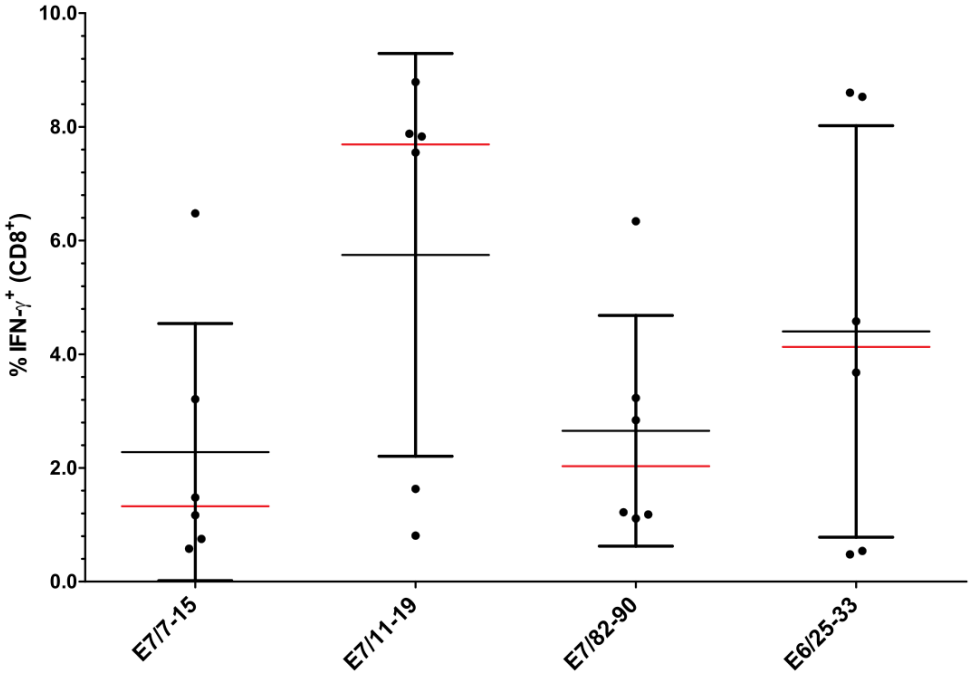

Figure 33. Immunogenicity of LPP-HPV16 E6/E7 epitopes

A2.DR1 mice (n=6) were injected with 50 nmol of the respective LPP construct mixed with 50 µg pIC on days 0, 7 and 14. Mice were sacrificed on day 21 and splenocytes were isolated and stimulated with the indicated cognate peptide in the presence of Golgi apparatus-transport inhibitors. After subsequent intracellular IFN-γ staining, the frequency of IFN-γ$^+$ (epitope-specific) CD8$^+$ T cells was determined by flow cytometry. Each dot represents one mouse. Mean (black bar), median (red bar) and SD are depicted.

Additionally, we compared the expression levels of IFN-γ measured as the geometric mean fluorescence intensity (MFI) for the IFN-γ flow cytometry channel in the IFN-γ$^+$ CD8$^+$ T cells after restimulation with either the irrelevant or the cognate peptide (Figure 34). This analysis showed that the IFN-γ MFI after restimulation with the cognate peptide in the IFN-γ$^+$ CD8$^+$ T cells was significantly higher in all four treatment groups than after restimulation with the irrelevant peptide, demonstrating the specificity of the CD8$^+$ T cells for the respective cognate epitope. Furthermore, IFN-γ expression was significantly higher in IFN-γ$^+$ CD8$^+$ T cells specific for E7/11-19 than in the ones specific for E7/7-15. All other comparisons were not statistically significant.

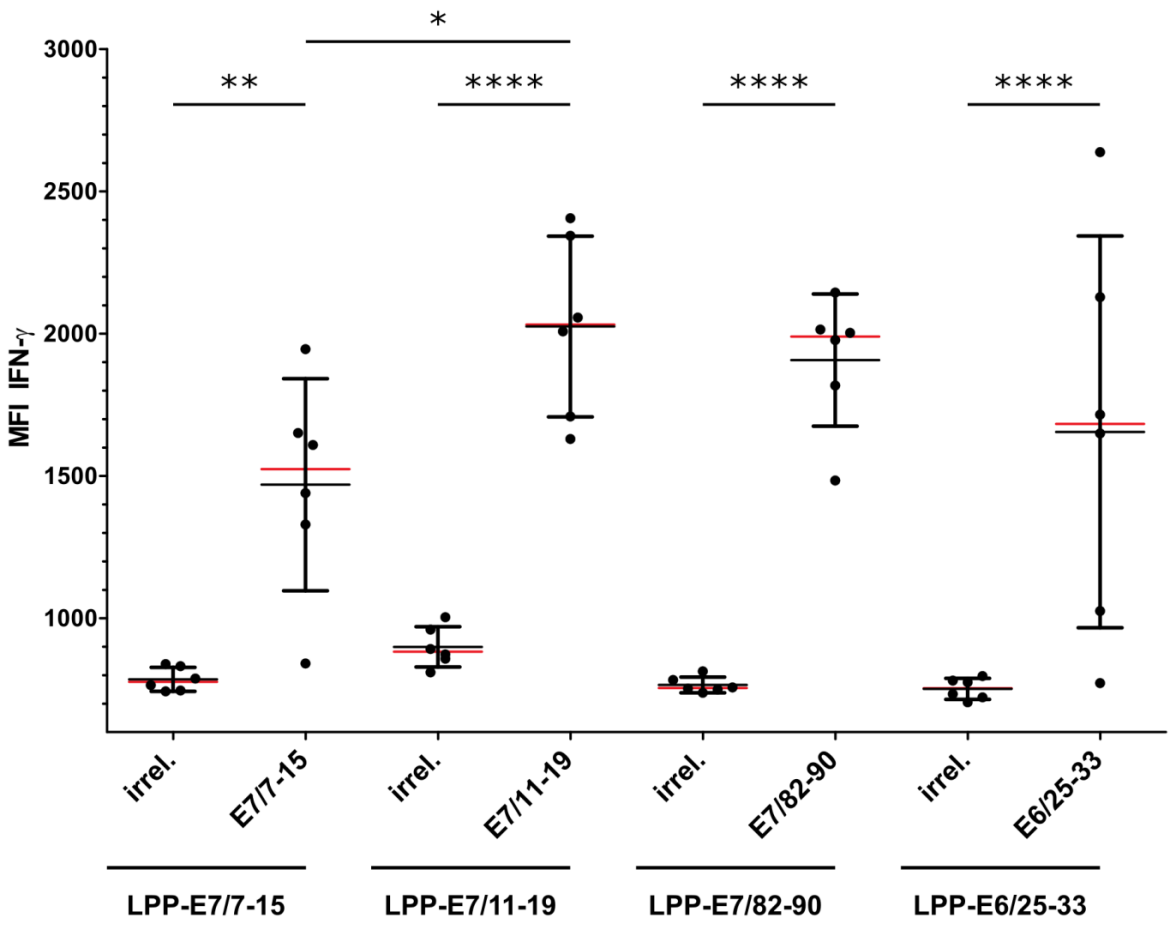

Figure 34. IFN-γ expression of LPP-induced CD8⁺ T cells

A2.DR1 mice (n=6) were injected with 50 nmol of the indicated LPP construct mixed with 50 µg pIC on days 0, 7 and 14. Mice were sacrificed on day 21 and splenocytes were isolated and stimulated with the irrelevant peptide or the indicated cognate peptide in the presence of Golgi apparatus-transport inhibitors. After subsequent intracellular IFN-γ staining, the geometric mean fluorescence intensity (MFI) of IFN-γ⁺ CD8⁺ T cells was determined by flow cytometry. Each dot represents one mouse. Mean (black bar), median (red bar) and SD are depicted. Mean and SD are depicted. *p≤0.05, **p≤0.01, ****p≤0.0001 (one-way ANOVA with Bonferroni's multiple comparison test).

4.3.2.2 Cytokine profile of vaccination-induced T cells

Several studies show that multifunctional T cells, i.e. T cells capable of expressing more than one cytokine, are more effective than monofunctional T cells in eradicating viruses and cancer cells ((van Duikeren *et al.*, 2012; Van Der Sluis *et al.*, 2015) and reviewed in (Seder, Darrah and Roederer, 2008)). Therefore, we assessed the ability of LPP-E7/11-19-induced CD8⁺ T cells to express TNF-α in addition to IFN-γ. Indeed, especially among the CD8⁺ T cells specific for E7/11-19, many cells that were IFN-γ⁺ were also found to be positive for TNF-α

(0.61 %) (Figure 35). Thus, on average more than 10 % of the E7/11-19-specific CD8$^+$ T cells produced TNF-α in addition to IFN-γ. Interestingly, we barely observed any TNF-α single-positive cells in all four tested groups, meaning that virtually all epitope-specific CD8$^+$ T cells respond to activation with IFN-γ expression.

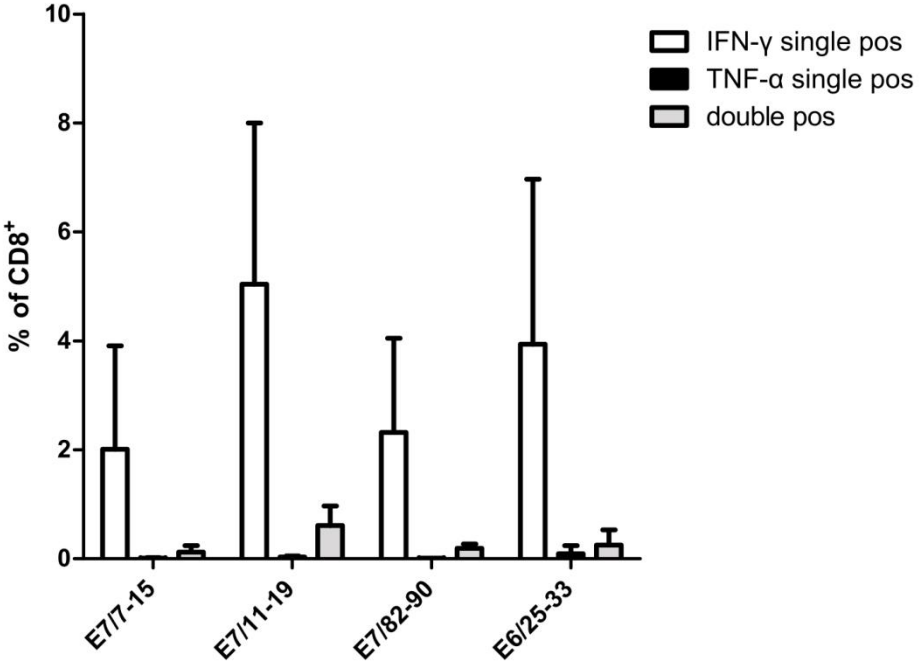

Figure 35. Cytokine profile of vaccination-induced T cells after cognate epitope stimulation

A2.DR1 mice (n=6) were injected with 50 nmol of the indicated LPP construct mixed with 50 µg pIC on days 0, 7 and 14. Mice were sacrificed on day 21 and splenocytes were isolated and stimulated with the irrelevant peptide or the indicated cognate peptide in the presence of Golgi apparatus-transport inhibitors. After subsequent intracellular TNF-α/IFN-γ staining, the frequency of TNF-α$^+$, IFN-γ$^+$ and TNF-α$^+$/IFN-γ$^+$ double-positive CD8$^+$ T cells was determined by flow cytometry. Mean and SD are depicted.

4.3.2.3 Cytotoxicity of vaccination-induced T cells

To assess the ability of the vaccination-induced CD8$^+$ T cells to kill target cells in an epitope-dependent manner, we used the Vital-FR assay, a highly sensitive flow cytometry-based cytotoxicity assay (Stanke *et al.*, 2010) that was initially designed for human T cells and that we adapted for the use with murine A2.DR1-derived, vaccination-induced T cells. This assay is based on the coculture of differentially labeled specific and unspecific target cells together with T cells. Specific killing is thus indicated by a decline in the relative frequency of specific target cells to unspecific target cells when more T cells are added (Figure 36).

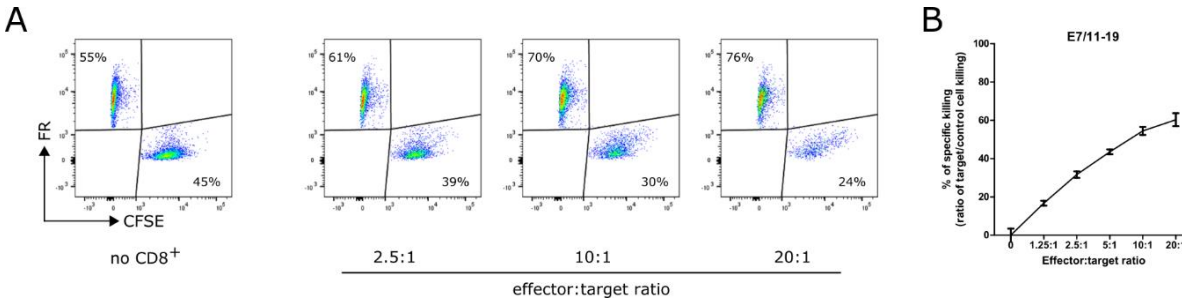

Figure 36. Working principle of the Vital-FR flow cytometry-based cytotoxicity assay

Effector cells (in this case CD8$^+$ T cells that were MACS-isolated from splenocytes of LPP-E7/11-19-vaccinated A2.DR1 mice which had been cultured for 7 days in the presence of E7/11-19 peptide) are added at different effector-to-target (E:T) ratios to wells containing a 1:1 mixture of specific target cells labeled in green (here: PAP-A2 cells, CFSE-labeled) and unspecific target cells labeled in red (here: the parental untransduced 2277NS cells, FR-labeled). 48 h after addition of CD8$^+$ T cells, target cells are trypsinized, fixed and analyzed by flow cytometry.

(A) Exemplary flow cytometry plots. With increasing E:T ratios, more specific target cells (CFSE-labeled) are killed and their relative amount decreases in the flow cytometry plots, while the absolute number of unspecific target cells (FR-labeled) remains the same, thus their relative amount increases. (B) The ratio of specific/unspecific target cells is plotted as "% of specific killing". An increase with increasing E:T ratios is indicative of specific killing of the specific target cells compared to the unspecific target cells.

First, we assessed the cytotoxic potential of the E7/7-15-, E7/11-19-, E7/82-90- and E6/25-33-specific CD8$^+$ T cells induced by LPP vaccination (Figure 37). This was achieved by using cognate epitope-loaded 2277NS cells as specific target cells and irrelevant epitope-loaded 2277NS cells as unspecific target cells. We observed that with increasing numbers of spleen-derived CD8$^+$ T cells from mice vaccinated with the respective LPP construct, the frequency of specific target cells was reduced in comparison to the frequency of unspecific target cells, which indicates specific killing. For three (E7/7-15, E7/11-19, E7/82-90) of the four CD8$^+$ T cell specificities, specific killing of more than 70 % was observed (Figure 37). Only for E6/25-33-specific CD8$^+$ T cells, specific killing was less pronounced and reached only approximately 40 %.

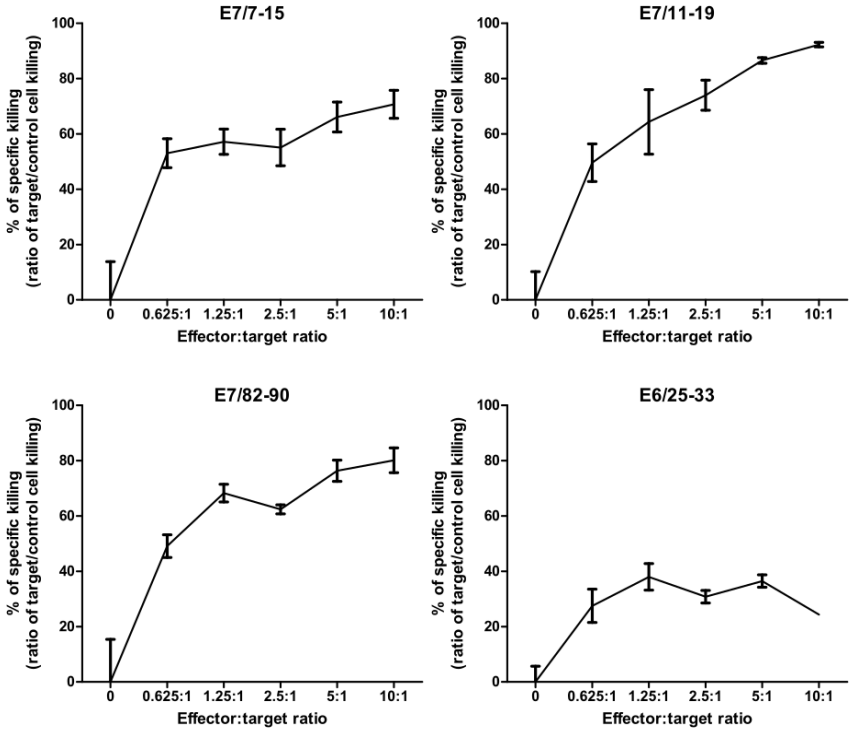

Figure 37. Cytotoxicity of vaccination-induced CD8$^+$ T cells towards epitope-loaded 2277NS target cells

Splenocytes of LPP-vaccinated A2.DR1 mice were isolated and cultured 7 days in the presence of the respective indicated cognate peptide. CD8$^+$ T cells were isolated by untouched MACS isolation. CD8$^+$ T cells (effector cells) were added to wells containing a 1:1 mixture of specific target cells (2277NS loaded with the indicated peptide, CFSE-labeled) and unspecific target cells (277NS cells loaded with an irrelevant HLA-A2-binding epitope, FR-labeled). 48 h after addition of CD8$^+$ T cells, cells were analyzed by flow cytometry. "% of specific killing" was calculated from the ratio of specific to unspecific target cell killing. The experiment was performed in triplicates; error bars: SD.

In a second step we used the verified killing capabilities of the vaccination-induced T cells to find out if the E6/E7 proteins expressed by PAP-A2 cells are processed into the respective MHC class I epitopes and subsequently presented on HLA-A2 on the cell surface. Using PAP-A2 cells as specific target cells, 2277NS cells as unspecific target cells and vaccination-induced, epitope-specific CD8$^+$ T cells as effector cells, we observed that PAP-A2 cells were specifically killed by CD8$^+$ T cells of all four specificities (E7/7-15, E7/11-19, E7/82-90, E6/25-33) (Figure 38). This result demonstrated that E6 and E7 are indeed processed in PAP-A2 cells into the four epitopes, which are subsequently presented on HLA-A2 in

sufficient quantities to allow specific CD8$^+$ T cells to recognize these epitopes and kill the presenting cell.

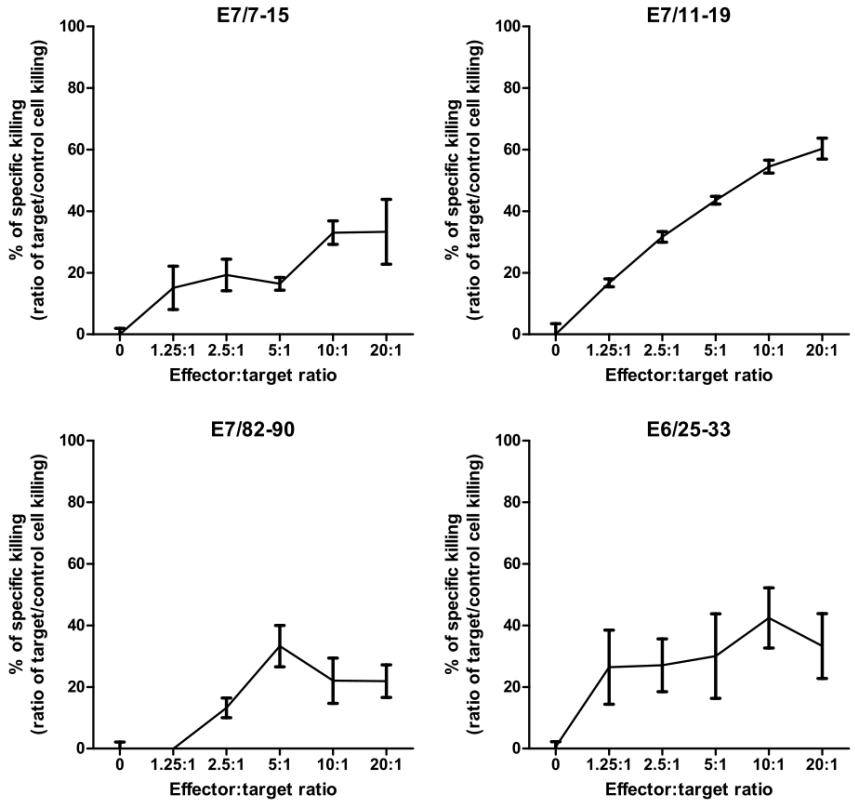

Figure 38. Cytotoxicity of vaccination-induced CD8$^+$ T cells towards PAP-A2 target cells

Splenocytes of LPP-vaccinated A2.DR1 mice were isolated and cultured 7 days in the presence of the respective indicated cognate peptide. CD8$^+$ T cells were isolated by untouched MACS isolation. CD8$^+$ T cells (effector cells) were added to wells containing a 1:1 mixture of specific PAP-A2 target cells (CFSE-labeled) and unspecific target cells (parental 2277NS cells, FR-labeled). 48 h after addition of CD8$^+$ T cells, cells were analyzed by flow cytometry. "% of specific killing" was calculated from the ratio of specific to unspecific target cell killing. The experiment was performed in triplicates; error bars: SD.

4.3.2.4 Vaccination with combinations of HPV16 E6/E7 LPPs

We hypothesized that by administering several LPPs simultaneously, it should be possible to increase the overall numbers of HPV16 E6/E7-reactive and thus potentially tumor-reactive CD8$^+$ T cells. To test this hypothesis, we injected mice with all possible combinations of LPP-E7/11-19 with the other LPPs that were previously found to be immunogenic.

As we utilized a new batch of LPP-E7/11-19 in the combination experiments, we repeated the LPP-E7/11-19 single vaccination to establish the functionality of this batch (Figure 39,

panel A). The median frequency of E7/11-19-specific $CD8^+$ T cells induced by this batch (3.58 %) was lower than the median frequencies induced by the other used batches (13.2 % and 7.4 %). However, the induced frequencies are still comparable, especially when considering the single data points which showed that also the new batch was capable of inducing 16.5 % of E7/11-19-specific $CD8^+$ T cells in one mouse.

Remarkably, the frequencies of HPV16 epitope-specific $CD8^+$ T cells were much lower in combination vaccinations when compared to the single LPP immunizations (Figure 39, panels B-D, Figure 40). The combination of LPP-E7/11-19 and LPP-E7/7-15 resulted in median frequencies of E7/7-15-specific $CD8^+$ T cells of only 0.4 % (compared to 1.4 % in the single LPP-E7/7-15 immunization) and median frequencies of E7/11-19 $CD8^+$ T cells of only 0.47 % (compared to 3.58 % in the single LPP-E7/11-19 immunization). The combination of LPP-E7/11-19 and LPP-E7/82-90 lowered the median frequency of E7/82-90-specific $CD8^+$ T cells from 2.03 % in the single LPP-E7/82-90 vaccination to 1.1 % and for E7/11-19-specific $CD8^+$ T cells from 3.58 % to 0.39 %. A similar observation was made for the combination of LPP-E7/11-19 and LPP-E6/25-33, since in the single LPP-E6/25-33 vaccination the median frequency of E6/25-33-specific $CD8^+$ T cells was 4.1 %, but in the combination immunization the median frequency of E6/25-33-specific $CD8^+$ T cells was only 1.4 %. For E7/11-19 specific $CD8^+$ T cells, the frequency was reduced from 3.58 % to 0.49 %, respectively. Interestingly, in all three groups there was one mouse that responded exceptionally strongly against either E7/11-19 or the other epitope that was used for vaccination. Therefore, the median frequencies of IFN-γ^+ $CD8^+$ T cells are more suitable to describe the population as a whole than the mean frequencies (Figure 39).

The mice that received the combination of two LPPs had low but detectable $CD8^+$ T cells responses against two different epitopes that are presented on PAP-A2 tumor cells (see 4.3.2.3). Therefore, to compare the potential anti-tumor efficacy of the combination vaccinations, the total frequency of tumor-reactive $CD8^+$ T cells is relevant. This number was calculated by adding the frequencies of the E7/11-19-specific T cells to the frequencies of $CD8^+$ T cells specific for the respective other epitope (= total potentially tumor-reactive $CD8^+$ T cells). Remarkably, the median sums of total potentially tumor-reactive $CD8^+$ T cells (0.84 % for 7+11, 1.55 % for 82+11, 2.81 % for 25+11) were all lower than the median frequencies of potentially tumor-reactive $CD8^+$ T cells in the single vaccinations (1.4 % for E7/7-15, 3.58 %

for E7/11-19, 2.85 % for E7/82-90, 4.1 % for E6/25-33). In addition to calculating the sum of the total potentially tumor-reactive $CD8^+$ T cells, we also experimentally determined the frequency of potentially tumor-reactive $CD8^+$ T cells by incubating splenocytes from the vaccinated mice with a mixture of all epitopes used for that vaccination. We observed some differences between the two numbers (e.g. in 11+25 for mouse 4) but in general the two ways of evaluation gave very similar results.

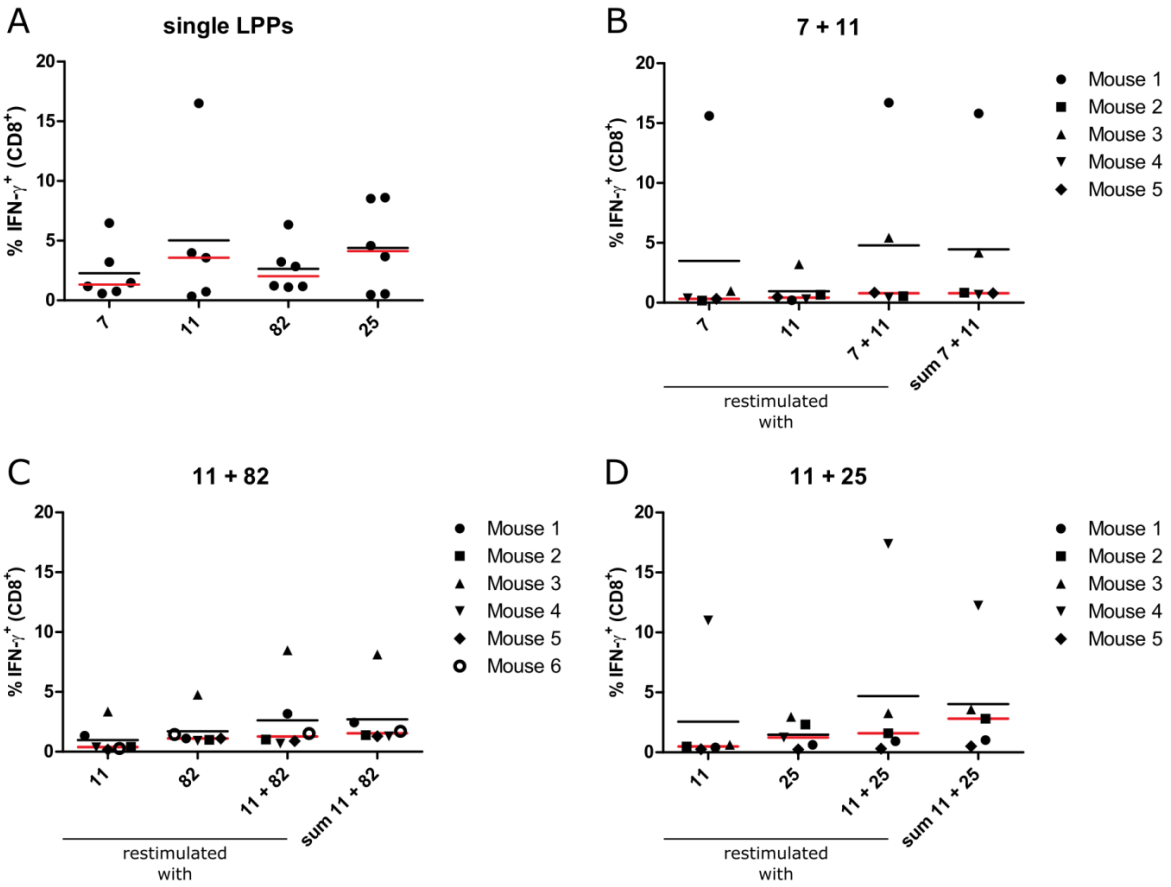

Figure 39. Vaccination with combinations of two different HPV16 LPPs leads to epitope-specific immunosuppression

Panel A represents the data for E7/7-15, E7/82-90 and E6/25-33 single LPP vaccinations as shown in Figure 33 for comparison purposes. The LPP-E7/11-19 single vaccination shown in A was conducted according to the same regimen as for the other epitopes with the same batch of LPP-E7/11-19 that was used for B-D. For the LPP combination experiments, A2.DR1 mice (n=5-6) were injected with 50 nmol of each of the LPP constructs indicated in the title of each graph together with 50 µg pIC per mouse on days 0, 7 and 14. Mice were sacrificed on day 21 and splenocytes were isolated and stimulated with the indicated peptides or the indicated peptide mix in the presence of Golgi apparatus-transport inhibitors. After subsequent intracellular IFN-γ staining, the frequency of IFN-γ^+ (epitope-specific) $CD8^+$ T cells was determined by flow cytometry. The fourth group ("sum") in the graphs B-D shows the calculated sum of the frequency of IFN-γ^+ ($CD8^+$) for the respective single epitope restimulations. Each dot represents one mouse. Mean (black bar) and median (red bar) are depicted. Abbreviations: 7 = E7/7-15, 11 = E7/11-19, 82 = E7/82-90, 25 = E6/25-33.

The vaccination of A2.DR1 mice with combinations of three or four different HPV16-epitope LPPs yielded similar results (Figure 40) as the vaccination with two different LPPs (Figure 39). Again, the median frequencies of E7/11-19-specific $CD8^+$ were very low (7+11+82: 0.11 %, 7+11+25: 0.09 %, 11+82+25: 0.23 %, 7+11+82+25: 0.12 %) and thus similar to the ones in

vaccinations with two LPPs. The response to E7/7-15 was diminished in all three treatment groups that were treated with this epitope (median frequencies of E7/7-15-specific $CD8^+$ T cells: 7+11+82: 0.3 %, 7+11+25: 0.27 %, 7+11+82+25: 0.12 %) compared to single LPP-E7/7-15 vaccination (median frequency of E7/7-15-specific $CD8^+$ T cells: 1.4 %). In combinations in which E7/82-90 was used, the response to this epitope was always the most pronounced when compared to the responses to the three other epitopes (median frequencies of E7/82-90-specific $CD8^+$ T cells: 7+11+82: 1.97 %, 11+82+25: 2.12 %, 7+11+82+25: 1.97 %) and very similar to the median frequency of E7/82-90-specific $CD8^+$ T cells in the E7/82-90 single vaccination (2.03 %). Only the combination 7+11+25 gave rise to substantial median frequencies of E6/25-33-specific $CD8^+$ T cells (median frequencies of E6/25-33-specific $CD8^+$ T cells: 7+11+25: 2.63 %, 11+82+25: 0.26 %, 7+11+82+25: 0.17 %). However, even the 2.63 % of E6/25-33-specific $CD8^+$ T cells were still lower than the median frequency of these T cells in E6/25-33 single vaccination (4.1 %).

When analyzing the sum of the potentially tumor-reactive $CD8^+$ T cells in the combination experiments with three or four different LPPs, it was observed that the median sum was similar in all 4 treatments (median sum of the potentially tumor-reactive $CD8^+$ T cells: 7+11+82: 3.33 %, 7+11+25: 4.22 %, 11+82+25: 2.64 %, 7+11+82+25: 3.66 %). These numbers are mostly dependent on the contribution of E7/82-90-specific $CD8^+$ T cells.

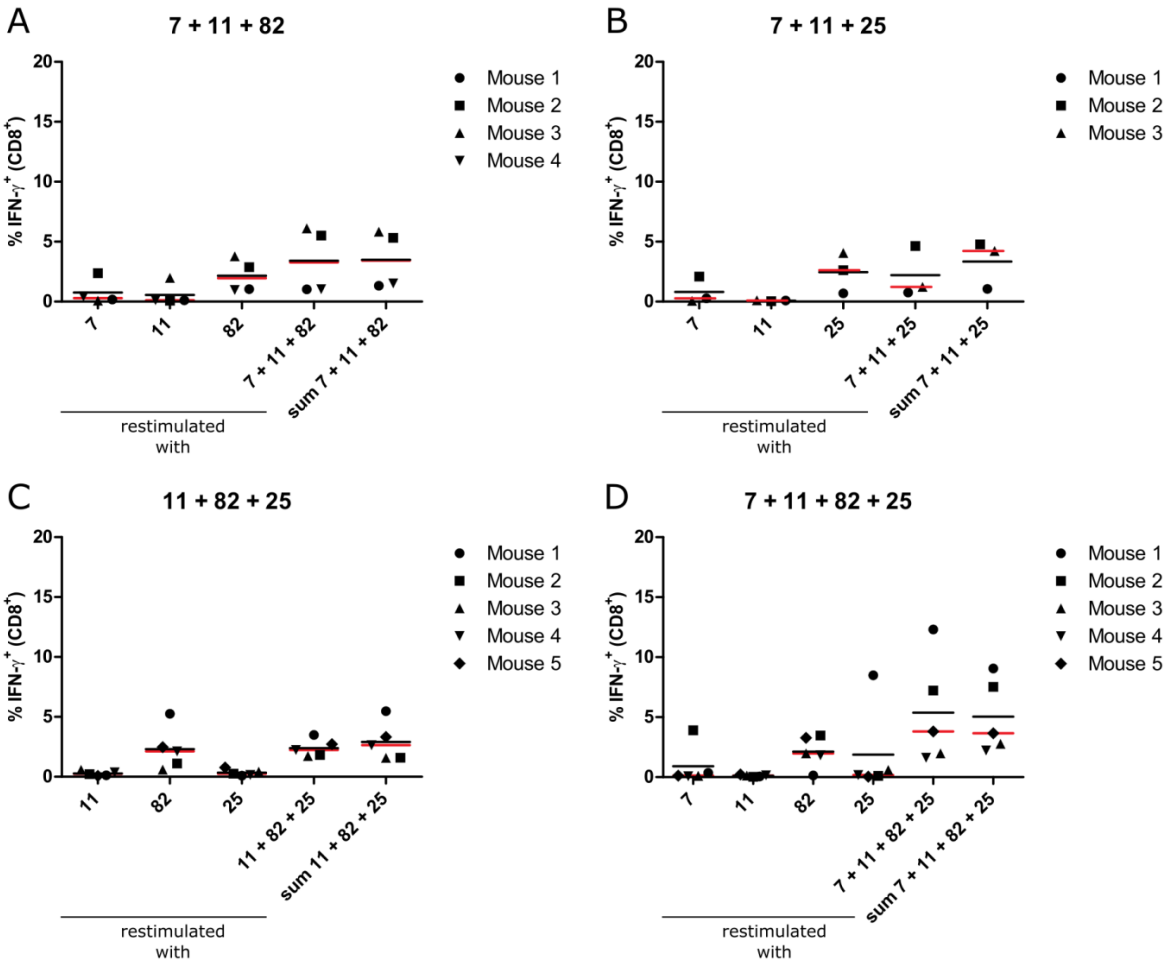

Figure 40. Vaccination with combinations of three or four different HPV16 LPPs leads to epitope-specific immunosuppression

A2.DR1 mice (n=3-5) were injected with 50 nmol of each of the LPP constructs indicated in the title of each graph together with 50 µg pIC per mouse on days 0, 7 and 14. Mice were sacrificed on day 21 and splenocytes were isolated and stimulated with the indicated peptides or the indicated peptide mix in the presence of Golgi apparatus-transport inhibitors. After subsequent intracellular IFN-γ staining, the frequency of IFN-γ$^+$ (epitope-specific) CD8$^+$ T cells was determined by flow cytometry. The group titled "sum" shows the calculated sum of the frequency of IFN-γ$^+$ (CD8$^+$) for the respective single epitope restimulations. Each dot represents one mouse. Mean (black bar) and median (red bar) are depicted. Abbreviations: 7 = E7/7-15, 11 = E7/11-19, 82 = E7/82-90, 25 = E6/25-33.

4.3.3 Anti-tumor vaccinations

4.3.3.1 Prophylactic vaccination with LPP-E7/11-19

After having established the cytotoxic potential of the vaccination-induced CD8$^+$ T cells, we tested their anti-tumor capabilities in a prophylactic tumor vaccination experiment with PAP-A2 tumor cells. The prophylactic vaccination with LPP-E7/11-19 significantly enhanced

the overall survival of mice that were subsequently challenged with 1.5x10^6 PAP-A2 cells compared to the vehicle control-injected or the untreated mice (Figure 41). The median survival time of LPP-E7/11-19-treated mice was twice as long as that of vehicle control-treated animals (mean survival for the LPP-E7/11-19-vaccinated group: 41 days, mean survival for vehicle control-treated mice: 17 days). In the LPP-E7/11-19-vaccinated group, 33 % of the animals rejected the tumor cells completely; in contrast to 20 % in both the vehicle control-treated and the untreated group.

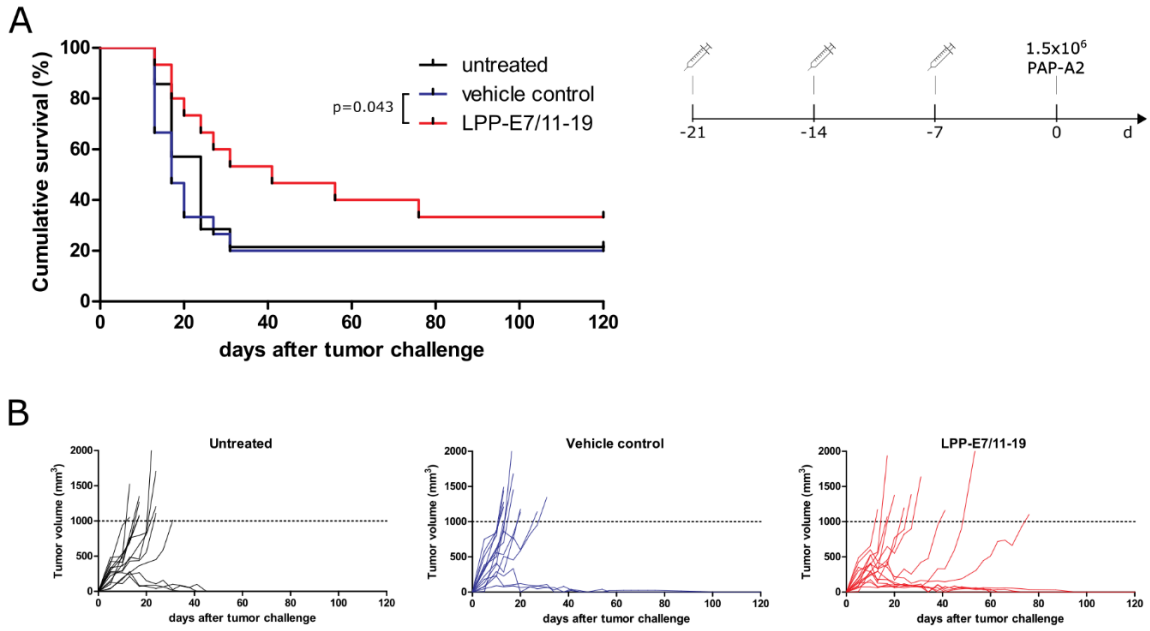

Figure 41. Prophylactic vaccination with LPP-E7/11-19

15 mice per group were either left untreated or injected three times with DSPE-PEG-maleimide as a vehicle control or LPP-E7/11-19. 7 days after the last vaccination, all mice were injected with 1.5x10^6 PAP-A2 cells. A), survival curves and treatment regimen, B) tumor growth curves of individual mice. Statistical analysis for differences in survival was performed with the Gehan-Breslow-Wilcoxon test.

4.3.3.2 Therapeutic vaccination with LPP-E7/11-19

The goal of our studies is the development of a therapeutic anti-HPV16 vaccine, which would be given to patients diagnosed with either a precursor lesion or an established cancer. Therefore, we tested the ability of our vaccines to induce control of tumor growth in a therapeutic vaccination experiment. For this, A2.DR1 mice were inoculated with 1.5x10^6 PAP-A2 cells and were injected after four days with LPP-E7/11-19, followed by two boost immunizations after 5 days each. In this experiment, vaccination with LPP-E7/11-19

led to complete tumor rejection in 50 % of the mice. These mice remained tumor-free until termination of the experiment (Figure 42). In contrast, 100 % of vehicle control-treated mice and 87.5 % of untreated mice had to be eliminated due to excessive tumor growth. However, since the division of the survival curves became only apparent after 40 days, this difference is statistically non-significant with the used number of mice.

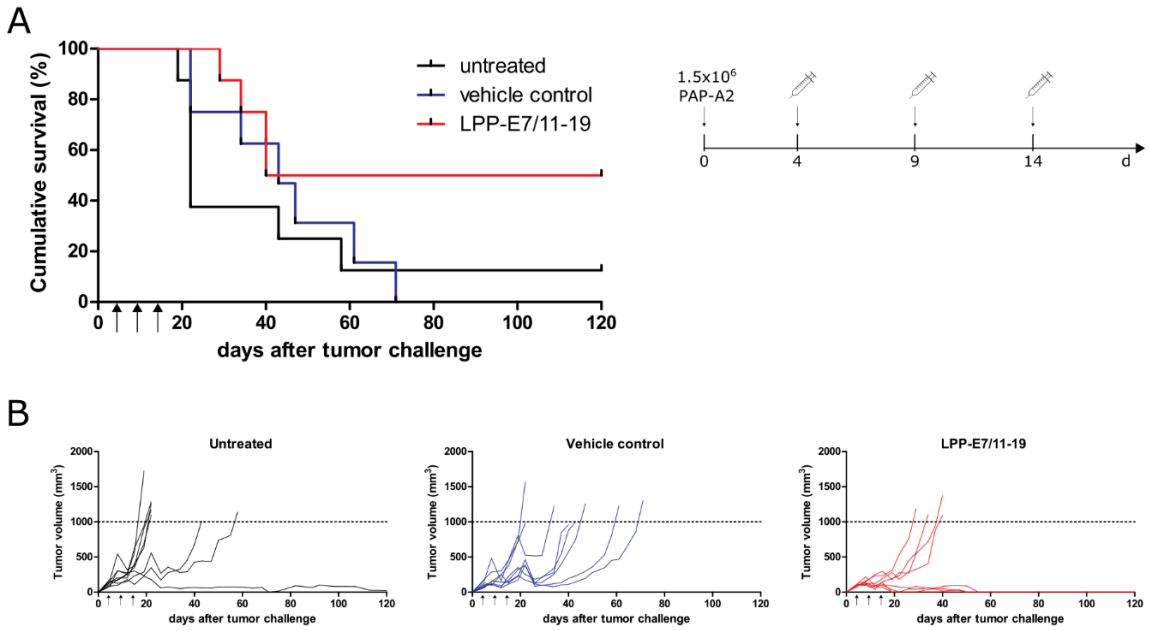

Figure 42. Therapeutic vaccination with LPP-E7/11-19

Mice were injected with $1.5x10^6$ PAP-A2 tumor cells on day 0. 8 mice per group were either left untreated or were injected three times with either DSPE-PEG-maleimide as a vehicle control or LPP-E7/11-19 beginning from day 4 after tumor injection. A), survival curves and treatment regimen, B) tumor growth curves of individual mice. Statistical analysis for differences in survival was performed with the Gehan-Breslow-Wilcoxon test and all differences were found to be non-significant.

4.3.3.3 Therapeutic vaccination with LPP-E7/7-15, LPP-E7/82-90 and LPP-E6/25-33

We also tested the efficacy of the other HPV16 epitopes used in this study to induce anti-tumor responses when administered as LPP together with pIC. In this experiment, exactly the same experimental approach as for the therapeutic LPP-E7/11-19 experiment was used and it was found that despite inducing small increases in overall survival, none of the three tested LPPs (LPP-E7/7-15, LPP-E7/82-90, LPP-E6/25-33) induced improvements in overall survival similar to LPP-E7/11-19.

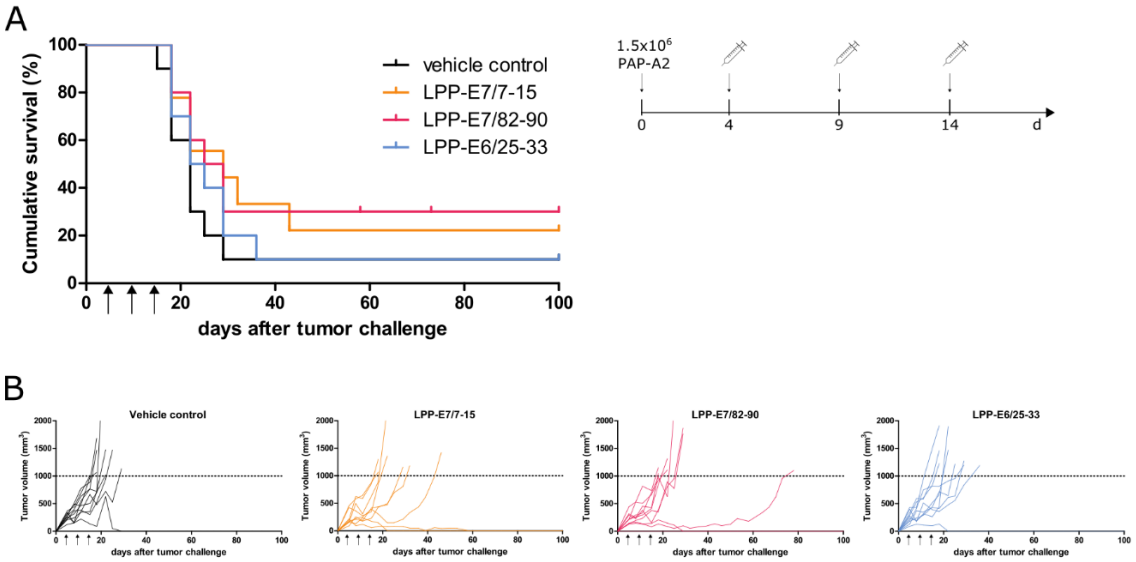

Figure 43. Therapeutic vaccination with the other LPP-HPV16 E6/E7 epitopes

Mice were injected with $1.5x10^6$ PAP-A2 tumor cells at day 0. 10 mice per group were either left untreated or injected three times with either DSPE-PEG-maleimide as a vehicle control or the indicated LPP construct beginning from day 4 after tumor injection. A), survival curves and treatment regimen, B) tumor growth curves of individual mice. Statistical analysis for differences in survival was performed with the Gehan-Breslow-Wilcoxon test and all differences were found to be non-significant.

4.3.3.4 Therapeutic vaccination with combinations of LPP-HPV16 E6/E7 epitopes

When we injected mice with different combinations of the four LPP constructs we observed suppressed T cell responses (see 4.3.2.4). We nevertheless tested if these reduced T cell responses would still result in anti-tumor responses in a therapeutic experiment with the very same experimental setup as was used for the single LPP vaccinations. Indeed, the combination of LPP-E7/11-19 with any one of the three other LPP-epitopes did not give rise to better anti-tumor effects than treatment with LPP-E7/11-19 alone (Figure 44, left panel). Furthermore, also the combination of three or four different LPP-epitopes did not induce better anti-tumor effects (Figure 44, right panel). The best combination formulation turned out to be 11+82, for which the overall survival benefit was statistically significant, but which did not induce a higher frequency of long-term tumor rejection than the vehicle control.

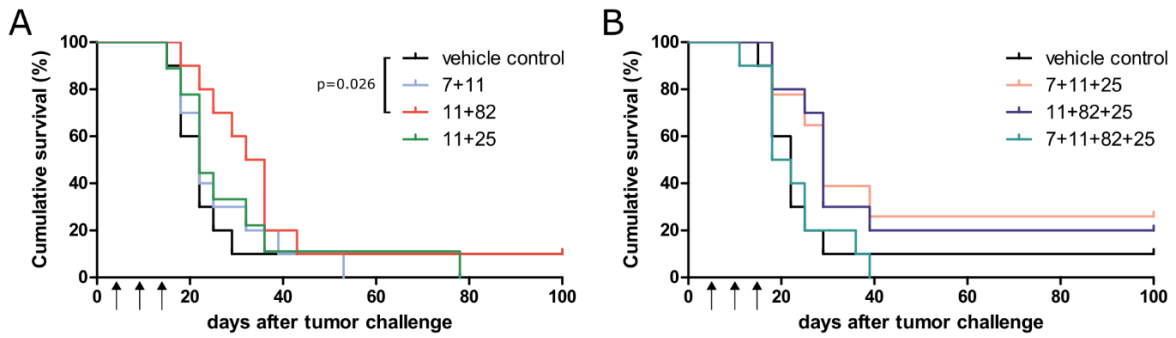

Figure 44. Therapeutic vaccination with combinations of LPP-HPV16 E6/E7 epitopes

Mice were injected with $1.5x10^6$ PAP-A2 tumor cells at day 0. 10 mice per group were either injected three times with either the indicated LPP combinations (50 nmol per compound) or 50 nmol of DSPE-PEG-maleimide and 50 µg of pIC beginning from day 4 after tumor injection. Statistical analysis for differences in survival was performed with the Gehan-Breslow-Wilcoxon test.

Taking together the results from therapeutic vaccinations with single LPP compounds and with combinations of different LPPs, it can be concluded that the best therapeutic anti-tumor results were achieved with the single LPP-E7/11-19 vaccination.

5 Discussion

Cervical cancer induced by high-risk HPVs is a major health concern, causing more than 530,000 cancer cases and approximately 270,000 deaths per year. Additionally, 100,000 anal, vulvar, penile and, importantly, oropharyngeal cancers are caused by HPV annually (de Martel *et al.*, 2017). In total, 5 % of all cancers worldwide are therefore estimated to be caused by HPVs (Plummer *et al.*, 2016). Furthermore, the incidence of precancerous lesions is by far higher than the number of cancer cases, since 250,000 to 1 million women are diagnosed with cervical intraepithelial neoplasia (CIN) lesions annually in the USA alone (Henk *et al.*, 2010). Treatment for CIN is therefore much more common in developed countries than occurrence of cervical cancer (Barken *et al.*, 2012). Treatment options to date include surgery, chemotherapy and radiation therapy. An emerging field of oncology is immuno-oncology that allows the harnessing of the immune system's specificity, powerful effector and long-lasting memory mechanisms as a treatment tool against cancer. Since the highly specific targeting system of T cells allows to selectively target cancer cells, the side effects of immunotherapy are expected to be much lower than those of conventional therapies (Gulley, 2013). HPV-induced cancers express viral proteins, such as E6 and E7, which are recognized by the immune system as foreign, making them especially attractive targets for immunotherapeutic interventions. Additionally, the expression of these proteins is indispensable for the malignant phenotype of the cancer cells, making immune evasion by silencing the respective genes virtually impossible. This is highlighted by the finding that mutations in E7 are extremely rare in cervical cancers since mutations abrogate the carcinogenic function of this protein (Mirabello *et al.*, 2017). Furthermore, the majority of HPV-induced cancers are caused by only one HPV type, HPV16 (de Martel *et al.*, 2017). This allows the treatment of a large number of patients with treatments that are specific for HPV16. Due to all the reasons mentioned, many attempts have been made to develop therapeutic vaccines against HPV16-induced cancers (see 1.2.3 and (Khallouf, Grabowska and Riemer, 2014; Chabeda *et al.*, 2018)). Many of these attempts have yielded very promising results in preclinical studies, however, clinical trials for the better part could not reproduce the favorable preclinical results.

To improve the translatability of the preclinical findings and to develop a clinically successful therapeutic HPV16 vaccine, we consider two aspects to be of special importance: First, the

vaccine should contain epitopes that are *bona fide* presented on cells of HPV16-induced cancer, since there is a large amount of evidence showing that HPV infection leads to altered antigen processing, which prevents the presentation of some possible epitopes. Second, promising vaccine candidates should be tested in a suitable *in vivo* model that allows the exclusive testing of immune responses restricted by human MHC, i.e. HLA molecules. This is of special importance since all models used to date allowed for immune responses restricted by murine H-2 molecules, thus misrepresenting the clinical situation.

Following these guidelines, we aimed at developing a therapeutic vaccine containing defined epitopes that are known to be presented on tumor cells. Furthermore, we aimed at generating a HPV16 tumor model in A2.DR1 mice, which do not express any murine MHC molecules. Testing the epitope-specific vaccine in this tumor model was therefore going to enable us to improve the clinical relevance of data generated in preclinical studies.

5.1 Characteristics of A2.DR1 mice

A2.DR1 mice are transgenic for HLA-A*0201 and HLA-DR1 and thus can mount immune responses that are restricted by HLA-types that are among the most prevalent HLA-types in the human population worldwide. Additionally, genetic manipulations via knockouts ensure that no murine MHC class I/class II molecules can present epitopes to immune cells. Thus, any immune response in these mice is necessarily restricted by HLA-A2 and HLA-DR1. For this reason, the A2.DR1 mouse represents an ideal mouse model for experimental situations where the exclusive study of HLA-restricted immune responses is important.

Prior to the start of this PhD project, A2.DR1 mice of our colony were accidentally crossed with C57BL/6 mice, rendering the offspring of these matings heterozygous for murine and human MHC molecules. Immune responses in these heterozygous animals can be restricted by human and by murine MHC molecules, which is why renewed contamination of the A2.DR1 breeding colony had to be avoided. To rule out the occurrence of renewed accidental interstrain breeding, we decided to monitor all animals used for breeding with genotyping PCRs. By compiling seven genotyping PCRs, we were able to routinely confirm the correct genetic background of our A2.DR1 breeding stock animals (Figure 11, Figure 13). We found that when using DNA from C57BL/6 mice as negative control templates for the HLA-DRA1 and HLA-DRB1 PCRs, a fragment of the length expected for HLA-DRA1 and HLA-DRB1 was

amplified in these PCR reactions, albeit with a lower yield than from the A2.DR1 DNA templates. We speculated that since murine and human MHC class II genes share high sequence homology, these fragments could be generated by cross binding of the HLA-DR1 primers to the murine MHC class II genes. This theory could be confirmed by using DNA from MHC class II KO mice as controls, since these samples did not give rise to any fragments of the size corresponding to the PCR-amplified HLA-DRA1 and HLA-DRB1 fragments (Figure 12). It is likely that the lower yield observed in the PCRs with C57BL/6 DNA as a template was caused by weaker affinity of the primers to the murine MHC class II genes than to their respective specific templates, HLA-DRA1 and HLA-DRB1.

Taken together, the successful compilation of genotyping PCRs and the continuous monitoring of the A2.DR1 breeding colony ensured the generation of results in homozygous A2.DR1 mice.

5.2 Tumor model generation

To generate an A2.DR1-compatible, HPV16 E6/E7-expressing tumor model, several options for parental cells were explored. After attempts of using lung cells and keratinocytes isolated from A2.DR1 mice had not given rise to tumorigenic cell lines (data not shown), we decided to use the already tumorigenic A2.DR1-derived sarcoma cell line 2277NS (Quandt, 2012; Schumacher *et al.*, 2014) as a parental cell line to be transduced with HPV16 E6/E7.

2277NS cells were generated by injection of a carcinogen (methylcholanthrene, MCA) into A2.DR1^{old} mice. As a result, these cells carry many somatic mutations, which are likely to also give rise to neoepitopes. In addition to MCA, 2277NS cells also were exposed to further genome destabilizing effects after transduction with the pWPI vector, since the expression of the E6 and E7 proteins leads to genome instability (McBride and Warburton, 2017). Other models such as TC-1 (Lin *et al.*, 1996) or HLF16 (Eiben *et al.*, 2002) presumably have fewer total mutations than 2277NS cells since their tumorigenicity was induced by transfecting somatic cells with vectors coding for constitutively activated versions of ras proteins (e.g. V12 h-ras). However, also these two cell lines started accumulating mutations after beginning to express E6 and E7 *in vitro*. It is reasonable to assume that the mutation profile that is induced by MCA is different from the one induced by the actions of E6 and E7. It is

important to keep all these differences in mind when comparing results generated in the different models.

2277NS cells are derived from a slightly different version of A2.DR1 mice (namely A2.DR1^{old}) than the A2.DR1 mice used in this study. The two versions differ in two points: First, in A2.DR1^{old} mice the H-2D^{b} gene is not knocked out as it is in A2.DR1 mice, but the absence of H-2D^{b} molecules on the surface is based on the fact that only complexes of epitope, MHC class I heavy chain and β2m are stably assembled and transported to the cell surface. Since A2.DR1^{old} mice are KO for murine β2m, no H-2D^{b} complexes should reach the cell surface. However, some reports mention that despite the KO of the murine β2m, H-2D^{b} heavy chains could be found on the cell surface of β2m KO mice (Allen *et al.*, 1986; Bix and Raulet, 1992). Second, while in A2.DR1 mice the complete MHC class II locus is knocked out, A2.DR1^{old} mice still express I-Eβ. This molecule could form atypical heterodimers with HLA-DRα and thus be present on the cell surface (Lawrance *et al.*, 1989). Due to these two differences there was a chance that the immune system of A2.DR1 mice might recognize the 2277NS cells as foreign and respond with a xenoreaction against the potentially present H-2D^{b} heavy chain and the atypical HLA-DRα/I-Eβ. We analyzed 2277NS cells via flow cytometry for cell surface expression of H-2D^{b} molecules, but we could not find any indication for the surface presentation of these molecules (data not shown). Nevertheless, before continuing to work with 2277NS cells, we tested if the injection of 2277NS cells into A2.DR1 mice would give rise to a xenoreaction against the putative non-self H-2D^{b} and HLA-DRα/I-Eβ, which could lead to the rejection of the 2277NS tumors. We did not observe any symptoms of a xenoreaction as the mice did not exhibit signs of discomfort or obvious signs of an immune response and the 2277NS cells formed tumors just as they are reported to do in A2.DR1^{old} mice (Figure 14). Even if residual amounts of H-2D^{b} heavy chains, too low to induce a xenoreaction, should be expressed on 2277NS cells, these molecules could not induce a specific CD8^{+} T cell-mediated response against H-2D^{b}-presented HPV16 E6/E7 epitopes, since no T cells were positively selected to recognize peptides presented on H-2D^{b} in the thymus of our A2.DR1 mice.

Another potential problem associated with the use of 2277NS cells was their relatively low HLA-A2 surface expression (Figure 15), which could make it difficult for T cells to recognize any tumor model based on this cell line. On the other hand, there is evidence that only one copy of a peptide presented on MHC is sufficient for T cells to recognize and kill an infected

cell (Sykulev *et al.*, 1996). Furthermore, two tumor models based on 2277NS cells have been previously used to demonstrate therapeutic effects of immunotherapeutic interventions (Schumacher *et al.*, 2014; Ochs *et al.*, 2017). However, it is reasonable to assume that very low target molecule expression on the cancer cell would make T cell-mediated killing more difficult and less frequent. This assumption is supported by the finding that many cancer types, among them cervical cancer as an example of HPV-induced cancers, downregulate their MHC class I expression, probably to make detection by the immune system more difficult (Bubeník, 2003). The fact that 2277NS cells show only low levels of HLA-A2 expression could therefore even be advantageous for obtaining experimental results that have better prognostic value for clinical studies than e.g. results obtained with TC-1 cells which exhibit pronounced MHC class I expression (data not shown). However, the HLA-A2 expression in 2277NS cells can be increased by IFN-γ treatment. If a few T cells recognize their epitope in the tumor despite low levels of HLA-A2 expression, they would get activated and secrete IFN-γ and thus induce the upregulation of HLA-A2 also in 2277NS cells. Interestingly, we found that the PAP-A2 cell line expressed higher levels of HLA-A2 than the parental cell line 2277NS, but still lower levels than e.g. the human cervical cancer cell line CaSki (data not shown). This is in contrast to the observation that the expression of E7 reduces the total abundance of MHC on the cell surface (Doorbar *et al.*, 2015). This discrepancy can be explained by the workflow we used for the generation of the PAP-A2 cell line as we selected the 2277NS (pWPI) clones with the highest HLA-A2 expression in this population (Figure 18).

After we had transduced 2277NS cells with the pWPI HPV16 E6/E7 vector, we analyzed the resulting polyclonal 2277NS (pWPI) cells for their expression of E6 and E7. The expression levels of E6 and E7 in 2277NS (pWPI) were considerably higher than the ones in CaSki cells, presumably as a consequence of the usage of the strong EF-1α promotor in the pWPI vector and the selection pressure applied through puromycin. However, after we had generated clonal cell lines from the polyclonal pool of 2277NS (pWPI) cells, we found that the E6/E7 expression levels were highly heterogeneous between clones. This finding, especially with correlating relative levels of E6 and E7 expression (Figure 19), makes multiple integration of the vector into the genome of 2277NS cells likely. It also makes it probable that E6 and E7 are actually expressed in an approximate 1:1 ratio (as expected if the P2A sequence works

properly (Kim *et al.*, 2011; Liu *et al.*, 2017)). Remarkably, several clones did not exhibit any E6/E7 expression at all after puromycin selection. This may be based on the fact that the puromycin gene is located behind the E6/E7 genes on the mRNAs (see vector map, Figure 16) but translation of the puromycin gene is initiated from an internal ribosome entry site (IRES) (Komar and Hatzoglou, 2011). Therefore, it is reasonable to assume that in some clones only the puromycin resistance cassette was translated.

In some E6/E7 WBs (Figure 19) we failed to detect E6 in CaSki and E7 in TC-1 cells. This result is likely due to the fact that the expression levels of both proteins are relatively low in the respective cell lines. However, we could confirm the expression of both proteins in both cell lines in different WBs (data not shown).

Only one of the five 2277NS (pWPI)-derived clonal cell lines that we injected into A2.DR1 mice formed a tumor and this only in one of 4 injected animals (Figure 21). This low tumor take could have different reasons, among them the expression levels of HLA-A2, E6 and E7 of the different clones. The IVA2 clone exhibited intermediate expression of HLA-A2, of E6 and of E7. One could speculate that clones with lower expression of these three proteins are less likely to be detected by the immune system. This speculation is strengthened by the finding that upon reisolation of the IVA2 tumor, these cells, then called PAP-A2, were found to express much lower levels of E6 and E7 than the parental IVA2 cell line (data not shown).

We found that a relatively large number of PAP-A2 cells were necessary to induce a high tumor take (Figure 24). We observed that $2.5x10^6$ PAP-A2 cells induced 100 % tumor take and very fast tumor growth, but that a reduction of the number of injected cells to $1x10^6$ cells induced tumors in only 60 % of mice. Extrapolating from these results, we decided to conduct further experiments with $1.5x10^6$ PAP-A2 cells, which should induce a high tumor-take but leave enough time for treatment intervention.

In summary, we established the PAP-A2 cell line as a new tumor model for HPV16-induced malignancies, which is suited for the use in fully MHC-humanized A2.DR1 mice.

5.3 Epitope-specific vaccinations against HPV16 E6/E7-positive tumors

Therapeutic vaccination against HPV-induced tumors should induce the strongest anti-tumor effect possible and should be easily applicable in the clinic. Most vaccine formulations tested

in clinical studies so far have only met the second criterion: They are easily applicable in the clinic because they do not require an additional patient selection process based on their immune characteristics. This is e.g. possible by using DNA vaccines coding for whole HPV proteins or a mix of SLPs in the vaccine formulation since they contain epitopes suitable for many HLA types (Kenter *et al.*, 2009).

These SLPs are quickly and efficiently processed and cross-presented (Rosalia *et al.*, 2013), which is a prerequisite for effective $CD8^+$ T cell responses. However, SLPs do not allow for the selection of truly tumor cell-presented peptides and therefore do not allow for choosing the peptides that give rise to a productive immune response in a specific patient. We hypothesize that meeting the first and most important prerequisite for a therapeutic HPV vaccine, achieving the strongest possible anti-tumor effect, will require focusing the immune responses on epitopes that are truly presented on the target cells. This can only be achieved by epitope-specific vaccines. However, epitope-specific vaccines have also disadvantages since they cannot be applied to all patients but have to be matched to the specific patient's HLA-type. In the age of ever more personalized medicine, epitope-specific vaccines matched to the patient's HLA type represent a realistic treatment option. HLA-typing nowadays requires only 48 h by next generation sequencing (NGS) (Illumina Inc, 2018) and the costs are no longer prohibitively high and can be expected to decrease further in the years to come (Wetterstrand, 2018). The potential workflow required for the application of an epitope-specific therapeutic vaccine would thus start with the detection of e.g. a CIN lesion. In this instance, a small biopsy such as a swab would be taken from the lesion to determine the HPV type causing the lesion by already approved tests such as the cobas® HPV test, a DNA-based test for HPV detection and typing (Wright *et al.*, 2011). The same sample, a blood sample or an oral swab would be used to determine the patient's HLA type. If the patient is found to express e.g. HLA-A2, she would be given a vaccine containing epitopes specifically for this HLA type. The combination of several epitopes restricted to different HLA-types in one vaccine is also an option, allowing the use of one vaccine for more than one HLA type. If the peptides are chosen carefully (meaning that the epitopes are only binding to a specific HLA-type), this would not lead to non-productive immune responses.

5.3.1 Comparison of vaccine formulations

In our mouse model, we used different vaccine formulations to induce $CD8^+$ T cell immune responses against mass spectrometry-confirmed HPV16 epitopes. As a lead epitope for the comparison of the different formulations we chose E7/11-19, since this epitope was found to be relatively abundantly presented on HLA-A2 on several $HPV16^+$ cell lines (Riemer *et al.*, 2010; Blatnik *et al.*, 2018). Our laboratory examined healthy female donors for HPV16 E6/E7-reactive T cells in their blood to detect memory responses that were indicative of a previous encounter with HPV16 (Blatnik *et al.*, 2018). In this analysis, 4 out of 8 HPV16-reactive healthy female donors had E7/11-19-specific T cells in their blood. Additionally, on average, the frequency of T cells being activated by a HPV epitope was the highest among the cultures that were stimulated with the E7/11-19 peptide.

The goal for the comparison of the vaccination formulations was to find the approach that induces the highest number of E7/11-19-specific $CD8^+$ T cells as magnitude of the T cell response is correlated with treatment success (Cho and Celis, 2010). The three assays most commonly used for the detection of epitope-specific T cells are the enzyme-linked immuno spot assay (ELISpot), the intracellular cytokine-staining assay (ICS) and the MHC multimer assay (Amara, 2009; Murphy *et al.*, 2016). Additional assays are the staining for the effector molecule granzyme B (Murphy *et al.*, 2016) and staining for the degranulation marker CD107a (Betts *et al.*, 2003).

The ELISpot assay is very sensitive and also allows the functional assessment of T cell effector functions (such as IFN-γ or TNF-α secretion). However, this assay does not permit the concomitant analysis of frequencies of T cell populations (e.g. frequencies of $CD8^+$ T cells). Therefore, we concentrated on the MHC multimer and IFN-γ ICS assays, which are both flow cytometry-based and thus allow the simultaneous analysis of the T cell populations. We tested various multimer constructs such as fully human HLA-A2 pentamers, single-chain trimers (MHC molecules with bound peptides formed from a single polypeptide chain) (Hansen *et al.*, 2010) with different α3 domains, and H-$2K^b$-HLA-A2 chimeric pentamers (data not shown). Fully human HLA-A2 multimers did not exhibit any staining of epitope-specific A2.DR1-derived $CD8^+$ T cells, thus confirming the findings concerning the incompatibility of murine CD8 and the α3 domain of HLA (Irwin, Heath and Sherman, 1989). H-$2K^b$-HLA-A2 chimeric pentamers, which are reported to specifically stain $CD8^+$ T cells of HLA-humanized

mice (Choi *et al.*, 2002), did exhibit specific staining to some extent – but their sensitivity was always lower than the sensitivity achieved in IFN-γ ICS analyses and also seemed to vary between epitopes (data not shown). This finding could be explained by the theory that the affinity of some murine T cell receptors to the human α1 and α2 domains of HLA-A2 is high enough to activate the T cell but not high enough to bind the cell to the fluorophore-coupled multimer for a time long enough to allow detection. Our method of choice was therefore IFN-γ/TNF-α ICS with subsequent flow cytometric analysis. Additionally, a clear advantage of the IFN-γ ICS is that only T cells that are activated are counted in the flow cytometer. A T cell that is stained with an MHC multimer does not have to be functional but only to express a suitable TCR with an affinity high enough for prolonged binding to the multimer. In contrast, a T cell that is able to express IFN-γ after epitope recognition is capable of fulfilling one of its most important effector functions.

We compared three different vaccine formulation types which differ greatly in their mechanism of action: emulsion-based formulations, mRNA vaccines and several amphiphilic compounds. In the emulsion-based approach and the amphiphilic compounds we used synthetic short peptides (SSP). SSPs are, as SLPs, considered safe, stable and are easy to produce (Chabeda *et al.*, 2018). SSPs also induce powerful activation of $CD8^+$ T cells (Rosalia *et al.*, 2013). However, synthetic short peptides can also be presented by non-professional APCs by binding to MHC class I present on the outside of the cell by e.g. replacing the naturally presented ligand (Eisen *et al.*, 2012). Since non-professional APCs do not supply T cells with signals 2 and 3 (see Figure 2), this process can lead to immune tolerance (Bijker *et al.*, 2007), which is a strategy to prevent autoimmunity. Both vaccine formulations used in this study reduce the presentation of epitopes on non-professional APCs. The oil emulsion of IFA is mostly taken up by professional phagocytes (Murphy *et al.*, 2016) and the amphiphilic vaccines have been shown to bind to albumin and thus migrate along with albumin to the lymph node in which they are taken up by DCs and macrophages (Liu *et al.*, 2014). The mRNA vaccine could potentially also induce tolerance if non-professional APCs take up the mRNA, express the encoded peptides and present them as an internally generated epitope on MHC class I. However, the lipoplex formulation of this vaccine ensures that the mRNA is virtually exclusively taken up by professional APCs, in particular DCs (Kranz *et al.*, 2016).

We used an emulsion-based formulation for our first experiments with E7/11-19. E7/11-19 epitope vaccination has, to the best of our knowledge, never been performed in HLA-A2-humanized mice before. Emulsion-based formulations have long been the gold standard for the induction of $CD8^+$ T cells, and thus also for therapeutic anti-cancer vaccines. To verify the immunogenicity of E7/11-19 also in A2.DR1 mice, we used a water-in-oil emulsion based on the mineral oil ISA51. Indeed, we could observe E7/11-19-specific $CD8^+$ T cells after one injection of this formulation. To date, there is only one study that quantifies frequencies of anti-HPV16 $CD8^+$ T cells in HLA-A2-humanized mice in response to vaccination with emulsion-based vaccines (Daftarian *et al.*, 2007). These authors report frequencies of approximately 1 % of splenocytes specific for E7/82-90 and 0.65 % specific for E7/11-20 in one mouse each after a single vaccination with VacciMax®, an emulsion-based vaccine adjuvanted with CpG. However, these results were obtained in HLA-A2 transgenic mice in which the HLA-A2 molecule was not altered to contain a murine α3 domain. Therefore, the authors speculate that the TCRs in this mouse model have a particularly high affinity for their MHC:peptide complex to allow binding despite the murine CD8/human α3 HLA domain incompatibility. It is unclear what the frequency of $CD8^+$ T cells is among the splenocytes of these mice, which would be important to know for being able to compare these results directly with the ones obtained in A2.DR1 mice. Nevertheless, the results obtained in our experiments seem to be within the same range and showed with certainty that E7/11-19 is immunogenic in A2.DR1 mice. However, the obtained T cell numbers did not justify testing this formulation in an anti-tumor setting. Especially in the light of recent publications showing the immune response-debilitating effects of depot vaccines (Hailemichael *et al.*, 2013, 2018) we hypothesized that inducing E7/11-19-specific $CD8^+$ T cells via different formulations would yield better anti-tumor responses than the use of emulsion-based vaccines.

As a second formulation to induce E7/11-19-specific $CD8^+$ T cells, we tested mRNA vaccines in collaboration with the company BioNTech (Mainz). The advantages of mRNA vaccines are their relatively fast production, which permits the synthesis of personalized vaccines; the mRNA's self-adjuvanting characteristics; and its capability to be immediately translated once taken up by cells. The resultant peptides are directly transported into the ER and loaded onto MHC class I, making cross-presentation unnecessary. This is facilitated by a C-terminal MITD sequence that further enhances epitope presentation on MHC class I and class II (Kreiter *et*

al., 2007). Furthermore, a phosporothioate cap on the 5' end of the RNA introduced into the RNA vaccines of BioNTech protects the RNA from degradation in the target cells and enhances translation specifically in immature DCs (Kuhn *et al.*, 2010). mRNA delivered in BioNTech's systemically applied liposomes is mostly taken up by professional APCs which prime T cells in lymph nodes all over the body, making the priming of T cells very efficient (Kranz *et al.*, 2016). This mechanism of action of the lipoplex formulation also ensures that the professional APC that expresses the mRNA provides the necessary additional two signals to prime T cells, since the mRNA itself is a TLR agonist and thus activates the professional APC taking up the mRNA construct. One of the disadvantages of mRNA vaccines is that mRNA is susceptible to degradation by RNases, therefore careful handling of all substances and tools used for the generation of RNA vaccines is of paramount importance. BioNTech's mRNA vaccines are currently tested in several clinical trials (e.g. NCT02410733, NCT02035956). Among these is a first-in-human phase I/II trial in patients with $HPV16^+$ positive cancers with E6/E7 mRNA that is complexed in lipids (Eudra CT No.: 2014-002061-30).

In a preliminary experiment with E7 full length mRNA we did not observe an induction of E7-specific T cells. This experiment was conducted with only one mouse per construct with the objective to screen several different mRNAs in a setting in which the availability of the in-house bred A2.DR1 mice was limited. Since in this experiment only one mouse was used and since E7 full length mRNA induced strong anti-E7 responses in other mouse models (personal communication Dr. Christian Grunwitz) this result should be regarded with caution. The lack of induction of E7/11-19-specific $CD8^+$ T cells after injection of mRNA encoding only E7/11-19 (Figure 26) was an expected result since also in previous experiments conducted by BioNTech elongation of the minimal epitope by three amino acids up- and downstream of the epitope was necessary to induce an immune response (personal communication Dr. Christian Grunwitz). Following this approach, we observed $CD8^+$ T cells specific for this epitope after vaccination with two constructs (E7/8-21 +/- PADRE) that included three amino acids before and after the E7/11-19 sequence to allow correct antigen processing. The induced frequencies of E7/11-19-specific $CD8^+$ T cells were relatively low (approximately 1 % of $CD8^+$ T cells), but since the mRNA vaccines also increased the overall frequency of $CD8^+$ T cells in the spleen of the treated animals to approximately 13.5 %, the frequencies of E7/11-19-specific $CD8^+$ T cells cannot be compared directly with the frequencies of E7/11-19-specific

$CD8^+$ T cells in mice treated with other vaccines. Accounting for this confounding factor, the overall number of E7/11-19-specific $CD8^+$ T cells was still lower in mRNA treated animals than in animals treated with the most successful amphiphilic vaccines (Figure 32).

In addition, we observed a response against an epitope that was created by the linker sequences connecting the mRNA backbone and the E7/8-21 sequence (SLHEYMLDL). The immune response directed against this epitope was approximately two times stronger than the one against the target epitope E7/11-19. Since it is our explicit aim to exclude unproductive immune responses, this finding was highly unfavorable. Therefore, steps were undertaken to ensure that induced immune responses were exclusively directed against the target epitope. To do so, we changed the anchor amino acid leucine of the artificial SLHEYMLDL epitope to an alanine, which should abrogate binding of this peptide to HLA-A2. After this amino acid exchange, we did not observe any immune responses directed against E7/11-19 or against SAHEYMLDL (data not shown). We hypothesize that the most likely reason for this finding is that the new amino acid sequence is not processed by peptidases into the respective epitopes. An *in silico* test with the proteasome cleavage prediction server NetChop 3.1 (Keşmir *et al.*, 2002; Nielsen *et al.*, 2005) gave backing to this hypothesis. Using a combination of MHC epitope binding prediction servers (NetMHC 4.0 and SYFPEITHI) and NetChop we found that the exchange of the serine contained in the linker sequence to other amino acids than alanine could lead to mRNAs that can induce immune responses specifically against E7/11-19. These mRNAs will be tested in future experiments for the exclusive induction of $CD8^+$ T cells recognizing E7/11-19.

Amphiphilic vaccines are reported to function by albumin hitchhiking of the peptide-containing compounds to lymph nodes (Liu *et al.*, 2014). Apparently, in addition to lymph node targeting, amphiphilic vaccines also result in improved uptake by DCs (Wang *et al.*, 2018). The albumin binding strategy has previously been used together with nanoparticles (Zhu *et al.*, 2017) and amphiphilic vaccines were also successfully combined with other immunotherapeutic interventions such as anti-tumor ABs, IL-2 and checkpoint blockade (Moynihan *et al.*, 2016). We adapted two different approaches from the literature to make minimal epitopes amphiphilic: the Pam2 approach developed by Cho *et al.* (Cho *et al.*, 2013) and the LPP approach developed by Liu *et al.* (Liu *et al.*, 2014). Furthermore, we generated two more compounds that were designed with the rationale to improve the applicability of

the Pam2 approach by allowing easier and more specific synthesis (Pam1 and Stea2 compounds).

All compounds were tested for their ability to induce $CD8^+$ T cell responses against our lead epitope E7/11-19. Except Pam1-E7/11-19, all compounds induced substantial frequencies of E7/11-19-specific $CD8^+$ T cells in A2.DR1 mice. Since the only difference between Pam1-E7/11-19 and Pam2-E7/11-19 is that Pam2-E7/11-19 contains one more palmitic acid, it is likely that the lack of a T cell immune response after vaccination with Pam1-E7/11-19 is founded in this difference. This finding matches the observations of Liu *et al.* that CpG coupled to a monoacylated compound does not migrate to lymph nodes as readily as CpG coupled to a diacylated compound. This decrease in lymph node localization could explain the decrease in vaccination efficacy.

Putting the results obtained with the amphiphilic vaccines in A2.DR1 mice in relation to results of other groups with these compounds is difficult since no results of experiments with these compounds in humanized mice have been published so far. Nevertheless, some conclusions can be drawn from observations made in this study that have an impact on the general understanding of the working principle of amphiphilic vaccines.

Cho *et al.* report that their Pam2 compounds only elicit very high frequencies of epitope-specific $CD8^+$ T cells when pIC is used as a TLR agonist and not with other TLR agonists such as CpG (Cho *et al.*, 2013). The LPP compound was also tested with pIC and an amphiphilic variant of CpG and it was shown that this amphiphilic CpG was a better adjuvant than non-amphiphilic CpG to be used in conjunction with LPP, since this combination induced higher frequencies of epitope-specific $CD8^+$ T cells (Liu *et al.*, 2014). Interestingly, our LPP-E7/11-19 adjuvanted with CpG did not elicit substantial $CD8^+$ T cell responses, which is in contrast to LPP-E7/11-19 adjuvanted with pIC (Figure 30). Therefore, our results regarding the TLR agonist to be used to adjuvant amphiphilic epitopes are more in line with the findings made by Cho *et al.*. However, we did not use amphiphilic versions of either CpG or pIC.

One major difference between pIC and CpG is that TLR9, which recognizes CpG, is different in mice and humans (Bauer *et al.*, 2001). Different CpG motifs are needed to boost immune responses in these two species. In contrast, TLR3, is of sufficient similarity between mice and humans to recognize pIC in both species (Martins, Bavari and Salazar, 2015). Therefore,

results generated with pIC in mice can be more directly translated into the human setting than results generated with CpG.

Another interesting observation that we made concerns the optimal route of injection. Cho *et al.* report that intravenous injection of the Pam2 compounds was approximately three times more effective in inducing epitope-specific $CD8^+$ T cells than the subcutaneous injection route. We could not reproduce these findings as the chemically extremely similar compound Stea2-E7/11-19 induced slightly more epitope-specific $CD8^+$ T cells when injected subcutaneously (Figure 28). In the study by Liu *et al.*, the LPP compounds were always injected subcutaneously. We speculated that the intravenous injection of LPPs could increase the vaccines' efficacy – as had been shown before by Cho *et al.* with their amphiphilic compound. Remarkably, we could not confirm this hypothesis since the intravenous injection of LPP did not give rise to any epitope-specific T cells. This surprising result may be explained by the different chemical structures of the Pam2 and the LPP compound. Due to the long PEG spacer, the LPP compound is much larger than the Pam2 compound. It is possible that the LPP compound is more easily taken up by e.g. liver cells and thus taken out of the circulation before a DC has the chance to take it up. This process would not be relevant in subcutaneously injected LPP because the subcutaneous liquid is not passed through the liver before albumin binding and transport to the lymph nodes takes place.

We compared the efficacy of the various vaccination approaches by their capability to induce high frequencies of E7/11-19-specific $CD8^+$ T cells. Due to experimental reasons, we used the frequency of specific $CD8^+$ T cells among $CD19^-$ splenocytes as a surrogate for the whole-body frequency of specific $CD8^+$ T cells in the animals. This surrogate is justified because the vast majority of specific $CD8^+$ T cells have left the lymph nodes and have entered the circulation (and thus can be found in the spleen) seven days after the last vaccination.

One of the most important factors that determine if a therapeutic vaccination will be successful is the total number of tumor-reactive T cells in the individual, if the quality of these cells is held constant. This can be seen in studies in which animals were treated with adoptive transfer of T cells. In these studies, higher total numbers of tumor-reactive T cells are correlated with better treatment efficacy (Klebanoff *et al.*, 2012). Knowing the frequency

of epitope-specific $CD8^+$ T cells within the $CD8^+$ T cell compartment is therefore not enough, because the size of the $CD8^+$ T cell compartment is also important. The total size of the $CD8^+$ T cell compartment can be described as the mathematical product of two factors: The total number of immune cells and the percentage of $CD8^+$ T cells among the immune cells. To determine the second factor, we quantified the percentage of $CD8^+$ T cells among the immune cells in the spleen. In this analysis, we observed a remarkable increase in the frequency of $CD8^+$ T cells among $CD19^-$ splenocytes after vaccination with mRNA and all amphiphilic constructs but not after vaccination with emulsion-based vaccines (Figure 31). The most remarkable increase in the frequency of $CD8^+$ T cells could be observed in the mice that were treated with mRNA. In this group, the mean overall frequency of $CD8^+$ T cells among splenocytes was 13.5 % (compared to 5 % in naïve A2.DR1 mice). The mean overall $CD8^+$ frequency in animals treated with amphiphilic vaccines was approximately 8 %.

As mentioned before, it is not feasible to determine the total number of immune cells or $CD8^+$ T cells in a whole animal and the spleen represents a potential surrogate measure. Due to interexperimental uncertainties regarding the comparability of the number of splenocytes per mouse, we chose not to include the differences we observed in these assays into our analysis (see 4.3.1.4). Therefore, it is important to estimate the size of a potential error introduced by omitting this factor and if this could change the outcome of the comparison between the groups. We observed splenocyte counts between $30x10^6$ and $55x10^6$ splenocytes per spleen in naïve mice (data not shown). Splenocyte counts in vaccinated animals usually ranged from $30x10^6$ to $75x10^6$ splenocytes per mouse. Only in exceptional cases the splenocyte count was as high as $150x10^6$ per spleen. We observed these high counts only in experiments in which mRNA had been injected. Therefore, the treatment group most affected by not including the spleen size is the mRNA group since we observed the highest number of splenocytes per spleen in this group. Assuming the largest possible error resulting from the difference between $30x10^6$ and $150x10^6$, the median frequency of E7/11-19-specific $CD8^+$ T cells induced by vaccination with mRNA vaccines could be underestimated by a factor of five. To correct for this potential error, the median frequencies of E7/11-19-specific $CD8^+$ T cells among $CD19^-$ splenocytes induced by the mRNA vaccines (0.065 %) have to be multiplied by five. The resulting frequency of 0.325 % can then be directly compared with the frequency of E7/11-19 specific $CD8^+$ T cells that are induced by

LPP-E7/11-19 (0.63 %). Thus, the mRNA vaccines would still only induce half the median frequency of E7/11-19-specific $CD8^+$ T cells that are induced by LPP-E7/11-19. Therefore, it can be concluded that the chosen comparison approach excludes a critical underestimation of some vaccines' performance that could have altered the outcome of the comparison between the vaccine formulations.

All amphiphilic vaccines that induced substantial frequencies of specific $CD8^+$ T cells (Pam2 i.v. pIC, Stea2 s.c. pIC, LPP s.c. pIC) induced more E7/11-19-specific $CD8^+$ T cells than the emulsion-based vaccines and the mRNA vaccines by direct comparison of frequencies of E7/11-19-specific $CD8^+$ T cells and also when taking into account the increase in overall $CD8^+$ T cell frequencies (Figure 32). The injected quantities of these three compounds were not perfectly comparable due to the impurities mainly in the Pam2 compound that motivated us to generate the Stea2 compound. Even with this slight limitation in comparability, we found the LPP compound to have the most favorable overall performance in terms of induction of E7/11-19-specific $CD8^+$ T cells, ease of production and handling.

5.3.2 Characterization of immune responses induced by LPP vaccines

Therefore, we used the modular synthesis scheme of this compound that facilitates the use of various peptides to generate three further HPV16 minimal epitope LPPs (LPP-E7/7-15, LPP-E7/82-90 and LPP-E6/25-33). We chose the two additional HPV16 E7 epitopes because $CD8^+$ T cells against these epitopes could be found in healthy donors and the presentation of these epitopes on CaSki cells was confirmed by mass spectrometry (Blatnik *et al.*, 2018). This study showed that E7/7-15 and E7/82-90, in addition to E7/11-19, represent target structures on cancer cells and that $CD8^+$ T cell responses against these epitopes are immunodominant enough to appear during a natural infection. An additional reason to focus on E7-derived epitopes was that the E7 sequences found in cervical cancers are virtually devoid of any mutations, whereas conservation of E6 does not seem to be as critical for carcinogenesis (Mirabello *et al.*, 2017). We still decided to also include one E6-derived epitope, LPP-E6/25-33. In our experiments, we found that all of the three additional LPPs induced substantial frequencies of epitope-specific $CD8^+$ T cells (Figure 33) when they were injected subcutaneously together with pIC.

It has been reported that T cells that produce more than one cytokine, which are therefore called multifunctional, particularly contribute to tumor clearance (van Duikeren *et al.*, 2012). Therefore, we tested the ability of the vaccination-induced, epitope-specific $CD8^+$ T cells to express TNF-α in addition to IFN-γ. T cells of all four specificities responded to activation with TNF-α expression. This was most pronounced in the E7/11-19-specific $CD8^+$ T cells in which approximately 10 % expressed TNF-α in addition to IFN-γ. Liu *et al.* found approximately 12 % of epitope-specific $CD8^+$ to be expressing TNF-α, which matches our results for E7/11-19-specific $CD8^+$ T cells. Interestingly, only very few $CD8^+$ T cells responded to activation with only TNF-α expression and no IFN-γ expression.

To be considered fully functional, $CD8^+$ T cells have to exhibit cytotoxicity in addition to cytokine production – hence the term „cytotoxic T cells“ (CTLs), which is often used interchangeably to „$CD8^+$ T cells”. In this study, we observed specific killing of peptide-loaded target cells (Figure 37) for $CD8^+$ T cells of all four specificities of interest (E7/7-15-, E7/11-19-, E7/82-90- and E6/25-33-specific) and were therefore able to confirm that these vaccination-induced $CD8^+$ T cells truly are fully functional cytotoxic T cells. However, it is important to keep in mind that the setting of externally loaded target cells with peptides added in high concentrations does not resemble the natural situation where, usually, only few MHC molecules on the cell surface present the respective epitope.

To test the T cells’ killing capacity in a more natural scenario, we made use of the newly developed PAP-A2 cell line that expresses HPV16 E6 and E7. Thus, PAP-A2 cells should also present internally processed peptides contained in the E6/E7 sequence on MHC class I. The expression levels of E7 in PAP-A2 are much lower than in CaSki cells (Figure 23), a human cell line that was derived from a HPV16-induced cervical carcinoma. It is therefore reasonable to assume that PAP-A2 cells present fewer copies of E7-derived peptides on their surface than CaSki cells. The killing of PAP-A2 cells by E7-specific cytotoxic T cells should consequently represent a bigger challenge than the killing of CaSki cells. Nevertheless, we observed specific killing of PAP-A2 cells by T cells of all four specificities, which was especially pronounced in the case of E7/11-19-specific $CD8^+$ T cells. This result demonstrates that murine PAP-A2 cells process and present the respective epitopes on HLA-A2, proving the suitability of our newly generated tumor model to test anti-tumor vaccinations with these epitopes. This result is in contrast to the findings of Street *et al.* who report that E7/82-90-

specific T cells derived from AAD mice were unable to kill cells endogenously expressing HPV16 E6/E7 (Street *et al.*, 2002). Since in that study it was found that the same E7/82-90-specific T cells were able to kill target cells that were externally loaded with E7/82-90 peptide, the authors concluded that there are differences in the epitope-processing machinery of mice and humans that do not allow the processing of E7 into E7/82-90. Consistent with their findings, the group argues that due to these differences the value of humanized mouse models for the study of therapeutic vaccines is limited. The results obtained in this PhD project cannot support this hypothesis, since all four epitopes, among them E7/82-90, that were found on naturally transformed HPV16$^+$ human cells were generated from endogenously expressed E6/E7 and presented on our PAP-A2 murine cells.

The magnitude of killing of epitope-loaded target cells and PAP-A2 target cells can be directly compared as for both experiments T cells from the very same culture were used. The less pronounced killing of PAP-A2 compared to epitope-loaded 2277NS cells by E7/7-15-, E7/11-19- and E7/82-90-specific CD8$^+$ T cells could be explained by the theory that fewer HLA-A2 epitope complexes with these epitopes can be found on the surface of the PAP-A2 cells than on 2277NS cells that were externally loaded with synthetic minimal epitopes. It is however not possible to compare the killing capacities of the CD8$^+$ T cells of different specificities because the numbers of epitope-specific CD8$^+$ T cells within the T cell cultures were not controlled in this experiment. Adjusting the numbers of specific CD8$^+$ T cells to equal numbers would have required an additional ICS staining, which was not possible with the limited cell material at our disposal. However, if one was to control for the number of cells and observe a difference in the killing capacity of CD8$^+$ T cells of different specificities, two explanations for this are possible: First, the TCRs have different affinities for their respective MHC:peptide complex and second, the different HLA-A2-binding affinities and/or the differences in efficiency of the processing of the epitopes lead to different abundance of the respective epitopes presented on HLA-A2 and therefore alter the number of potential target molecules on the cells, and thus the likelihood of a T cell finding its specific target complex.

In a test experiment (data not shown) we observed that the mixing and injection of LPP-E7/11-19 and LPP-E7/82-90 resulted in a median frequency of E7/11-19-specific CD8$^+$ T cells of 0.44 % (compared to 4.2-13 % in a single vaccination). We also found that the median

frequency of E7/82-90-specific $CD8^+$ T cells was slightly diminished compared to single vaccination (1.5 %, compared to a median frequency of 2.0 % in single E7/82-90-vaccination). However, since we observed precipitation of the two LPPs that were mixed, the finding of reduced frequencies of epitope-specific $CD8^+$ T cells may have been explained by the precipitation, since precipitated LPPs e.g. might not attach well to albumin. To exclude effects caused by precipitation before injection, we injected different combinations of HPV16 LPPs into different subcutaneous injection sites in a follow-up experiment (see 4.3.2.4). We found that the anti-E7/11-19 $CD8^+$ T cell response was again greatly diminished compared to the single LPP immunization (median of 4.2-13 % in single vaccinations, approximately 0.45 % in combinations) by administering different LPPs at the same point of time. Furthermore, also the frequencies of the $CD8^+$ T cells specific for the other injected epitope(s) were reduced. This resulted in a generally lower frequency of potentially tumor-reactive $CD8^+$ T cells as evaluated by incubating the splenocytes with a combination of the different epitopes in one well and by adding up the frequencies of IFN-γ^+ $CD8^+$ T cells after incubation with the single epitopes used in the treatment. The small differences between the two methods used could be explained by different affinities of the epitopes to HLA-A2 leading to competition for HLA-A2-binding and therefore also differential T cell activation in the restimulation with all peptides combined in one well.

After the first test experiment we considered immunodominance as a potential reason since the magnitude of the response against E7/82-90 was only slightly diminished compared to single LPP-E7/82-90 vaccination, while the E7/11-19 response was nearly completely suppressed. However, in the follow-up experiment we observed reduced frequencies of $CD8^+$ T cells specific for all the epitopes when combined. Thus, immunodominance of one epitope over the others can be excluded as a potential reason.

In the combination experiments, the total pIC amount of 50 µg per mouse was distributed equally to all injection sites. Potentially, this reduced local amount of pIC may have led to reduced DC activation, which in turn resulted in less T cell activation. However, also in other experiments the 50 µg pIC per mouse were distributed over a larger area, namely in all experiments in which amphiphilic vaccines (Stea2-E7/11-19, Pam2-E7/11-19) were injected intravenously. In these experiments, the priming of E7/11-19-specific $CD8^+$ T cells was not impaired.

Another potential reason for the impaired activation of epitope-specific $CD8^+$ T cells may lie in the LPP dose, which was twice as high as in the single immunizations (three times and four times for the combinations with three and four LPPs, respectively). Potentially, the high amount of fatty acids could either cause mechanical problems, such as impaired lymph drainage of the injection sites, or impair DC behavior. This hypothesis could be tested by injecting a double dose of LPP-E7/11-19. If this vaccination, despite the injection of a large amount of LPP, gives rise to similarly high frequencies of E7/11-19-specific $CD8^+$ T cells as observed in single LPP-E7/11-19 vaccination, the theory of an impairing effect of too high a concentration of fatty acids would be falsified.

Taken together, our results argue for the use of minimal epitopes which need to be matched carefully to avoid epitope-specific immunosuppression, if a combination of epitopes is desired (Figure 39, Figure 40).

VGX-3100 is the most successful therapeutic vaccine in clinical trials so far and the DNA in this vaccine encodes for longer stretches of E6/E7 sequences (Trimble *et al.*, 2015). It would be interesting to see if the epitope-specific immunosuppression would also be observed after immunization with this construct. Since this vaccine showed clinical efficacy, the specificity of the induced $CD8^+$ T cells is of large interest. This DNA vaccine may not induce epitope-specific immunosuppression, or the potentially very wide breadth of T cell specificities allows the development of high enough total numbers of tumor-reactive T cells to have a therapeutic effect.

5.3.3 Efficacy of anti-tumor vaccinations

Thus far, we have shown the establishment of the tumorigenic HPV16 E6/E7-expressing cell line PAP-A2 and of a vaccination formulation (LPP) that induces high frequencies of HPV16 epitope-specific $CD8^+$ T cells. We were able to show in *in vitro* experiments that the vaccination-induced, epitope-specific $CD8^+$ T cells are capable of killing the PAP-A2 cells. After these successful experiments, it remained to be seen if this *in vitro* anti-tumor cell effect would also translate into an anti-tumor effect *in vivo*.

To test if this was the case, we first chose a prophylactic vaccination approach, i.e. we vaccinated A2.DR1 mice with LPP-E7/11-19 and subsequently challenged them with PAP-A2 tumor cells (Figure 41). This approach was also chosen to rule out potential anti-tumor

effects by a general stimulation of the immune system by pIC injection, since the last pIC injection took place seven days before the tumor challenge. This hypothesis was confirmed by the finding that the survival curves of the untreated group overlapped with the vehicle control-treated group. In this experiment, we observed a significant difference in mean survival times as well as in overall survival between the vehicle control-treated group and the LPP-E7/11-19-treated group. Since the only difference in treatment between these two groups was the inclusion of the E7/11-19 epitope in the vaccine formulation, the difference in survival is most likely based on the induction of E7/11-19-specific $CD8^+$ T cells in the LPP-E7/11-19 group.

Since our declared goal is the development of a therapeutic HPV16 vaccine that can be used against precursor lesions and cancer, it was necessary to test the LPP-E7/11-19 efficacy also in a therapeutic experimental setting (Figure 42). In this experiment, we observed complete tumor rejection in 50 % of the LPP-E7/11-19-vaccinated mice, which is substantially more than in the untreated (12.5 %) or the vehicle control-treated (0 %) groups. Studies of therapeutic HPV16 vaccines in C57BL/6 mice with TC-1 tumors have sometimes reported higher tumor rejection rates than the ones observed in our experiments (Cho *et al.*, 2013; Liu *et al.*, 2014; Bissa *et al.*, 2015; Heidenreich *et al.*, 2015; Kranz *et al.*, 2016). However, in the TC-1 model, immune responses are often induced against the extremely immunogenic H-$2D^b$-restricted E7/49-57 epitope. It is likely that the HLA-A2-restricted E7/11-19-epitope is less immunogenic than E7/49-57 and therefore induces lower frequencies of epitope-specific $CD8^+$ T cells with direct influence on treatment success. For example, Liu *et al.* observed frequencies of more than 20 % E7/49-57-specific $CD8^+$ T cells among all $CD8^+$ T cells with LPP-E7/49-57 and only one booster injection instead of the two booster injections used in our treatment regimen. Cho *et al.* even report that more than 40 % of all $CD8^+$ T cells were specific for E7/49-57 after two injections of Pam2-E7/49-57 in C57BL/6 mice. In addition to the potential difference in immunogenicity of the two used epitopes, it is important to keep in mind that not only the tumor inoculation and treatment schemes in the various studies were different (such as numbers of injected cells and time until treatment initiation), but that in the other studies a completely different cell line and mouse model was used. Naïve C57BL/6 mice have approximately threefold higher frequencies of total $CD8^+$ T cells (15 % of $CD19^-$ cells in splenocytes, (BioRad, 2018)) compared to A2.DR1 mice (5 % of $CD19^-$ cells in

splenocytes, Figure 31). This is most likely due to inferior affinities of murine TCRs to HLA-A2, leading to negative selection during the thymic development of T cells in A2.DR1 mice. The difference in overall $CD8^+$ T cell numbers certainly has a direct influence on the overall number of epitope-specific $CD8^+$ T cells in each given mouse. Furthermore, the susceptibility of TC-1 tumors and PAP-A2 tumors to T cell-mediated killing may be completely different. Susceptibility to T cell killing depends on MHC class I expression, expression of immune modulatory surface molecules by the tumor cells and a tumor microenvironment (such as the presence of myeloid-derived suppressor cells (MDSC) (reviewed in (Umansky *et al.*, 2016)) or hypoxic areas in the tumor) that is more or less permissive for $CD8^+$ T cell actions (reviewed in (Gajewski, Schreiber and Fu, 2013)). The same caveats about tumor cell line-inherent differences also hold true for results obtained in AAD mice with e.g. HLF16 cells.

Therapeutic vaccination with other LPP-HPV16 epitopes did not induce anti-tumor effects as strong as LPP-E7/11-19, even though treatment with LPP-E7/7-15 and LPP-E7/82-90 resulted in a small increase in tumor rejection compared to the vehicle control-treated animals (Figure 43). This is especially interesting in the light of the result that all four LPP compounds induced similar frequencies of epitope-specific $CD8^+$ T cells (Figure 33). However, we observed a significant difference in IFN-γ expression between E7/7-15 and E7/11-19-specific $CD8^+$ T cells, which could explain the better performance of E7/11-19 (Figure 34). On the other hand, the IFN-γ expression between E7/82-90-, E6/25-33- and E7/11-19-specific $CD8^+$ T cells was not different, making this hypothesis unlikely. Of course, different affinities of the respective TCRs to their MHC:peptide complex could explain this phenomenon. Similarly, a lower avidity of the TCR of the $CD8^+$ T cells specific for E7/7-15, E7/82-90 and E6/25-33 to the tumor cells could also explain the observed results. This explanation would also take into account differential antigen processing in the tumor cells. The hypothesis of differential antigen processing in tumor cells is supported by the finding that in mass spectrometry analysis of HPV16 epitopes presented on HLA-A2 on CaSki cells, E7/11-19 was the most abundantly detected epitope (Riemer *et al.*, 2010). Another potential explanation is based on the observation that the highest frequencies of multi-cytokine expressing epitope-specific $CD8^+$ T cells were detected in animals treated with LPP-E7/11-19. The multifunctional $CD8^+$ T cells could mediate much stronger anti-tumor effects than T cells only expressing IFN-γ after activation, as was reported before (van Duikeren *et al.*, 2012).

Interestingly, we often observed a two-armed distribution of mice in regard to their ability to mount an epitope-specific $CD8^+$ T cell response in vaccination experiments in non-tumor bearing mice. Some mice responded with considerably higher frequencies of specific $CD8^+$ T cells than others within the same group. This seems to be a characteristic of the A2.DR1 mice, since we observed this phenomenon with all vaccine formulations including the LPP formulation (Figure 28, Figure 30, Figure 33). Unfortunately, we could not assess if this observation translates into corresponding survival in tumor-bearing mice, since the readout with IFN-γ ICS requires more cells than can be isolated from a blood sample from a single live mouse, and thus necessitates sacrificing of mice and spleen isolation. However, it is tempting to speculate that the animals which exhibited less pronounced anti-tumor effects within a group indeed also belonged to the group of animals with fewer vaccination-induced $CD8^+$ T cells.

When we vaccinated tumor-bearing mice with combinations of the previously tested HPV16 minimal epitope constructs, we observed anti-tumor effects that were similar in magnitude to single immunizations with E7/7-15, E7/82-90 and E6/25-33 and that were therefore inferior to single immunization with E7/11-19. Since we also observed reduced overall frequencies of $CD8^+$ T cells that were specific for the four used epitopes upon combination vaccination with LPPs (4.3.2.4) it is likely that the inferior anti-tumor efficacy is based on reduced frequencies of these cells. This is in contrast to the findings of Daftarian *et al.* (Daftarian *et al.*, 2007) who reported equal anti-tumor effects with E7/82-90 in a single epitope-vaccine and in a mix with three additional HPV16 minimal epitopes (E7/11-20, E7/86-93 and E6/29-38). However, the epitopes were supplied in an emulsion-based vaccine, which could lead to equal immune responses against all these epitopes. The observed results could therefore be explained by differences in delivery form (emulsion-based vaccine vs. LPP) and the different epitopes.

One way to prevent the suppression of $CD8^+$ T cell responses against single epitopes upon injection of several LPP compounds in our system could be to use LPPs with different epitopes in an alternating vaccination regime such as 1^{st} injection: LPP-E7/11-19, 2^{nd} injection: LPP-E7/82-90, 3^{rd} injection: LPP-E7/11-19 et cetera. However, the question would remain if the additional presence of even high frequencies of e.g. E7/82-90-specific $CD8^+$ T cells would result in a pronounced increase in anti-tumor effects, since also the single

immunization with LPP-E7/82-90 did not induce large anti-tumor effects. This is underlined by the fact that the median frequencies of potentially tumor-reactive $CD8^+$ T cells were not very low in the combination treatments (7+11+82: 3.33 %, 7+11+25: 4.22 %, 11+82+25: 2.64 %, 7+11+82+25: 3.66 %). Nevertheless, these T cells, which contained close to no E7/11-19-specific $CD8^+$ T cells, did not induce pronounced anti-tumor effects. Therefore, it seems likely that of the T cell specificities thus far induced in the A2.DR1/PAP-A2 tumor model, only E7/11-19-specific $CD8^+$ T cells mediate pronounced anti-tumor effects.

Overall, the therapeutic and prophylactic tumor vaccination experiments show that single immunization with LPP-E7/11-19 induces strong anti-tumor effects that are more pronounced than the ones induced by the other tested HPV16 LPP minimal epitope constructs or by combinations of different HPV16 minimal epitope LPPs.

The fact that an E7-derived epitope was effective in the mediation of anti-tumor effects in our PAP-A2 model is especially promising since the E7-expression levels of PAP-A2 cells are markedly lower than in the human cervical cancer cell line CaSki (Figure 23). Therefore, it is likely that CaSki cells – and maybe other naturally HPV16-induced tumors – present higher amounts of E7/11-19 epitopes on their surface, which would in turn facilitate T cell-mediated killing.

Taking into account the results of this PhD thesis when evaluating the results of clinical studies that have used therapeutic peptide HPV vaccines, several observations can be made. Overall, only two completed clinical studies have treated patients of a specific HLA-type with defined epitopes. These studies have used either lipidated E7/86-93 peptide (Steller *et al.*, 1998) or E7/12-20 in an oil-emulsion with or without the addition of lipidated E7/86-93 (Muderspach *et al.*, 2000). These trials have shown only very moderate or no success in terms of disease reduction. Contributing to the poor performance of the treatment is the fact that all patients enrolled in the first study had advanced metastatic disease (Steller *et al.*, 1998). However, both studies demonstrated the immunogenicity of the chosen peptides, but immune responses were not induced in all patients and were weak. This could be due to the fact that the lipopeptides in both studies were injected without TLR agonists and therefore activation of the innate immune system was not induced, leading to limited T cell priming.

Human T cell lines specific for E7/86-93 and E7/11-20 can effectively kill CaSki cells (Ressing *et al.*, 1995), therefore these epitopes must be presented by these cancer cell line. Also in the course of our studies E7/11-20 was found on the surface of CaSki cells by mass spectrometry (Blatnik *et al.*, 2018). The epitope E7/86-93 (TLGIVCPI) could not be confirmed to be presented on CaSki cells by Blatnik *et al.* because this peptide contains a cysteine at position 6. In the Blatnik study, cysteine-containing peptides were not monitored as the reactivity of cysteines allows the formation of many potential adducts that prevent detection by the employed targeted mass spectrometry approach (Blatnik *et al.*, 2018).

The study by Muderspach *et al.* and nearly all other clinical studies using peptide vaccines, including the most recent studies ((van Poelgeest *et al.*, 2013; de Vos van Steenwijk *et al.*, 2014; Takeuchi *et al.*, 2015), NCT02128126, NCT02426892, NCT02865135), have used SLPs or minimal epitopes in emulsion-based formulations, mostly ISA51, which was also used in this thesis. ISA51-based vaccines, in particular if used without the addition of TLR agonists such as MPLA, induced only very low frequencies of E7/11-19-specific $CD8^+$ T cells compared to the amphiphilic formulations in this study (Figure 32). In addition to the low induction of epitope-specific $CD8^+$ T cells, these few specific T cells are sequestered to the vaccination site where persistent granulomas form in some cases (van Doorn *et al.*, 2016). We never observed such granulomas or other vaccination-related adverse effects in animals treated with amphiphilic vaccines, which represents another advantage of these formulations.

In the light of the results of this PhD thesis, the suboptimal outcomes of the clinical studies mentioned above are not surprising. Future clinical studies will be able to benefit from the experiences gained in this thesis and the previous clinical studies and will hopefully yield better results.

Taken together, the data presented in this thesis show that amphiphilic vaccines induce the highest frequencies of epitope-specific $CD8^+$ T cells among the tested formulations, that vaccination-induced $CD8^+$ T cells can specifically kill the newly established PAP-A2 cell line and that therapeutic vaccination with E7/11-19 induces strong anti-tumor effects.

6 Summary & Outlook

Cancer immunotherapy holds the possibility to become a major pillar of future oncologic treatments. HPV16-induced cancers represent ideal targets for cancer immunotherapy, due to the obligatory expression of the HPV16 proteins E6/E7, against which no central tolerization has taken place. However, some hurdles still have to be overcome before anti-HPV16 immunotherapies will become standard therapies in the clinic. Therefore, the aim of this study was to further improve the efficacy of anti-HPV16 immunotherapy by targeting problems that are specifically connected to this cancer entity.

To this end, we established a new tumor model of HPV16 E6/E7-positive cancers in fully MHC-humanized A2.DR1 mice. Furthermore, several epitope-specific vaccination approaches were compared for their induction of cytotoxic T cells directed against mass spectrometry-verified HPV16 epitopes. Finally, a therapeutic vaccine formulation based on lipo-PEG-peptides (LPPs) generated in this study was successfully tested for its anti-tumor effect in the novel mouse tumor model.

In our experiments, we used pIC as an adjuvant for the LPP vaccine. In contrast, the initial study by Liu *et al.* used an amphiphilic version of CpG to adjuvant their LPP formulation (Liu *et al.*, 2014). This amphiphilic version of CpG reduced systemic toxicity and improved vaccination success since it is, like the LPP, trafficked to lymph nodes and taken up by professional APCs. A potential option to further increase the immune response in response to LPP vaccination would therefore be to generate an amphiphilic version of pIC.

We achieved the best anti-tumor responses using the E7/11-19 epitope. This epitope is currently also tested in the clinic in a phase Ib/II trial in HLA-A*02$^+$ patients with incurable HPV16-related oropharyngeal, cervical, or anal cancer (NCT02865135). The goal of this trial is to assess the safety and efficacy of DPX-E7, an emulsion-based vaccine containing E7/11-19 in combination with cyclophosphamide. Emulsion-based formulations were the ones with the worst performance in our experiments. Therefore, it remains to be seen if the E7/11-19 epitope can confer substantial anti-tumor effects in this setting.

When we vaccinated A2.DR1 mice with combinations of HPV16 LPPs we observed a general decrease in the epitope-specific CD8$^+$ T cell immune responses. So far, the precise reasons for this phenomenon have not been determined. Overcoming the problems that were

associated with the use of combinations of LPPs could diversify the anti-tumor immune response and thus also increase the overall number of tumor-reactive $CD8^+$ T cells leading to improved anti-tumor effects.

So far, MHC class II-restricted epitopes have not been used as LPPs for vaccinations. MHC class II-restricted $CD4^+$ T cell responses provide help for $CD8^+$ T cell responses and can therefore increase the efficacy of vaccinations aimed at expanding tumor-specific $CD8^+$ T cells. In future experiments, we will test MHC class II (HLA-DR)-restricted responses in our A2.DR1 mice. Potential epitopes to be coupled to the amphiphilic construct can be either universally applicable non-natural epitopes like PADRE or be derived from HPV16 E6/E7. Epitopes that promiscuously bind to several MHC class II types are of particular interest since they can be used in larger groups of patients. Several MHC class II epitopes that promiscuously bind to HLA-DR molecules have been defined by our group (Grabowska, Kaufmann and Riemer, 2014) which represent the ideal starting point for *in vivo* vaccination studies with MHC class II LPP constructs.

Furthermore, our laboratory is currently using the PAP-A2 cell line that was generated during this PhD thesis to establish orthotopic models of HPV16-induced cancers. For this, the PAP-A2 cells were transfected with a vector coding for luciferase, which makes the observation of tumor growth possible even when the tumor is not accessible and therefore cannot be measured with calipers. The use of orally and vaginally placed tumors as orthotopic models will enable researchers to modify the vaccination approach tested in this study to make it suitable for inducing strong immune responses in the mucosal environment with its special characteristics. So far, no orthotopic model of HPV-induced cancers has been established for MHC-humanized mice and the orthotopic models under development are expected to further increase the translational value of the results generated in this PhD thesis. Since the mucosal microenvironment is different from the subcutaneous microenvironment and since subcutaneously induced T cells do not readily migrate to mucosal sites, different methods to induce migration of the vaccination-induced T cells to the mucosal tumor will have to be tested. Potential ways to influence the migration of T cells towards the tumors would be special vaccination regimens (Çuburu *et al.*, 2017), the local application of the chemokines CXCL9 and CXCL10 (Shin and Iwasaki, 2012) and the local application of immune modulators/TLR agonists such as R848 (Soong *et al.*, 2014).

In addition to the above-mentioned future goals of our group several other approaches to improve anti-HPV cancer immunotherapy are used by other groups. Immune checkpoint blockade has been the major breakthrough in oncology during the last years (Sharma and Allison, 2015). The boosting of vaccine-induced immune responses by concomitant application of checkpoint blockade ABs is a very attractive option to achieve better treatment results. Several clinical studies targeting HPV16-induced malignancies are already using this strategy. Among these are studies using the DNA vaccine VGX-3100 together with a PD-L1 AB (NCT03162224) and a study that combines the emulsion-based SLP vaccine ISA101 with nivolumab (NCT02426892). The use of checkpoint blockade ABs is especially interesting against HPV-induced cancers since these cancer cells do not only express virus-derived epitopes but also express many mutation-derived neoepitopes (Alexandrov *et al.*, 2013) due to the genome destabilizing actions of E6/E7-expression (McBride and Warburton, 2017).

Another focus to improve anti-HPV immunotherapies lies in the combination of therapeutic vaccination with concomitant chemotherapy or radiation therapy. Chemotherapy can improve the vaccination results by depleting T_{reg} (reviewed in (Emens and Middleton, 2015)) and low dose radiation therapy induces a reprogramming of the tumor microenvironment (Klug *et al.*, 2013), immunogenic cell death and an influx of professional APCs that prime T cells that are either specific for tumor mutation-derived neoantigens or viral epitopes (reviewed in (Golden and Apetoh, 2015)). These treatment options are pursued in clinical studies such as one trial combining ISA101 with paclitaxel and carboplatin (NCT02128126) or the previously mentioned trial using E7/11-19 in the DPX-E7 formulation that uses cyclophosphamide (NCT02865135).

We advocate the use of epitope-specific vaccines. However, many successful preclinical experiments show effectivity also for vaccine formulations that are not epitope specific. So far, these could not be tested in a mouse model without the bias introduced by the immunodominant E7/49-57 epitope. Our new tumor model in combination with A2.DR1 mice now allows the test of such vaccines in humanized mice. The models and results generated in this study will thus help to increase the translatability of preclinical studies to clinical situations in the future.

7 References

Adams, S. (2009) 'Toll-like receptor agonists in cancer therapy.', *Immunotherapy*, 1(6), pp. 949–64. doi: 10.2217/imt.09.70.

Albrechtsen, S. *et al.* (2008) 'Pregnancy outcome in women before and after cervical conisation: population based cohort study.', *BMJ*, 337(7673), p. a1343. doi: 10.1136/bmj.a1343.

Alexander, J. *et al.* (1997) 'Derivation of HLA-A11/Kb transgenic mice: functional CTL repertoire and recognition of human A11-restricted CTL epitopes.', *Journal of Immunology*, 159(10), pp. 4753–61.

Alexandrov, L. B. *et al.* (2013) 'Signatures of mutational processes in human cancer.', *Nature*, 500(7463), pp. 415–21. doi: 10.1038/nature12477.

Allen, H. *et al.* (1986) 'Beta 2-microglobulin is not required for cell surface expression of the murine class I histocompatibility antigen H-2Db or of a truncated H-2Db.', *Proceedings of the National Academy of Sciences of the United States of America*, 83(19), pp. 7447–51.

Altmann, D. M. *et al.* (1995) 'The T cell response of HLA-DR transgenic mice to human myelin basic protein and other antigens in the presence and absence of human CD4.', *The Journal of Experimental Medicine*, 181(3), pp. 867–875.

Amara, R. R. (2009) 'Methods for quantitating antigen-specific T cell responses using functional assays in rhesus macaques.', *Methods in Molecular Biology (Clifton, N.J.)*, 485, pp. 417–24. doi: 10.1007/978-1-59745-170-3_28.

Arbyn, M. *et al.* (2018) 'Prophylactic vaccination against human papillomaviruses to prevent cervical cancer and its precursors.', *The Cochrane Database of Systematic Reviews*, 5, p. CD009069. doi: 10.1002/14651858.CD009069.pub3.

Barken, S. S. *et al.* (2012) 'Frequency of cervical intraepithelial neoplasia treatment in a well-screened population', *International Journal of Cancer*, 130(10), pp. 2438–2444. doi: 10.1002/ijc.26248.

Bauer, S. *et al.* (2001) 'Human TLR9 confers responsiveness to bacterial DNA via species-specific CpG motif recognition.', *Proceedings of the National Academy of Sciences of the United States of America*, 98(16), pp. 9237–42. doi: 10.1073/pnas.161293498.

BenMohamed, L. *et al.* (2000) 'Induction of CTL response by a minimal epitope vaccine in HLA A*0201/DR1 transgenic mice: dependence on HLA class II restricted T(H) response.', *Human Immunology*, 61(8), pp. 764–79. doi: 10.1016/S0198-8859(00)00139-7.

Bennett, S. R. *et al.* (1998) 'Help for cytotoxic-T-cell responses is mediated by CD40 signalling.', *Nature*, 393(6684), pp. 478–80. doi: 10.1038/30996.

Berard, F. *et al.* (2000) 'Cross-priming of naive CD8 T cells against melanoma antigens using dendritic cells loaded with killed allogeneic melanoma cells.', *The Journal of Experimental Medicine*, 192(11), pp. 1535–44. doi: 10.1084/jem.192.11.1535.

Bernard, H.-U. *et al.* (2010) 'Classification of papillomaviruses (PVs) based on 189 PV types and proposal of taxonomic amendments.', *Virology*, 401(1), pp. 70–9. doi: 10.1016/j.virol.2010.02.002.

Berraondo, P. *et al.* (2007) 'Eradication of large tumors in mice by a tritherapy targeting the innate, adaptive, and regulatory components of the immune system', *Cancer Research*, 67(18), pp. 8847–8855. doi: 10.1158/0008-5472.CAN-07-0321.

Betts, M. R. *et al.* (2003) 'Sensitive and viable identification of antigen-specific CD8+ T cells by a flow cytometric assay for degranulation.', *Journal of Immunological Methods*, 281(1–2), pp. 65–78.

Bijker, M. S. *et al.* (2007) 'CD8+ CTL priming by exact peptide epitopes in incomplete Freund's adjuvant induces a vanishing CTL response, whereas long peptides induce sustained CTL reactivity.', *Journal of Immunology*, 179(8), pp. 5033–40.

BioRad (2018) *BioRad - Cell frequencies*. Available at: https://www.bio-rad-antibodies.com/flow-cytometry-cell-frequency.html (Accessed: 13 July 2018).

Bissa, M. *et al.* (2015) 'A prime/boost strategy using DNA/fowlpox recombinants expressing the genetically attenuated E6 protein as a putative vaccine against HPV-16-associated cancers', *Journal of Translational Medicine*, 13(1), p. 80. doi: 10.1186/s12967-015-0437-9.

Bix, M. and Raulet, D. (1992) 'Functionally conformed free class I heavy chains exist on the surface of beta 2 microglobulin negative cells.', *The Journal of Experimental Medicine*, 176(3), pp. 829–34. doi: 10.1084/jem.176.3.829.

Blander, J. M. and Medzhitov, R. (2006) 'Toll-dependent selection of microbial antigens for presentation by dendritic cells.', *Nature*, 440(7085), pp. 808–812. doi: 10.1038/nature04596.

Blatnik, R. *et al.* (2018) 'A targeted LC-MS strategy for low-abundant HLA class I-presented peptide detection identifies novel human papillomavirus T-cell epitopes', *Proteomics*, 18(11), p. e1700390. doi: 10.1002/pmic.201700390.

Bonhoure, F. and Gaucheron, J. (2006) 'Montanide ISA 51 VG as Adjuvant for Human Vaccines', *Journal of Immunotherapy*, 29(6), pp. 647–648.

Borenstein, S. H. *et al.* (2000) 'CD8+ T cells are necessary for recognition of allelic, but not locus-mismatched or xeno-, HLA class I transplantation antigens.', *Journal of Immunology,* 165(5), pp. 2341–2353. doi: 10.4049/jimmunol.165.5.2341.

Bosch, F. X. *et al.* (2013) 'Comprehensive Control of Human Papillomavirus Infections and Related Diseases', *Vaccine*, 31 Suppl 7, pp. H1–H31. doi: 10.1016/j.vaccine.2013.10.003.

Boshart, M. *et al.* (1984) 'A new type of papillomavirus DNA, its presence in genital cancer biopsies and in cell lines derived from cervical cancer.', *The EMBO journal*, 3(5), pp. 1151–7. doi: 10.1002/J.1460-2075.1984.TB01944.X.

Brake, T. *et al.* (2003) 'Comparative analysis of cervical cancer in women and in a human papillomavirus-transgenic mouse model: identification of minichromosome maintenance protein 7 as an informative biomarker for human cervical cancer.', *Cancer Research*, 63(23), pp. 8173–80.

Bravo, I. G., de Sanjosé, S. and Gottschling, M. (2010) 'The clinical importance of understanding the evolution of papillomaviruses', *Trends in Microbiology*, 18(10), pp. 432–438. doi: 10.1016/j.tim.2010.07.008.

Bruni, L. *et al.* (2016) 'Global estimates of human papillomavirus vaccination coverage by region and income level: A pooled analysis', *The Lancet Global Health*, 4(7), pp. e453–e463. doi: 10.1016/S2214-109X(16)30099-7.

Bubeník, J. (2003) 'Tumour MHC class I downregulation and immunotherapy (Review).', *Oncology Reports*, 10(6), pp. 2005–8.

van der Burg, S. H. *et al.* (2016) 'Vaccines for established cancer: overcoming the challenges posed by immune evasion.', *Nature Reviews Cancer*, 16(4), pp. 219–33. doi: 10.1038/nrc.2016.16.

Carmon, L. *et al.* (2000) 'Novel breast-tumor-associated MUC1-derived peptides: characterization in Db-/- x beta2 microglobulin (beta2m) null mice transgenic for a chimeric HLA-A2.1/Db-beta2 microglobulin single chain.', *International Journal of Cancer*, 85(3), pp. 391–7.

Carpino, L. A. and Han, G. Y. (1972) 'The 9-Fluorenylmethoxycarbonyl amino-protecting group', *The Journal of Organic Chemistry*, 37(22), pp. 3404–3409. doi: 10.1021/jo00795a005.

Chabeda, A. *et al.* (2018) 'Therapeutic vaccines for high-risk HPV-associated diseases', *Papillomavirus Research*, pp. 46–58. doi: 10.1016/j.pvr.2017.12.006.

Charles River (2018) *Charles River,*. Available at: https://www.criver.com/products-services/find-model/c3h-mouse?region=23 (Accessed: 23 May 2018).

Cheever, M. A. *et al.* (2009) 'The prioritization of cancer antigens: A National Cancer Institute pilot project for the acceleration of translational research', *Clinical Cancer Research*, 15(17), pp. 5323–5337. doi: 10.1158/1078-0432.CCR-09-0737.

Cho, H.-I. *et al.* (2013) 'BiVax: a peptide/poly-IC subunit vaccine that mimics an acute infection elicits vast and effective anti-tumor CD8 T-cell responses.', *Cancer Immunology, Immunotherapy : CII*, 62(4), pp. 787–99. doi: 10.1007/s00262-012-1382-6.

Cho, H.-I. and Celis, E. (2010) 'Overcoming doubts and other obstacles in the development of effective peptide-based therapeutic vaccines against cancer.', *Expert Review of Vaccines*, 9(4), pp. 343–5. doi: 10.1586/erv.10.13.

Choi, E. M. *et al.* (2002) 'The use of chimeric A2Kb tetramers to monitor HLA A2 immune responses in HLA A2 transgenic mice', *Journal of Immunological Methods*, 268(1), pp. 35–41. doi: 10.1016/S0022-1759(02)00198-9.

Chow, E. P. F. *et al.* (2017) 'Quadrivalent vaccine-targeted human papillomavirus genotypes in heterosexual men after the Australian female human papillomavirus vaccination programme: a retrospective observational study.', *The Lancet. Infectious Diseases*, 17(1), pp. 68–77. doi: 10.1016/S1473-3099(16)30116-5.

Crum, C. P. *et al.* (1986) 'In situ hybridization analysis of HPV 16 DNA sequences in early cervical neoplasia.', *The American Journal of Pathology*, 123(1), pp. 174–82.

Çuburu, N. *et al.* (2017) 'Adenovirus vector-based prime-boost vaccination via heterologous routes induces cervicovaginal CD8 $^{+}$ T cell responses against HPV16 oncoproteins', *International Journal of Cancer*, 142(7), pp. 1467-1479. doi: 10.1002/ijc.31166.

Daftarian, P. M. *et al.* (2007) 'Rejection of large HPV-16 expressing tumors in aged mice by a single immunization of VacciMax encapsulated CTL/T helper peptides.', *Journal of Translational Medicine*, 5, p. 26. doi: 10.1186/1479-5876-5-26.

Day, P. M. *et al.* (2004) 'Establishment of papillomavirus infection is enhanced by promyelocytic leukemia protein (PML) expression', *Proceedings of the National Academy of Sciences of the United States of America*, 101(39), pp. 14252–14257. doi: 10.1073/pnas.0404229101.

Day, P. M. *et al.* (2010) 'In vivo mechanisms of vaccine-induced protection against HPV infection.', *Cell Host & Microbe*, 8(3), pp. 260–70. doi: 10.1016/j.chom.2010.08.003.

Day, P. M. *et al.* (2013) 'Identification of a role for the trans-Golgi network in human papillomavirus 16 pseudovirus infection.', *Journal of Virology*, 87(7), pp. 3862–70. doi: 10.1128/JVI.03222-12.

Decrausaz, L. *et al.* (2011) 'A novel mucosal orthotopic murine model of human papillomavirus-associated genital cancers', *International Journal of Cancer*, 128(9), pp. 2105–2113. doi: 10.1002/ijc.25561.

Denny, L. A. *et al.* (2012) 'Human papillomavirus, human immunodeficiency virus and immunosuppression.', *Vaccine*, 30 Suppl 5, pp. F168-74. doi: 10.1016/j.vaccine.2012.06.045.

Deschuyteneer, M. *et al.* (2010) 'Molecular and structural characterization of the L1 virus-like particles that are used as vaccine antigens in Cervarix™, the AS04-adjuvanted HPV-16 and -18 cervical cancer vaccine.', *Human Vaccines*, 6(5), pp. 407–19.

Domingos-Pereira, S. *et al.* (2013) 'Intravaginal TLR agonists increase local vaccine-specific CD8 T cells and human papillomavirus-associated genital-tumor regression in mice.', *Mucosal Immunology*, 6(2), pp. 393–404. doi: 10.1038/mi.2012.83.

Doorbar, J. (2005) 'The papillomavirus life cycle.', *Journal of Clinical Virology*, 32 Suppl 1, pp. S7-15. doi: 10.1016/j.jcv.2004.12.006.

Doorbar, J. (2013) 'The E4 protein; structure, function and patterns of expression', *Virology*, 445(1–2), pp. 80–98. doi: 10.1016/j.virol.2013.07.008.

Doorbar, J. *et al.* (2015) 'Human papillomavirus molecular biology and disease association.', *Reviews in Medical Virology*, 25 Suppl 1, pp. 2–23. doi: 10.1002/rmv.1822.

van Doorn, E. *et al.* (2016) 'Safety and tolerability evaluation of the use of Montanide ISA^{TM}51 as vaccine adjuvant: A systematic review', *Human Vaccines & Immunotherapeutics*, 12(1), pp. 159–169. doi: 10.1080/21645515.2015.1071455.

Van Doorslaer, K. *et al.* (2013) 'The Papillomavirus Episteme: a central resource for papillomavirus sequence data and analysis.', *Nucleic Acids Research*, 41(Database issue), pp. D571-8. doi: 10.1093/nar/gks984.

Van Doorslaer, K. *et al.* (2017) 'The Papillomavirus Episteme: a major update to the papillomavirus sequence database.', *Nucleic Acids Research*, 45(D1), pp. D499–D506. doi: 10.1093/nar/gkw879.

Drexler, I. *et al.* (2003) 'Identification of vaccinia virus epitope-specific HLA-A*0201-restricted T cells and comparative analysis of smallpox vaccines', *Proceedings of the National Academy of Sciences of the United States of America*, 100(1), pp. 217–222. doi: 10.1073/pnas.262668999.

van Duikeren, S. *et al.* (2012) 'Vaccine-Induced Effector-Memory CD8+ T Cell Responses Predict Therapeutic Efficacy against Tumors', *The Journal of Immunology*, 189(7), pp. 3397–3403. doi: 10.4049/jimmunol.1201540.

Dürst, M. *et al.* (1983) 'A papillomavirus DNA from a cervical carcinoma and its prevalence in cancer biopsy samples from different geographic regions.', *Proceedings of the National Academy of Sciences of the United States of America*, 80(12), pp. 3812–3815. doi: 10.1073/pnas.80.12.3812.

Dyson, N. *et al.* (1989) 'The human papilloma virus-16 E7 oncoprotein is able to bind to the retinoblastoma gene product.', *Science*, 243(4893), pp. 934–7.

Egawa, N. *et al.* (2015) 'Human papillomaviruses; Epithelial tropisms, and the development of neoplasia', *Viruses*, 7(7), pp. 3863–3890. doi: 10.3390/v7072802.

Eiben, G. L. *et al.* (2002) 'Establishment of an HLA-A*0201 human papillomavirus type 16 tumor model to determine the efficacy of vaccination strategies in HLA-A*0201 transgenic mice.', *Cancer Research*, 62(20), pp. 5792–9.

Einstein, M. H. *et al.* (2014) 'Comparison of long-term immunogenicity and safety of human papillomavirus (HPV)-16/18 AS04-adjuvanted vaccine and HPV-6/11/16/18 vaccine in healthy women aged 18-45 years: End-of-study analysis of a Phase III randomized trial', *Human Vaccines and Immunotherapeutics*, 10(12), pp. 3435–3445. doi: 10.4161/hv.36121.

Eisen, H. N. *et al.* (2012) 'Promiscuous binding of extracellular peptides to cell surface class I MHC protein.', *Proceedings of the National Academy of Sciences of the United States of America*, 109(12), pp. 4580–5. doi: 10.1073/pnas.1201586109.

Emens, L. A. and Middleton, G. (2015) 'The interplay of immunotherapy and chemotherapy: harnessing potential synergies.', *Cancer Immunology Research*, 3(5), pp. 436–43. doi: 10.1158/2326-6066.CIR-15-0064.

Fehrmann, F., Klumpp, D. J. and Laimins, L. A. (2003) 'Human papillomavirus Type 31 E5 Protein Supports Cell Cycle Progression and Activates Late Viral Functions upon Epithelial Differentiation.', *Journal of Virology*, 77(5), pp. 2819–2831. doi: 10.1128/JVI.77.5.2819.

Feltkamp, M. C. *et al.* (1993) 'Vaccination with cytotoxic T lymphocyte epitope-containing peptide protects against a tumor induced by human papillomavirus type 16-transformed cells.', *European Journal of Immunology*, 23(9), pp. 2242–2249. doi: 10.1002/eji.1830230929.

Fernando, G. J. *et al.* (1998) 'Th2-type CD4+ cells neither enhance nor suppress antitumor CTL activity in a mouse tumor model', *Journal of Immunology*, 161(5), pp. 2421–2427. doi: 10.4049/jimmunol.173.5.3148.

Firat, H. *et al.* (1999) 'H-2 class I knockout, HLA-A2.1-transgenic mice: a versatile animal model for preclinical evaluation of antitumor immunotherapeutic strategies.', *European Journal of Immunology*, 29(10), pp. 3112–21. doi: 10.1002/(SICI)1521-4141(199910)29:10<3112::AID-IMMU3112>3.0.CO;2-Q.

Foged, C. (2011) 'Subunit vaccines of the future: the need for safe, customized and optimized particulate delivery systems.', *Therapeutic Delivery*, 2(8), pp. 1057–77.

Formana, D. *et al.* (2012) 'Global burden of human papillomavirus and related diseases', *Vaccine*, 30(Suppl.5), pp. F12–F23. doi: 10.1016/j.vaccine.2012.07.055.

Freeman, G. J. *et al.* (2000) 'Engagement of the PD-1 immunoinhibitory receptor by a novel B7 family member leads to negative regulation of lymphocyte activation.', *The Journal of Experimental Medicine*, 192(7), pp. 1027–34.

Gajewski, T. F., Schreiber, H. and Fu, Y.-X. (2013) 'Innate and adaptive immune cells in the tumor microenvironment.', *Nature Immunology*, 14(10), pp. 1014–22. doi: 10.1038/ni.2703.

Gallez-Hawkins, G. *et al.* (2003) 'Use of transgenic HLA A*0201/Kb and HHD II mice to evaluate frequency of cytomegalovirus IE1-derived peptide usage in eliciting human CD8 cytokine response.', *Journal of Virology*, 77(7), pp. 4457–62. doi: 10.1128/JVI.77.7.4457.

Galloway, D. A. *et al.* (2005) 'Regulation of telomerase by human papillomaviruses', *Cold Spring Harbor Symposia on Quantitative Biology*, 70, pp. 209–215. doi: 10.1101/sqb.2005.70.041.

Genther, S. M. *et al.* (2003) 'Quantitative role of the human papillomavirus type 16 E5 gene during the productive stage of the viral life cycle.', *Journal of Virology*, 77(5), pp. 2832–42. doi: 10.1128/JVI.77.5.2832.

Geraets, D. *et al.* (2012) 'Detection of rare and possibly carcinogenic human papillomavirus genotypes as single infections in invasive cervical cancer', *Journal of Pathology*, 228(4), pp. 534–543. doi: 10.1002/path.4065.

Ghimire, T. R. (2015) 'The mechanisms of action of vaccines containing aluminum adjuvants: an in vitro vs in vivo paradigm', *SpringerPlus,* 4(1), p. 181. doi: 10.1186/s40064-015-0972-0.

Golden, E. B. and Apetoh, L. (2015) 'Radiotherapy and immunogenic cell death.', *Seminars in Radiation Oncology*, 25(1), pp. 11–7. doi: 10.1016/j.semradonc.2014.07.005.

González-Galarza, F. F. *et al.* (2015) 'Allele frequency net 2015 update: New features for HLA epitopes, KIR and disease and HLA adverse drug reaction associations', *Nucleic Acids Research*, 43(D1), pp. D784–D788. doi: 10.1093/nar/gku1166.

Grabowska, A. K., Kaufmann, A. M. and Riemer, A. B. (2014) 'Identification of promiscuous HPV16-derived T helper cell epitopes for therapeutic HPV vaccine design', *International Journal of Cancer*, 136(1), pp. 212-24. doi: 10.1002/ijc.28968.

Grabowska, A. K. and Riemer, A. B. (2012) 'The invisible enemy - how human papillomaviruses avoid recognition and clearance by the host immune system.', *The Open Virology Journal*, 6, pp. 249–56. doi: 10.2174/1874357901206010249.

Gulley, J. L. (2013) 'Therapeutic vaccines: The ultimate personalized therapy?', *Human Vaccines and Immunotherapeutics*, 9(1), pp. 219–221. doi: 10.4161/hv.22106.

Gunter, C. (2002) 'Human biology by proxy', *Nature*, 420(6915), p. 509. doi: 10.1038/420509a.

Gutcher, I. and Becher, B. (2007) 'APC-derived cytokines and T cell polarization in autoimmune inflammation.', *The Journal of Clinical Investigation*, 117(5), pp. 1119–27. doi: 10.1172/JCI31720.

Hailemichael, Y. *et al.* (2013) 'Persistent antigen at vaccination sites induces tumor-specific CD8+ T cell sequestration, dysfunction and deletion', *Nature Medicine*, 19(4), pp. 465–472. doi: 10.1038/nm.3105.

Hailemichael, Y. *et al.* (2018) 'Cancer vaccine formulation dictates synergy with CTLA-4 and PD-L1 checkpoint blockade therapy', *Journal of Clinical Investigation*, 128(4), pp. 1338–1354. doi: 10.1172/JCI93303.

Hancock, G., Hellner, K. and Dorrell, L. (2018) 'Therapeutic HPV vaccines.', *Best Practice & Research. Clinical Obstetrics & Gynaecology*, 47, pp. 59–72. doi: 10.1016/j.bpobgyn.2017.09.008.

Hansen, T. H. *et al.* (2010) 'Basic and translational applications of engineered MHC class I proteins.', *Trends in Immunology*, 31(10), pp. 363–9. doi: 10.1016/j.it.2010.07.003.

Harada, N. *et al.* (2017) 'Generation of a Novel HLA Class I Transgenic Mouse Model Carrying a Knock-in Mutation at the β_2-Microglobulin Locus', *The Journal of Immunology*, 198(1), pp. 516–527. doi: 10.4049/jimmunol.1502367.

zur Hausen, H. (2002) 'Papillomaviruses and cancer: from basic studies to clinical application.', *Nature Reviews Cancer*, 2(5), pp. 342–50. doi: 10.1038/nrc798.

Heidenreich, R. *et al.* (2015) 'A novel RNA-based adjuvant combines strong immunostimulatory capacities with a favorable safety profile', *International Journal of Cancer*, 137(2), pp. 372-84. doi: 10.1002/ijc.29402.

Henk, H. J. *et al.* (2010) 'Incidence and costs of cervical intraepithelial neoplasia in a US commercially insured population.', *Journal of Lower Genital Tract Disease*, 14(1), pp. 29–36. doi: 10.1097/LGT.0b013e3181ac05e9.

Hildesheim, A. *et al.* (2007) 'Effect of human papillomavirus 16/18 L1 virus like particle vaccine among young women with pre-existing infection: a randomized trial', *JAMA*, 298(7), pp. 743–753. doi: 10.1001/jama.298.7.743.

Hildesheim, A. *et al.* (2016) 'Impact of human papillomavirus (HPV) 16 and 18 vaccination on prevalent infections and rates of cervical lesions after excisional treatment.', *American Journal of Obstetrics and Gynecology*, 215(2), p. 212.e1-212.e15. doi: 10.1016/j.ajog.2016.02.021.

Hozumi, N. and Tonegawa, S. (1976) 'Evidence for somatic rearrangement of immunoglobulin genes coding for variable and constant regions.', *Proceedings of the National Academy of Sciences of the United States of America*, 73(10), pp. 3628–32.

IARC Working Group on the Evaluation of Carcinogenic Risk to Humans (2007) *Human Papillomaviruses.* Available at: https://www.ncbi.nlm.nih.gov/books/NBK321770/.

Illumina Inc (2018) *Illumina - HLA typing*. Available at: https://emea.illumina.com/clinical/hla-sequencing.html?langsel=/de/.

Irwin, M. J., Heath, W. R. and Sherman, L. A. (1989) 'Species-restricted interactions between CD8 and the alpha 3 domain of class I influence the magnitude of the xenogeneic response.', *The Journal of Experimental Medicine*, 170(4), pp. 1091–101. doi: 10.1084/jem.170.4.1091.

Isaacson Wechsler, E. *et al.* (2012) 'Reconstruction of Human Papillomavirus Type 16-Mediated Early-Stage Neoplasia Implicates E6/E7 Deregulation and the Loss of Contact Inhibition in Neoplastic Progression', *Journal of Virology*, 86(11), pp. 6358–6364. doi: 10.1128/JVI.07069-11.

Iwai, Y. *et al.* (2002) 'Involvement of PD-L1 on tumor cells in the escape from host immune system and tumor immunotherapy by PD-L1 blockade.', *Proceedings of the National Academy of Sciences of the United States of America*, 99(19), pp. 12293–7. doi: 10.1073/pnas.192461099.

Jemon, K. *et al.* (2016) 'Suppression of the CD8 T cell response by human papillomavirus type 16 E7 occurs in Langerhans cell-depleted mice', *Scientific Reports*, 6(1), p. 34789. doi: 10.1038/srep34789.

Ji, H. *et al.* (1998) 'Antigen-specific immunotherapy for murine lung metastatic tumors expressing human papillomavirus type 16 E7 oncoprotein.', *International Journal of Cancer*, 78(1), pp. 41–5.

de Jong, A. *et al.* (2004) 'Human papillomavirus type 16-positive cervical cancer is associated with impaired CD4+ T-cell immunity against early antigens E2 and E6.', *Cancer Research*, 64(15), pp. 5449–55. doi: 10.1158/0008-5472.CAN-04-0831.

Joura, E. A. *et al.* (2015) 'A 9-Valent HPV Vaccine against Infection and Intraepithelial Neoplasia in Women', *New England Journal of Medicine*, 372(8), pp. 711–723. doi: 10.1056/NEJMoa1405044.

Kalinke, U., Arnold, B. and Hämmerling, G. J. (1990) 'Strong xenogeneic HLA response in transgenic mice after introducing an alpha 3 domain into HLA B27.', *Nature*, 348(6302), pp. 642–4. doi: 10.1038/348642a0.

Kanodia, S., Fahey, L. M. and Kast, W. M. (2007) 'Mechanisms used by human papillomaviruses to escape the host immune response.', *Current Cancer Drug Targets*, 7(1), pp. 79–89. doi: 10.2174/156800907780006869.

Kärre, K. *et al.* (1986) 'Selective rejection of H-2-deficient lymphoma variants suggests alternative immune defence strategy.', *Nature*, 319(6055), pp. 675–8. doi: 10.1038/319675a0.

Kawana, K. *et al.* (2014) 'Oral vaccination against HPV E7 for treatment of cervical intraepithelial neoplasia grade 3 (CIN3) elicits E7-specific mucosal immunity in the cervix of CIN3 patients', *Vaccine*, 32(47), pp. 6233–6239. doi: 10.1016/j.vaccine.2014.09.020.

Kenter, G. G. *et al.* (2009) 'Vaccination against HPV-16 Oncoproteins for Vulvar Intraepithelial Neoplasia', *New England Journal of Medicine*, 361(19), pp. 1838–1847. doi: 10.1056/NEJMoa0810097.

Keşmir, C. *et al.* (2002) 'Prediction of proteasome cleavage motifs by neural networks', *Protein Engineering, Design and Selection*, 15(4), pp. 287–296. doi: 10.1093/protein/15.4.287.

Khallouf, H., Grabowska, A. and Riemer, A. (2014) 'Therapeutic Vaccine Strategies against Human Papillomavirus', *Vaccines (Basel)*, 2 (2), pp. 422–462. doi: 10.3390/vaccines2020422.

Kim, H. J. and Kim, H.-J. (2017) 'Current status and future prospects for human papillomavirus vaccines.', *Archives of pharmacal research*. Pharmaceutical Society of Korea, 40(9), pp. 1050–1063. doi: 10.1007/s12272-017-0952-8.

Kim, J. H. *et al.* (2011) 'High cleavage efficiency of a 2A peptide derived from porcine teschovirus-1 in human cell lines, zebrafish and mice', *PLoS ONE*, 6(4), pp. 318556. doi: 10.1371/journal.pone.0018556.

Kiyono, T. *et al.* (1998) 'Both Rb/p16(INK4a) inactivation and telomerase activity are required to immortalize human epithelial cells', *Nature*, 396(6706), pp. 84–88. doi: 10.1038/23962.

Klaes, R. *et al.* (2001) 'Overexpression of p16(INK4A) as a specific marker for dysplastic and neoplastic epithelial cells of the cervix uteri.', *International Journal of Cancer*, 92(2), pp. 276–84.

Klebanoff, C. A. *et al.* (2012) 'Determinants of successful CD8+ for large established tumors in mice T cell adoptive immunotherapy', *Clinical Cancer Research,* 17(16), pp. 5343–5352. doi: 10.1158/1078-0432.CCR-11-0503.

Klingelhutz, A. J., Foster, S. A. and McDougall, J. K. (1996) 'Telomerase activation by the E6 gene product of human papillomavirus type 16.', *Nature*, 380(6569), pp. 79–82. doi: 10.1038/380079a0.

Klitz, W. *et al.* (2003) 'New HLA haplotype frequency reference standards: High-resolution and large sample typing of HLA DR-DQ haplotypes in a sample of European Americans', *Tissue Antigens*, 62(4), pp. 296–307. doi: 10.1034/j.1399-0039.2003.00103.x.

Klug, F. *et al.* (2013) 'Low-dose irradiation programs macrophage differentiation to an iNOS$^+$/M1 phenotype that orchestrates effective T cell immunotherapy.', *Cancer Cell*, 24(5), pp. 589–602. doi: 10.1016/j.ccr.2013.09.014.

Koller, B. H. *et al.* (1990) 'Normal development of mice deficient in beta 2M, MHC class I proteins, and CD8+ T cells.', *Science*, 248(4960), pp. 1227–1230. doi: 10.1126/science.2112266.

Kollnberger, S. *et al.* (2004) 'HLA-B27 heavy chain homodimers are expressed in HLA-B27 transgenic rodent models of spondyloarthritis and are ligands for paired Ig-like receptors.', *Journal of Immunology,* 173(3), pp. 1699–710. doi: 10.4049/jimmunol.173.3.1699.

Komar, A. A. and Hatzoglou, M. (2011) 'Cellular IRES-mediated translation: the war of ITAFs in pathophysiological states.', *Cell Cycle*, 10(2), pp. 229–40. doi: 10.4161/cc.10.2.14472.

Kranz, L. M. *et al.* (2016) 'Systemic RNA delivery to dendritic cells exploits antiviral defence for cancer immunotherapy.', *Nature*, 534(7607), pp. 396–401. doi: 10.1038/nature18300.

Kreiter, S. *et al.* (2007) 'Increased Antigen Presentation Efficiency by Coupling Antigens to MHC Class I Trafficking Signals', *Journal of Immunology*, 180(1), pp. 309–318. doi: 10.4049/jimmunol.180.1.309.

Kreiter, S. *et al.* (2015) 'Mutant MHC class II epitopes drive therapeutic immune responses to cancer.', *Nature*, 520(7549), pp. 692–6. doi: 10.1038/nature14426.

Kruse, S. *et al.* (2018) 'Therapeutic vaccination using minimal HPV16 epitopes in a novel MHC-humanized murine HPV tumor model', *Oncoimmunology*. doi: 10.1080/2162402X.2018.1524694.

Kuhn, A. N. *et al.* (2010) 'Phosphorothioate cap analogs increase stability and translational efficiency of RNA vaccines in immature dendritic cells and induce superior immune responses in vivo', *Gene Therapy*, 17(8), pp. 961–971. doi: 10.1038/gt.2010.52.

Kuhs, K. A. L. *et al.* (2014) 'Effect of different human papillomavirus serological and dnacriteria on vaccine efficacy estimates', *American Journal of Epidemiology*, 180(6), pp. 599–607. doi: 10.1093/aje/kwu168.

Kuon, W. *et al.* (1997) 'Recognition of chlamydial antigen by HLA-B27-restricted cytotoxic T cells in HLA-B*2705 transgenic CBA (H-2k) mice.', *Arthritis and Rheumatism*, 40(5), pp. 945–54. doi: 10.1002/1529-0131(199705)40:5<945::AID-ART23>3.0.CO;2-L.

Kuon, W. *et al.* (2004) 'Identification of novel human aggrecan T cell epitopes in HLA-B27 transgenic mice associated with spondyloarthropathy.', *Journal of Immunology*, 173(8), pp. 4859–66. doi: 10.4049/jimmunol.173.8.4859.

Laemmli, U. K. (1970) 'Cleavage of structural proteins during the assembly of the head of bacteriophage T4', *Nature*, 227(5259), pp. 680–685. doi: 10.1038/227680a0.

Laurson, J. *et al.* (2010) 'Epigenetic repression of E-cadherin by human papillomavirus 16 E7 protein', *Carcinogenesis*, 31(5), pp. 918–926. doi: 10.1093/carcin/bgq027.

Lawrance, S. K. *et al.* (1989) 'Transgenic HLA-DR alpha faithfully reconstitutes IE-controlled immune functions and induces cross-tolerance to E alpha in E alpha 0 mutant mice.', *Cell*, 58(3), pp. 583–94.

Lehtinen, M. *et al.* (2012) 'Overall efficacy of HPV-16/18 AS04-adjuvanted vaccine against grade 3 or greater cervical intraepithelial neoplasia: 4-year end-of-study analysis of the randomised, double-blind PATRICIA trial', *The Lancet Oncology*, 13(1), pp. 89–99. doi: 10.1016/S1470-2045(11)70286-8.

Lin, K. Y. *et al.* (1996) 'Treatment of established tumors with a novel vaccine that enhances major histocompatibility class II presentation of tumor antigen', *Cancer Research*, 56(1), pp. 21–26. doi: 8548765.

Lipovsky, A. *et al.* (2013) 'Genome-wide siRNA screen identifies the retromer as a cellular entry factor for human papillomavirus.', *Proceedings of the National Academy of Sciences of the United States of America*, 110(18), pp. 7452–7. doi: 10.1073/pnas.1302164110.

Liu, H. *et al.* (2014) 'Structure-based programming of lymph-node targeting in molecular vaccines.', *Nature*, 507(7493), pp. 519–22. doi: 10.1038/nature12978.

Liu, Z. *et al.* (2017) 'Systematic comparison of 2A peptides for cloning multi-genes in a polycistronic vector', *Scientific Reports*, 7(1), p. 2193. doi: 10.1038/s41598-017-02460-2.

Macri, C. *et al.* (2016) 'Targeting dendritic cells: a promising strategy to improve vaccine effectiveness', *Clinical & Translational Immunology*, 5(3), p. e66. doi: 10.1038/cti.2016.6.

Madsen, L. *et al.* (1999) 'Mice lacking all conventional MHC class II genes.', *Proceedings of the National Academy of Sciences of the United States of America*, 96(18), pp. 10338–43.

Mage, M. G. *et al.* (1992) 'A recombinant, soluble, single-chain class I major histocompatibility complex molecule with biological activity.', *Proceedings of the National Academy of Sciences of the United States of America*, 89(22), pp. 10658–62. doi: 10.1073/pnas.89.22.10658.

Di Marco, M., Peper, J. K. and Rammensee, H.-G. (2017) 'Identification of Immunogenic Epitopes by MS/MS.', *Cancer Journal*, 23(2), pp. 102–107. doi: 10.1097/PPO.0000000000000252.

de Martel, C. *et al.* (2017) 'Worldwide burden of cancer attributable to HPV by site, country and HPV type', *International Journal of Cancer*, 141(4), pp. 664–670. doi: 10.1002/ijc.30716.

Martins, K. A. O., Bavari, S. and Salazar, A. M. (2015) 'Vaccine adjuvant uses of poly-IC and derivatives.', *Expert Review of Vaccines*, 14(3), pp. 447–59. doi: 10.1586/14760584.2015.966085.

McBride, A. A. and Warburton, A. (2017) 'The role of integration in oncogenic progression of HPV-associated cancers.', *PLoS Pathogens*, 13(4), p. e1006211. doi: 10.1371/journal.ppat.1006211.

McCredie, M. R. *et al.* (2008) 'Natural history of cervical neoplasia and risk of invasive cancer in women with cervical intraepithelial neoplasia 3: a retrospective cohort study', *The Lancet Oncology*, 9(5), pp. 425–434. doi: 10.1016/S1470-2045(08)70103-7.

Merrifield, R. B. (1963) 'Solid Phase Peptide Synthesis. I. The Synthesis of a Tetrapeptide', *Journal of the American Chemical Society*, 85(14), pp. 2149–2154. doi: 10.1021/ja00897a025.

Mestecky, J., Moldoveanu, Z. and Russell, M. W. (2005) 'Immunologic Uniqueness of the Genital Tract: Challenge for Vaccine Development', *American Journal of Reproductive Immunology*, 53(5), pp. 208–214. doi: 10.1111/j.1600-0897.2005.00267.x.

Mirabello, L. *et al.* (2017) 'HPV16 E7 Genetic Conservation Is Critical to Carcinogenesis', *Cell*, 170(6), p. 1164–1174.e6. doi: 10.1016/j.cell.2017.08.001.

Mirkovic, J. *et al.* (2015) 'Carcinogenic HPV infection in the cervical squamo-columnar junction.', *The Journal of Pathology*, 236(3), pp. 265–71. doi: 10.1002/path.4533.

Modis, Y., Trus, B. L. and Harrison, S. C. (2002) 'Atomic model of the papillomavirus capsid.', *The EMBO journal*, 21(18), pp. 4754–62. doi: 10.1093/emboj/cdf494.

Moody, C. A. and Laimins, L. A. (2010) 'Human papillomavirus oncoproteins: Pathways to transformation', *Nature Reviews Cancer*, 10(8), pp. 550–560. doi: 10.1038/nrc2886.

Moynihan, K. D. *et al.* (2016) 'Eradication of large established tumors in mice by combination immunotherapy that engages innate and adaptive immune responses.', *Nature Medicine*, 22(12), pp. 1402–1410. doi: 10.1038/nm.4200.

Muderspach, L. *et al.* (2000) 'A Phase I Trial of a Human Papillomavirus (HPV) Peptide Vaccine for Women with High-Grade Cervical and Vulvar Intraepithelial Neoplasia Who Are HPV 16 Positive', *Clinical Cancer Research*, 6(9), pp. 3406–3416.

Mullis, K. *et al.* (1986) 'Specific enzymatic amplification of DNA in vitro: the polymerase chain reaction.', *Cold Spring Harbor Symposia on Quantitative Biology*, 51 Pt 1, pp. 263–73.

Muñoz, N. *et al.* (1992) 'The causal link between human papillomavirus and invasive cervical cancer: a population-based case-control study in Colombia and Spain.', *International Journal of Cancer*, 52(5), pp. 743–9.

Murphy, K. *et al.* (2016) *Janeway's immunobiology, 9th ed.* New York: Garland Science.

Nabel, G. J. (2013) 'Designing Tomorrow's Vaccines', *New England Journal of Medicine*, 368(6), pp. 551–560. doi: 10.1056/NEJMra1204186.

Nardelli-Haefliger, D., Dudda, J. C. and Romero, P. (2013) 'Vaccination route matters for mucosal tumors', *Science Translational Medicine*, 5(172), pp. 172fs4. doi: 10.1126/scitranslmed.3005638.

Newberg, M. H. *et al.* (1996) 'Importance of MHC class 1 alpha2 and alpha3 domains in the recognition of self and non-self MHC molecules', *Journal of Immunology*, 156(7), pp. 2473–2480.

Nielsen, M. *et al.* (2005) 'The role of the proteasome in generating cytotoxic T-cell epitopes: insights obtained from improved predictions of proteasomal cleavage.', *Immunogenetics*, 57(1–2), pp. 33–41. doi: 10.1007/s00251-005-0781-7.

Ochs, K. *et al.* (2017) 'K27M-mutant histone-3 as a novel target for glioma immunotherapy', *Oncoimmunology*, 6(7), p. e1328340. doi: 10.1080/2162402X.2017.1328340.

Pajot, A., Michel, M.-L., *et al.* (2004) 'A mouse model of human adaptive immune functions: HLA-A2.1-/HLA-DR1-transgenic H-2 class I-/class II-knockout mice.', *European Journal of Immunology*, 34(11), pp. 3060–9. doi: 10.1002/eji.200425463.

Pajot, A., Pancré, V., *et al.* (2004) 'Comparison of HLA-DR1-restricted T cell response induced in HLA-DR1 transgenic mice deficient for murine MHC class II and HLA-DR1 transgenic mice expressing endogenous murine MHC class II molecules.', *International Immunology*, 16(9), pp. 1275–82. doi: 10.1093/intimm/dxh129.

Paolini, F. *et al.* (2013) 'Immunotherapy in new pre-clinical models of HPV-associated oral cancers', *Human Vaccines and Immunotherapeutics*, 9(3), pp. 534–543. doi: 10.4161/hv.23232.

Pascolo, S. *et al.* (1997) 'HLA-A2.1-restricted education and cytolytic activity of CD8(+) T lymphocytes from beta2 microglobulin (beta2m) HLA-A2.1 monochain transgenic H-2Db beta2m double knockout mice.', *The Journal of Experimental Medicine*, 185(12), pp. 2043–2051.

Pascolo, S. (2005) 'HLA class I transgenic mice: development, utilisation and improvement.', *Expert Opinion on Biological Therapy*, 5(7), pp. 919–938. doi: 10.1517/14712598.5.7.919.

Pastrana, D. V. *et al.* (2001) 'NHPV16 VLP vaccine induces human antibodies that neutralize divergent variants of HPV16.', *Virology*, 279(1), pp. 361–9. doi: 10.1006/viro.2000.0702.

Pattillo, R. a. *et al.* (1977) 'Tumor antigen and human chorionic gonadotropin in CaSki cells: a new epidermoid cervical cancer cell line.', *Science*, 196(4297), pp. 1456–8. doi: 10.1097/00006254-197801000-00022.

Le Pecq, J. B. and Paoletti, C. (1966) 'A new fluorometric method for RNA and DNA determination.', *Analytical Biochemistry*, 17(1), pp. 100–7.

Peng, S. *et al.* (2004) 'Development of a DNA vaccine targeting human papillomavirus type 16 oncoprotein E6.', *Journal of Virology*, 78(16), pp. 8468–76. doi: 10.1128/JVI.78.16.8468-8476.2004.

Peng, S. *et al.* (2006) 'Characterization of HLA-A2-restricted HPV-16 E7-specific CD8(+) T-cell immune responses induced by DNA vaccines in HLA-A2 transgenic mice.', *Gene Therapy*, 13(1), pp. 67–77. doi: 10.1038/sj.gt.3302607.

Plummer, M. *et al.* (2007) 'A 2-Year Prospective Study of Human Papillomavirus Persistence among Women with a Cytological Diagnosis of Atypical Squamous Cells of Undetermined Significance or Low-Grade Squamous Intraepithelial Lesion', *The Journal of Infectious Diseases*, 195(11), pp. 1582–1589. doi: 10.1086/516784.

Plummer, M. *et al.* (2016) 'Global burden of cancers attributable to infections in 2012: a synthetic analysis.', *The Lancet. Global health*, 4(9), pp. e609-16. doi: 10.1016/S2214-109X(16)30143-7.

van Poelgeest, M. I. E. *et al.* (2013) 'HPV16 synthetic long peptide (HPV16-SLP) vaccination therapy of patients with advanced or recurrent HPV16-induced gynecological carcinoma, a phase II trial', *Journal of Translational Medicine*, 11(1), p. 88. doi: 10.1186/1479-5876-11-88.

Pol, J. *et al.* (2015) 'Trial Watch: Peptide-based anticancer vaccines.', *Oncoimmunology*, 4(4), p. e974411. doi: 10.4161/2162402X.2014.974411.

Pyeon, D. *et al.* (2009) 'Establishment of human papillomavirus infection requires cell cycle progression.', *PLoS Pathogens*, 5(2), p. e1000318. doi: 10.1371/journal.ppat.1000318.

Quandt, J. (2012) *PhD thesis 'Common mutations in the tumor suppressor p53 & the oncogene Kras as targets for long peptide anti-cancer vaccination*'. Universität Heidelberg.

Rangan, L. *et al.* (2017) 'Identification of a novel PD-L1 positive solid tumor transplantable in HLA-A*0201/DRB1*0101 transgenic mice.', *Oncotarget*, 8(30), pp. 48959–48971. doi: 10.18632/oncotarget.16900.

Rathod, S. *et al.* (2015) 'A systematic review of quality of life in head and neck cancer treated with surgery with or without adjuvant treatment.', *Oral Oncology*, 51(10), pp. 888–900. doi: 10.1016/j.oraloncology.2015.07.002.

Redmond, W. L. and Sherman, L. A. (2005) 'Peripheral tolerance of CD8 T lymphocytes', *Immunity*, 22(3), pp. 275–284. doi: 10.1016/j.immuni.2005.01.010.

Reinhardt, R. L. *et al.* (2003) 'Preferential Accumulation of Antigen-specific Effector CD4 T Cells at an Antigen Injection Site Involves CD62E-dependent Migration but Not Local Proliferation', *The Journal of Experimental Medicine*, 197(6), pp. 751–762. doi: 10.1084/jem.20021690.

Ressing, M. E. *et al.* (1995) 'Human CTL epitopes encoded by human papillomavirus type 16 E6 and E7 identified through in vivo and in vitro immunogenicity studies of HLA-A*0201-binding peptides.', *Journal of Immunology*, 154(11), pp. 5934–5943.

Ridge, J. P., Di Rosa, F. and Matzinger, P. (1998) 'A conditioned dendritic cell can be a temporal bridge between a CD4+ T-helper and a T-killer cell.', *Nature*, 393(6684), pp. 474–8. doi: 10.1038/30989.

Riemer, A. B. *et al.* (2010) 'A conserved E7-derived cytotoxic T lymphocyte epitope expressed on human papillomavirus 16-transformed HLA-A2+ epithelial cancers', *Journal of Biological Chemistry*, 285(38), pp. 29608–29622. doi: 10.1074/jbc.M110.126722.

Robert Koch Institut (2018a) 'Epidemiologisches Bulletin', (1), pp. 8–9.

Robert Koch Institut (2018b) 'Epidemiologisches Bulletin', (26), pp. 1–19.

Roden, R. B. S. and Stern, P. L. (2018) 'Opportunities and challenges for human papillomavirus vaccination in cancer', *Nature Reviews Cancer*, 18(4), pp. 240–254. doi: 10.1038/nrc.2018.13.

Rosa, M. I. *et al.* (2008) 'Persistence and clearance of human papillomavirus infection: a prospective cohort study', *American Journal of Obstetrics and Gynecology*, 199(6), pp. 617.e1-7. doi: 10.1016/j.ajog.2008.06.033.

Rosalia, R. A. *et al.* (2013) 'Dendritic cells process synthetic long peptides better than whole protein, improving antigen presentation and T-cell activation', *European Journal of Immunology*, 43(10), pp. 2554–2565. doi: 10.1002/eji.201343324.

Saiki, R. K. *et al.* (1985) 'Enzymatic amplification of beta-globin genomic sequences and restriction site analysis for diagnosis of sickle cell anemia.', *Science*, 230(4732), pp. 1350–4.

Sandoval, F. *et al.* (2013) 'Mucosal imprinting of vaccine-induced $CD8^+$ T cells is crucial to inhibit the growth of mucosal tumors.', *Science Translational Medicine*, 5(172), p. 172ra20. doi: 10.1126/scitranslmed.3004888.

Santos, C. *et al.* (2017) 'HPV-transgenic mouse models: Tools for studying the cancer-associated immune response.', *Virus Research*, 235, pp. 49–57. doi: 10.1016/j.virusres.2017.04.001.

Schatz, D. G. (2004) 'V(D)J recombination.', *Immunological Reviews*, 200, pp. 5–11. doi: 10.1111/j.0105-2896.2004.00173.x.

Schiffman, M. *et al.* (2016) 'Carcinogenic human papillomavirus infection', *Nature Reviews Disease Primers*, 2, p. 16086. doi: 10.1038/nrdp.2016.86.

Schiller, J. T. and Müller, M. (2015) 'Next generation prophylactic human papillomavirus vaccines', *The Lancet Oncology*, 16(5), pp. e217–e225. doi: 10.1016/S1470-2045(14)71179-9.

Schneider, C. A., Rasband, W. S. and Eliceiri, K. W. (2012) 'NIH Image to ImageJ: 25 years of image analysis', *Nature Methods*, 9(7), pp. 671–675. doi: 10.1038/nmeth.2089.

Schoenberger, S. P. *et al.* (1998) 'T-cell help for cytotoxic T lymphocytes is mediated by CD40-CD40L interactions.', *Nature*, 393(6684), pp. 480–3. doi: 10.1038/31002.

Schumacher, T. *et al.* (2014) 'A vaccine targeting mutant IDH1 induces antitumour immunity', *Nature*, 512(7514), pp. 324–327. doi: 10.1038/nature13387.

Seder, R. A., Darrah, P. A. and Roederer, M. (2008) 'T-cell quality in memory and protection: Implications for vaccine design', *Nature Reviews Immunology*, 8(4), pp. 247–258. doi: 10.1038/nri2274.

Serrano, B. *et al.* (2015) 'Human papillomavirus genotype attribution for HPVs 6, 11, 16, 18, 31, 33, 45, 52 and 58 in female anogenital lesions', *European Journal of Cancer*, 51(13), pp. 1732–1741. doi: 10.1016/j.ejca.2015.06.001.

Sharma, P. and Allison, J. P. (2015) 'Immune checkpoint targeting in cancer therapy: Toward combination strategies with curative potential', *Cell*, 161(2), pp. 205–214. doi: 10.1016/j.cell.2015.03.030.

Shin, H. and Iwasaki, A. (2012) 'A vaccine strategy that protects against genital herpes by establishing local memory T cells.', *Nature*, 491(7424), pp. 463–7. doi: 10.1038/nature11522.

Sidney, J. *et al.* (2008) 'HLA class I supertypes: a revised and updated classification.', *BMC Immunology*, 9, p. 1. doi: 10.1186/1471-2172-9-1.

Van Der Sluis, T. C. *et al.* (2015) 'Vaccine-Induced tumor necrosis factor- Producing T cells synergize with cisplatin to promote tumor cell death', *Clinical Cancer Research*, 21(4), pp. 781–794. doi: 10.1158/1078-0432.CCR-14-2142.

Snell, G. D. and Higgins, G. F. (1951) 'Alleles at the histocompatibility-2 locus in the mouse as determined by tumor transplantation.', *Genetics*, 36(3), pp. 306–10.

Soong, R.-S. *et al.* (2014) 'Toll-like receptor agonist imiquimod facilitates antigen-specific CD8+ T-cell accumulation in the genital tract leading to tumor control through IFNγ.', *Clinical Cancer Research*, 20(21), pp. 5456–67. doi: 10.1158/1078-0432.CCR-14-0344.

Stanke, J. *et al.* (2010) 'A flow cytometry-based assay to assess minute frequencies of CD8+ T cells by their cytolytic function', *Journal of Immunological Methods*, 360(1–2), pp. 56–65. doi: 10.1016/j.jim.2010.06.005.

Stanley, M. A. (2012) 'Epithelial cell responses to infection with human papillomavirus', *Clinical Microbiology Reviews*, 25(2), pp. 215–222. doi: 10.1128/CMR.05028-11.

Steele, J. C. *et al.* (2002) 'Detection of CD4(+)- and CD8(+)-T-cell responses to human papillomavirus type 1 antigens expressed at various stages of the virus life cycle by using an enzyme-linked immunospot assay of gamma interferon release.', *Journal of Virology*, 76(12), pp. 6027–36. doi: 10.1128/JVI.76.12.6027.

Steinbach, A. *et al.* (2017) 'ERAP1 overexpression in HPV-induced malignancies: A possible novel immune evasion mechanism.', *Oncoimmunology*, 6(7), p. e1336594. doi: 10.1080/2162402X.2017.1336594.

Steller, M. A. *et al.* (1998) 'Cell-mediated immunologic responses in cervical and vaginal cancer patients with a lipidated epitope of human papillomavirus type 16 E7.', *Clinical Cancer Research*, 4(9), pp. 2103–2109.

Stern, P. L. *et al.* (2012) 'Therapy of human papillomavirus-related disease.', *Vaccine*, 30 Suppl 5(4), pp. F71-82. doi: 10.1016/j.vaccine.2012.05.091.

Stoler, M. H. *et al.* (1992) 'Human papillomavirus type 16 and 18 gene expression in cervical neoplasias', *Human Pathology*, 23(2), pp. 117–128. doi: 10.1016/0046-8177(92)90232-R.

Street, M. D. *et al.* (2002) 'Limitations of HLA-transgenic mice in presentation of HLA-restricted cytotoxic T-cell epitopes from endogenously processed human papillomavirus type 16 E7 protein', *Immunology*, 106(4), pp. 526–536. doi: 10.1046/j.1365-2567.2002.01442.x.

Sun, Y. *et al.* (2015) 'Intravaginal HPV DNA vaccination with electroporation induces local CD8+ T-cell immune responses and antitumor effects against cervicovaginal tumors', *Gene Therapy*, 22(7), pp. 528–535. doi: 10.1038/gt.2015.17.

Sykulev, Y. *et al.* (1996) 'Evidence that a single peptide-MHC complex on a target cell can elicit a cytolytic T cell response.', *Immunity*, 4(6), pp. 565–71.

Takeuchi, S. *et al.* (2015) 'Phase 2 studies of multiple peptides cocktail vaccine for treatment-resistant cervical and ovarian cancer.', *ASCO Meeting Abstracts* .

Tan, H.-X. *et al.* (2017) 'Induction of vaginal-resident HIV-specific CD8 T cells with mucosal prime–boost immunization', *Mucosal Immunology*, 11(3), pp. 994-1007. doi: 10.1038/mi.2017.89.

The Jackson Laboratory (2018a) *C57BL/6J*. Available at: https://www.jax.org/strain/000664 (Accessed: 22 May 2018).

The Jackson Laboratory (2018b) *Why mouse genetics?* Available at: https://www.jax.org/personalized-medicine/why-mouse-genetics (Accessed: 28 July 2018).

Theobald, M. *et al.* (1997) 'Tolerance to p53 by A2.1-restricted cytotoxic T lymphocytes', *The Journal of Experimental Medicine*, 185(5), pp. 833–41. doi: 10.1084/jem.185.5.833.

Tindle, R. W. *et al.* (1995) 'A vaccine conjugate of "ISCAR" immunocarrier and peptide epitopes of the E7 cervical cancer-associated protein of human papillomavirus type 16 elicits specific Th1- and Th2-type responses in immunized mice in the absence of oil-based adjuvants.', *Clinical and Experimental Immunology*, 101(2), pp. 265–71. doi: 10.1111/j.1365-2249.1995.tb08349.x.

Trimble, C. L. *et al.* (2010) 'Human papillomavirus 16-associated cervical intraepithelial neoplasia in humans excludes CD8 T cells from dysplastic epithelium.', *Journal of Immunology*, 185(11), pp. 7107–14. doi: 10.4049/jimmunol.1002756.

Trimble, C. L. *et al.* (2015) 'Safety, efficacy, and immunogenicity of VGX-3100, a therapeutic synthetic DNA vaccine targeting human papillomavirus 16 and 18 E6 and E7 proteins for cervical intraepithelial neoplasia 2/3: A randomised, double-blind, placebo-controlled phase 2b trial', *The Lancet*, 386(10008), pp. 2078–2088. doi: 10.1016/S0140-6736(15)00239-1.

Trimble, C. L. and Frazer, I. H. (2009) 'Development of therapeutic HPV vaccines', *The Lancet Oncology*, 10(10), pp. 975–980. doi: 10.1016/S1470-2045(09)70227-X.

Umansky, V. *et al.* (2016) 'The Role of Myeloid-Derived Suppressor Cells (MDSC) in Cancer Progression', *Vaccines (Basel)*, 4(4), p. 36. doi: 10.3390/vaccines4040036.

Ureta-Vidal, A. *et al.* (1999) 'Phenotypical and functional characterization of the CD8+ T cell repertoire of HLA-A2.1 transgenic, H-2KbnullDbnull double knockout mice.', *Journal of Immunology*, 163(5), pp. 2555–60.

Vici, P. *et al.* (2016) 'Targeting immune response with therapeutic vaccines in premalignant lesions and cervical cancer: hope or reality from clinical studies', *Expert Review of Vaccines*, 15(10), pp. 1327–1336. doi: 10.1080/14760584.2016.1176533.

De Villiers, E. M. *et al.* (2004) 'Classification of papillomaviruses', *Virology*, 324(1), pp. 17–27. doi: 10.1016/j.virol.2004.03.033.

Vitiello, A. *et al.* (1991) 'Analysis of the HLA-restricted influenza-specific cytotoxic T lymphocyte response in transgenic mice carrying a chimeric human-mouse class I major histocompatibility complex.', *The Journal of Experimental Medicine*, 173(4), pp. 1007–15. doi: 10.1084/jem.173.4.1007.

de Vos van Steenwijk, P. J. *et al.* (2012) 'A placebo-controlled randomized HPV16 synthetic long-peptide vaccination study in women with high-grade cervical squamous intraepithelial lesions.', *Cancer Immunology, Immunotherapy : CII*, 61(9), pp. 1485–92. doi: 10.1007/s00262-012-1292-7.

de Vos van Steenwijk, P. J. *et al.* (2014) 'The long-term immune response after HPV16 peptide vaccination in women with low-grade pre-malignant disorders of the uterine cervix: a placebo-controlled phase II study.', *Cancer Immunology, Immunotherapy : CII*, 63(2), pp. 147–60. doi: 10.1007/s00262-013-1499-2.

Walboomers, J. M. M. *et al.* (1999) 'Human papillomavirus is a necessary cause of invasive cervical cancer worldwide.', *The Journal of Pathology*, 189(1), pp. 12–9. doi: 10.1002/(SICI)1096-9896(199909)189:1<12::AID-PATH431>3.0.CO;2-F.

Walker, T. Y. *et al.* (2017) 'National, Regional, State, and Selected Local Area Vaccination Coverage Among Adolescents Aged 13-17 Years - United States, 2016.', *MMWR. Morbidity and Mortality Weekly Report*, 66(33), pp. 874–882. doi: 10.15585/mmwr.mm6633a2.

Wang, P. *et al.* (2018) 'An albumin-binding polypeptide both targets cytotoxic T lymphocyte vaccines to lymph nodes and boosts vaccine presentation by dendritic cells', *Theranostics*, 8(1), pp. 223–236. doi: 10.7150/thno.21691.

Waring, M. J. (1965) 'Complex formation between ethidium bromide and nucleic acids.', *Journal of Molecular Biology*, 13(1), pp. 269–82.

Werness, B., Levine, A. and Howley, P. (1990) 'Association of human papillomavirus types 16 and 18 E6 proteins with p53', *Science*, 248(4951), pp. 76–79. doi: 10.1126/science.2157286.

Wetterstrand, K. (2018) *DNA Sequencing Costs*, *DNA Sequencing Costs: Data from the NHGRI Genome Sequencing Program (GSP)*. Available at: https://www.genome.gov/sequencingcostsdata/ (Accessed: 20 July 2018).

WHO (2018) *WHO fact sheet: Human papillomavirus (HPV) and cervical cancer*. Available at: http://www.who.int/en/news-room/fact-sheets/detail/human-papillomavirus-(hpv)-and-cervical-cancer (Accessed: 18 July 2018).

Wieland, U., Kreuter, A. and Pfister, H. (2014) 'Human papillomavirus and immunosuppression.', *Current Problems in Dermatology*, 45, pp. 154–65. doi: 10.1159/000357907.

Wiesel, M. and Oxenius, A. (2012) 'From crucial to negligible: functional $CD8^+$ T-cell responses and their dependence on $CD4^+$ T-cell help.', *European Journal of Immunology*, 42(5), pp. 1080–8. doi: 10.1002/eji.201142205.

Williams, D. B. *et al.* (1989) 'Role of beta 2-microglobulin in the intracellular transport and surface expression of murine class I histocompatibility molecules.', *Journal of Immunology*, 142(8), pp. 2796–806.

Woodman, C. B. J., Collins, S. I. and Young, L. S. (2007) 'The natural history of cervical HPV infection: unresolved issues.', *Nature Reviews Cancer*, 7(1), pp. 11–22. doi: 10.1038/nrc2050.

World Health Organization (2014) *World Cancer Report 2014.*

Wright, T. C. *et al.* (2011) 'Evaluation of HPV-16 and HPV-18 genotyping for the triage of women with high-risk HPV+ cytology-negative results', *American Journal of Clinical Pathology*, 136(4), pp. 578–586. doi: 10.1309/AJCPTUS5EXAS6DKZ.

Yang, A. *et al.* (2016) 'Perspectives for therapeutic HPV vaccine development', *Journal of Biomedical Science*, 23(1), pp. 1–19. doi: 10.1186/s12929-016-0293-9.

Yarovinsky, F. *et al.* (2006) 'Toll-like Receptor Recognition Regulates Immunodominance in an Antimicrobial CD4+T Cell Response', *Immunity*, 25(4), pp. 655–664. doi: 10.1016/j.immuni.2006.07.015.

Zhu, G. *et al.* (2017) 'Albumin/vaccine nanocomplexes that assemble in vivo for combination cancer immunotherapy', *Nature Communications*, 8(1), p. 1954. doi: 10.1038/s41467-017-02191-y.

Zijlstra, M. *et al.* (1990) 'Beta 2-microglobulin deficient mice lack CD4-8+ cytolytic T cells', *Nature*, 344(6268), pp. 742–6. doi: 10.1038/344742a0.

Zottnick, S. (2017) *Master thesis 'Development of TC-1 mutanome-based DNA vaccines targeting tumour neo-epitopes'*. Universität Tübingen.

8 Annex

E6 Protein Sequence (from NCBI Reference Sequence: NC_001526.2):

MHQKRTAMFQDPQERPRKLPQLCTELQTTIHDIILECVYCKQQLLRREVYDFAFRDLCIVYRDGNPYAV
CDKCLKFYSKISEYRHYCYSLYGTTLEQQYNKPLCDLLIRCINCQKPLCPEEKQRHLDKKQRFHNIRGRWT
GRCMSCCRSSRTRRETQL

E7 Protein Sequence (from NCBI Reference Sequence: NC_001526.2):

MHGDTPTLHEYMLDLQPETTDLYCYEQLNDSSEEEDEIDGPAGQAEPDRAHYNIVTFCCKCDSTLRLCV
QSTHVDIRTLEDLLMGTLGIVCPICSQKP